THE JOURNAL
OF
CHEMICAL PHYSICS

VOLUME 16, NUMBER 10 OCTOBER, 1948

Physical Adsorption on Non-Uniform Surfaces

GEORGE HALSEY*
Department of Chemistry, Harvard University, Cambridge, Massachusetts
(Received March 9, 1948)

Analysis of adsorption on a uniform surface using the quasi-chemical theory of interaction shows that the hypotheses of the BET theory lead to substantially no adsorption beyond the first layer if $E_2=E_L$, and stepwise isotherms if $E_1>E_2>E_3>\cdots>E_L$. For the monolayer adsorption of gases on silver, platinum, and steel, the heterogeneous nature of the adsorbing surface is clearly indicated. Cooperative adsorption on the non-uniform surface is treated, and the cooperative analog of the Freundlich equation derived. The typical multi-layer isotherm is shown to be composed of three regions: non-cooperative adsorption on a strongly heterogeneous surface; cooperative adsorption on a still heterogeneous surface; and cooperative multi-layer adsorption induced by small van der Waals perturbations some distance from the surface.

The isotherm $p/p_0=\exp\{-a/\theta^r\}$ is derived and shown to be a good representation of adsorption data that conform to the BET Type I, II, or III shapes.

THE theory of physical adsorption has been greatly advanced by the idea that molecules of a vapor can be adsorbed to a depth of many monolayers. The development of the theory of multilayer adsorption is largely the work of Brunauer, Emmett, and Teller (BET).[1] The original theory has been the subject of many criticisms and refinements,[2] but the picture that the adsorbed layer is many molecules thick near the condensation pressure of the bulk liquid has not been invalidated. In other respects, however, it appears that a more refined treatment of adsorption or a uniform surface destroys rather than corrects the BET theory.

In what follows the notation of Brunauer[1] will be used.

I. CRITICISM OF THE BET THEORY

The original BET equation gives the coverage, measured in monolayers, as

$$\theta=v/v_m$$
$$=(p/p_0)/(1-p/p_0)\{1/c+(c-1/c)p/p_0\}. \quad (1)$$

In order to criticize the BET theory only the case $c=1$ need be considered. For $c\to\infty$, $\theta=\theta_{c=1}+1$, and the argument will be generalized to intermediate values of c.

$$\theta_{c=1}=(p/p_0)/(1-p/p_0). \quad (2)$$

This result is based on the quite untenable hypothesis that an isolated adsorbed molecule can adsorb a second molecule on top, yielding the full energy of liquefaction, and that in turn the second molecule can adsorb a third, and so on. However, it is more nearly true to assume that for hexagonal packing at least a triangular array of adsorbed molecules would be required to

* E. I. duPont de Nemours Postdoctoral Fellow, 1947–48.
[1] S. Brunauer, *The Adsorption of Gases and Vapors* (Princeton University Press, Princeton, New Jersey, 1943).
[2] T. L. Hill, J. Chem. Phys. **14**, 263, 441 (1946); **15**, 767 (1947); H. M. Cassel, J. Phys. Chem. **48**, 195 (1944).

adsorb another with the release of energy approaching the heat of liquefaction.

Consider the point $p/p_0=1/2$. Here the BET coverage in the first layer, θ_1, is 1/2. The fraction of sites in the second layer with filled triangular array beneath is $(1/2)^3$. If these sites are filled to the BET amount then $\theta_2=(1/2)^4$. The fraction of sites in the third layer with a filled triangular array beneath is then $(1/2)^{12}$! It is thus apparent that the third layer is effectively empty. θ_2 is then reduced to the Langmuir adsorption $(1/2)^3\times 1/3$ because it is not protected from evaporation by the BET coverage above. Therefore, θ_1 itself becomes almost unprotected and assumes the Langmuir coverage 1/3. This decrease further reduces θ_2 to the negligible value of $(1/3)^4$. Thus, at $p/p_0=1/2$ and below, only a monolayer exists, and the coverage is given by the Langmuir expression

$$\theta=(p/p_0)/(1+p/p_0). \tag{3}$$

It is apparent that unless θ_1 rises above *ca.* 1/3, the second layer is not formed in appreciable quantity. Keeping this fact in mind, attention may now be focused on the artificial problem where the second layer is prohibited from forming by a capillary wall. This problem is equivalent to the problem without such a wall as long as $\theta_1<1/3$. Equation (3) is the solution of this problem for the non-cooperative case.

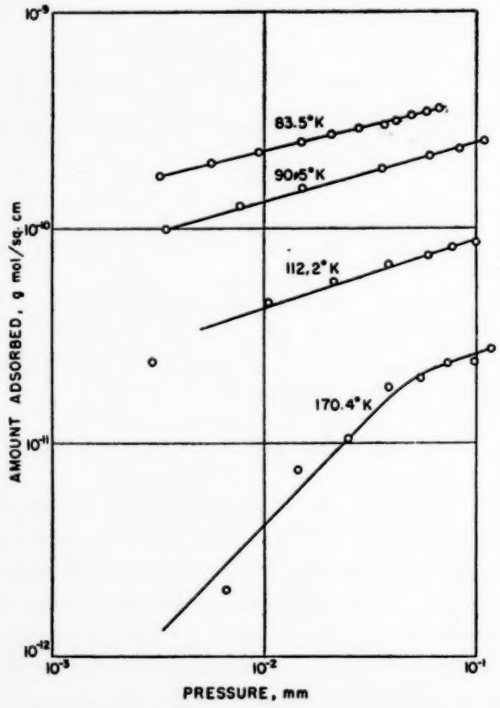

FIG. 1. The adsorption of nitrogen on platinum.

The refined (quasi-chemical) treatment of Fowler and Guggenheim[3] for localized monolayers will be used to obtain the solution for the cooperative case. Employing their notation the expression for pressure is (Eq. (1012.9))

$$p(\theta)=p^0(\theta/1-\theta)[(2-2\theta)/(\beta+1-2\theta)]^z,$$

where

$$\beta=[1-4\theta(1-\theta)(1-\exp\{-2w/zkT\})]^{1/2}.$$

(The constant p^0 is a reference pressure, not to be confused with p_0, the condensation pressure of the bulk liquid.)

In the case of attractive interaction (negative w) two-dimensional condensation begins at a θ_{conds} which is the smallest root of $p(\theta)=p(1/2)$. It will emerge that the square of this small θ can be neglected. Making this approximation, one finds

$$\theta_{\text{conds}}=\exp\{w/kT\}. \tag{4}$$

Because adsorption takes place on a liquid-like surface, the molal free energy of the completed film equals that of the liquid:

$$\log p_0=\int_0^1 \log p(\theta)d\theta.$$

Fowler and Guggenheim show that $\log p(\theta)/p(1/2)$ is an odd function of $\theta-1/2$. Thus

$$\int_0^1 \log p(\theta)d\theta=\log p(1/2),$$

$$p_0=p(1/2),$$

and therefore two-dimensional condensation begins when $p/p_0=1$, in harmony with the assumption of a liquid-like surface. Below condensation

$$\theta=(p/p_0)\exp\{w/kT\}.$$

Hexagonal packing will be assumed in order to find the value of w. There are six neighbors in a two-dimensional film and twelve in the liquid. Therefore, the energy of interaction in the film is

[3] R. H. Fowler and E. A. Guggenheim, *Statistical Thermodynamics* (Cambridge University Press, Teddington, England, 1939).

approximately $1/2E_L$. The number of pair interactions per molecule is $Z/2$. The energy per pair is $2w/Z$. Therefore, $(2w/Z)(Z/2)=-E_L/2$ and $-w=E_L/2$.

For the adsorption of nitrogen at 77°K, $E_L=1330$ cal./mole. Therefore, θ_{conds} (from Eq. (4)) $=0.015$. Trouton's rule indicates that a similar or smaller value is to be expected for most liquids at or below the boiling point. Thus, below $p/p_0=1$, θ remains below 2 percent coverage, justifying the assumptions that $\theta<1/3$ and that θ^2 can be neglected. Therefore, it appears that instead of observing the BET adsorption indicated by Eq. (2) or even the Langmuir adsorption of Eq. (3), a surface with the above properties is incapable of condensing further layers at any pressure below saturation. One must thus draw the conclusion that on the basis of the BET hypotheses the adsorption for any value of c is actually confined to the amount accommodated in the first layer. Adsorption in the second layer becomes the negligible quantity $\theta_1{}^3 p/p_0 \exp\{w/kT\}$, smaller by a factor $\theta_1{}^3$ than the adsorption on a liquid-like surface.

Discarding the hypothesis that $E_2=E_L$ is not sufficient to restore the BET theory. The treatment of cooperative adsorption can be extended to include surfaces whose adsorption energy is ΔE greater than that of the liquid. Two-dimensional condensation is found to begin at $\theta=\exp\{w/kT\}$ and

$$p/p_0=\exp\{-\Delta E/RT\}. \qquad (5)$$

It is reasonable to assume that w is unchanged by a change in the attraction between the surface and the adsorbed molecule. Thus, the value of θ at which condensation begins is unchanged. A multilayer isotherm based on the hypothesis $E_1>E_2>\cdots>E_L$ must lead to an isotherm composed of a series of steps.

When mobile adsorption is assumed, the results presented above are not altered significantly. If $\log p(\theta)/p(1/2)$ is an odd function of $\theta-1/2$ they are unchanged.

II. MONOLAYER ISOTHERMS

When adsorption data are fitted to the Langmuir equation, it is often found that the apparent maxima of adsorption are a function of temperature. F. J. Wilkins studied the adsorption of nitrogen, argon, and oxygen at temperatures from 77.3°K to 194.5°K.[4]

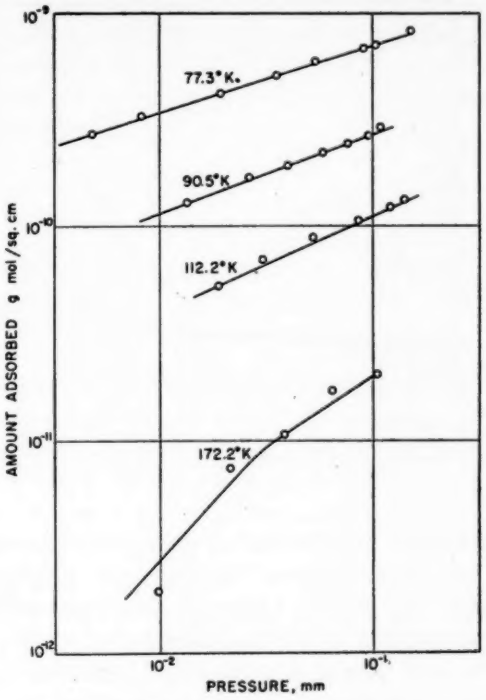

FIG. 2. The adsorption of argon on platinum.

The adsorption isotherms could be fitted by the Langmuir equation in most cases; but $V_{\max}$ varied 10–100 times with temperature. These data form an extreme case of the violation of the Langmuir postulate that the number of sites is constant. Wilkins' theoretical treatment directed at removing this limitation is not valid. He assumes that only a certain fraction of the surface area is available for adsorption, and that the size of this "island" varies continuously with temperature. Clearly, such an assumption presupposes a continuously non-uniform surface.

Contrary to this, Wilkins states (p. 502), "It has been tacitly assumed that the adsorption potential is constant throughout the adsorption volume." This inconsistent assumption allows him to develop the Langmuir equation within the "island."

It should be pointed out in passing that the correction applied to the Clausius-Clapeyron equation proposed by Wilkins, and discussed by

[4] F. J. Wilkins, Proc. Roy. Soc. **A164**, 496 (1938); *ibid.*, 510.

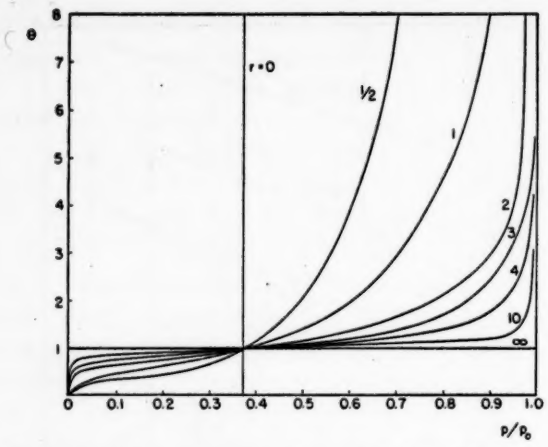

FIG. 3. The isotherm $p/p_0=\exp\{-1/\theta^r\}$ plotted for various values of r.

Armbruster and Austin[5] is erroneous. Corrected for gas imperfections, the equation is thermodynamically sound, as may be easily proven by the application of Gibbsian method.

The rejection of this equation apparently originated in the observation of McBain[6] that because of the varying maxima of adsorption obtained with the Langmuir isotherm, application of the equation was impossible; the answer is that the maxima are only apparent.

Halsey and Taylor have shown that the adsorption of hydrogen on tungsten is explained by a non-uniform surface,[7] characterized by an exponential distribution of adsorption energies. Such a distribution leads to an isotherm identical with the classical Freundlich isotherm. The widespread applicability of the Freundlich isotherm, and its origin in a distribution of adsorption energies are very significant when considered together. Although Zeldowitsh[8] derived the isotherm by an approximate process many years ago, textbooks dismiss it as the middle region of the Langmuir isotherm. Such an explanation can only apply over a limited pressure range while the Freundlich isotherm is often valid over many cycles of $\log p$.

It should be noted that strong repulsive interactions, dismissed on quantitative ground elsewhere,[7] do not lead naturally to the Freundlich law, but to an isotherm of the type $\log p \approx a\theta+b$. In addition, when adsorption takes place on a strongly non-uniform surface, it is quite proper to assume non-interactive adsorption when cooperation would take place on a uniform surface. This situation exists because it is quite reasonable to expect that the sites are so dispersed that the number of neighbors of a given energy is nearly zero. Finally, it will appear later that a distinction between cooperative and non-cooperative adsorption is not possible when the surface is very non-uniform.

Considering the success of the Freundlich plot in the case of hydrogen on tungsten, it is of interest to examine Wilkins' data on platinum in that form. Figures 1 and 2 show the data for nitrogen and argon, respectively. The general similarity to the Frankenburg data for tungsten is immediately apparent; it is as if a section, both with respect to temperature and pressure, were selected from Frankenburg's data.

The general similarity extends to the region of sparse coverage, where the slope on double logarithmic coordinates approaches unity, and the Langmuir equation becomes applicable. To infer from this that the Langmuir equation can also be applied to the high coverage isotherms is in error, because these Langmuir sites represent at most one percent of the total available sites.

When the data are plotted in this manner the achievement of the adsorption "maximum" at the higher temperatures clearly becomes illusory. An increase in pressure must ultimately lead to the total coverage of the surface, but for higher temperatures the pressures may have to become prohibitively large.

M. H. Armbruster's data[9] on the adsorption of gases on silver are similar to those of Wilkins, although considerably less extensive. The isotherms, over the limited range investigated, again conform to the Langmuir equation. The usual discrepancies are noted, however. Saturation maxima are a function of temperature. In fact, only a small fraction of the geometrical surface is covered. Only in the case of oxygen, where chemisorption is involved, does the fraction of

[5] M. H. Armbruster and J. B. Austin, J. Am. Chem. Soc. 66, 159 (1944).
[6] J. W. McBain, *Sorption of Gases and Vapours* (Routledge, London, 1932).
[7] G. Halsey and H. S. Taylor, J. Chem. Phys. 15, 624 (1947); see also R. Sips, J. Chem. Phys. 16, 490 (1948).
[8] J. Zeldowitsh, Acta Physicochimica U.R.S.S. 1, 961 (1934).
[9] M. H. Armbruster, J. Am. Chem. Soc. 64, 2545 (1942).

the geometrical surface covered approach unity. A non-uniform surface is thus indicated.

Armbruster and Austin[5] determined a large number of isotherms for gases on steel. The authors apply the methods of Wilkins to their data. It is pertinent to observe that they find: "The value of v_s [coverage at saturation] increases markedly with decreasing temperature, as is common in systems of this type." The non-uniform surface is again indicated.

Both Armbruster and Austin and Wilkins calculate the adsorption maxima, even when these are not reached, by using the Langmuir equation. It appears that the process might be deceptive. In attempting to discover a suitable isotherm for their data Armbruster and Austin remark "it [the Freundlich isotherm] fits very well over the low pressure range. . . . The equation fails, as it must as the surface approaches saturation." The slight bending over of the isotherm on the Freundlich plot, which the authors take to mean saturation cannot be considered conclusive. In many of the isotherms investigated the geometrical surface of the steel is not yet covered.

III. COOPERATIVE ADSORPTION AND THE FORMATION OF MULTILAYERS

Because on many surfaces the sites of low energy are much more numerous, the importance of cooperative adsorption increases with the progress of adsorption from the high energy sites to those of lower energy. Eventually the number of neighbors being adsorbed simultaneously may become large enough to cause cooperative condensation. If sites of nearly equal energies are localized into patches, this cooperation is facilitated because the number of effective neighbors is increased. Molecules adsorbed side by side but at differing pressures do not constitute neighbors in the cooperative sense because cooperation implies that the molecules influence one another's adsorption. A molecule adsorbed at a high pressure may contribute its energy to improve an adjacent site of lower energy; but, in doing so, it does not influence its own adsorption; it becomes evident that a knowledge of molecular topography is necessary to predict what kind of adsorption will take place.

If the surface is characterized by a distribution function of cooperative adsorption energies $N_{\Delta E}$, the pressure at which the sites with energy ΔE are filled is given by Eq. (5) and the expression for coverage is

$$\theta = \int_{-RT\log p/p_0}^{\infty} N_{\Delta E} d\Delta E.$$

If $N_{\Delta E}$ has the exponential form $c \exp\{-\Delta E/\Delta E_m\}$,

$$\theta = c'(p/p_0)^{RT/\Delta E_m}, \tag{7}$$

analogous to the Freundlich isotherm, which can be derived from the same distribution when interactions are not allowed. The only difference is that in the non-cooperative case the exponent must be less than unity because of the convergence condition $\Delta E_m/RT > 1$. If this condition is met, the two modes of adsorption are indistinguishable, while if $\Delta E_m/RT < 1$, the second derivative is positive, a phenomenon possible only with cooperative effects.

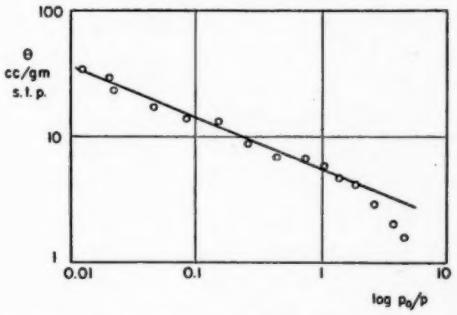

FIG. 4. Adsorption of water on anatase at 25°C plotted according to Eq. (11).

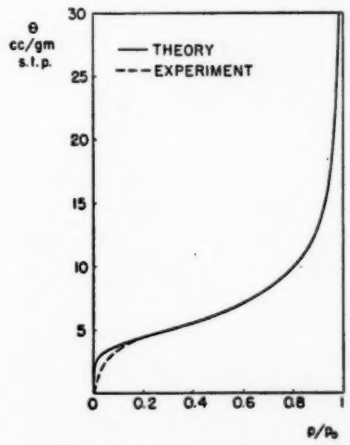

FIG. 5. The isotherm for water on anatase fitted to Eq. (10) with $r = 2.5$.

It is interesting to note that not only the Langmuir and the step-condensation isotherms lead to the Freundlich law when an exponential distribution is used. The isotherm $p(\theta)=\varphi(\theta)\exp\{-\Delta E/RT\}$ where $\varphi(\theta)$ is any function of θ independent of ΔE will lead to the same isotherm.

Owing to the neglect of the sites provided by the previously adsorbed gas, the generalized Freundlich isotherm does not approach $\theta=\infty$ at $p/p_0=1$. A modified treatment can provide for this situation. At some distance, x, from the surface, assume that the van der Waals energy ΔE falls off according to a law $E=\chi'(x)$. Now the volume adsorbed is proportional to the depth of the layer, so the energy can be written $E=\chi(\theta)$. Using Eq. (4), the isotherm becomes

$$p/p_0=\exp\{-\chi(\theta)/RT\}. \tag{8}$$

For the specific law $\Delta E=a\theta^{-r}$ the isotherm obtained is

$$p/p_0=\exp\{-a/RT\theta^r\}. \tag{9}$$

This equation not only satisfies the above requirements but is of general utility and it will be discussed in detail below.

The typical experimental isotherm can be divided into three parts. The first part consists of adsorption without cooperation on the more active parts of the surface, described in Part II. Secondly, a cooperative adsorption takes place on the still heterogeneous surface resulting from the initial adsorption. A certain amount of this subsequent adsorption takes place on bare surface, the remainder on the surface of the previously adsorbed gas, under the influence of transmitted van der Waals forces. In general, enough molecules are being adsorbed at once when $\Delta E\sim RT$ (or $p/p_0=1/e$) to allow cooperation. A clear

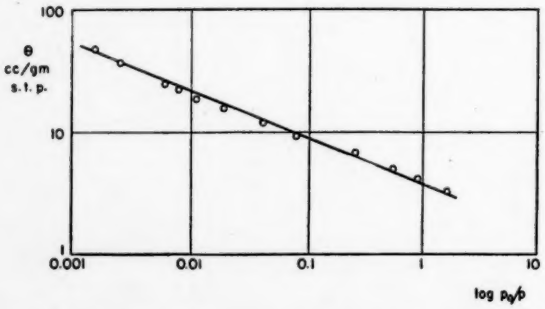

FIG. 6. Adsorption of nitrogen on anatase at −197°C fitted from $p/p_0=0.0026$ to 0.9936 by $r=2.67$.

manifestation of cooperation is a positive $d^2\theta/dp^2$. In the pressure region near condensation, the third part of the isotherm begins—a cooperative multilayer condensation under the influence of the weak van der Waals field transmitted from the surface. The intense forces acting at large distances required by the old potential theory are not needed, because only a small fraction of RT causes two-dimensional condensation at pressures near $p/p_0=1$, when the perturbation is added to the E_L provided by cooperation.

The three regions into which isotherms can be divided are not necessarily all manifest in a given isotherm; in the BET "type III" isotherm, where $d^2\theta/dp^2$ is always positive, the first region is missing. In Type I only the first portion is apparent. W. J. C. Orr's[10] adsorption isotherms for non-polar gases on KCl show the three regions nicely separated. Thus argon at 79.35°K is adsorbed without cooperation on a heterogeneous surface until pressure reaches 1.5 cm. Here an inflection point is reached, and cooperative adsorption begins. That this adsorption takes place on a limited surface is shown by its reaching an apparent saturation. This is followed by a second inflection point leading to multilayers and condensation. Nitrogen and oxygen behave similarly.

The calculated heat curves confirm this interpretation. The heat declines during the non-cooperative adsorption; it passes through a minimum and begins to increase as cooperative adsorption takes place. It reaches a maximum and declines as the monolayers add out into space.

It is to be emphasized that the explanation of any of the experimental isotherms in the BET classification (Types I to V) invokes the presence of a non-uniform surface. Paradoxically enough, the obeying of the Langmuir isotherm is frequently a positive indication that the surface is non-uniform enough to make cooperative adsorption impossible. It is for this reason that the Langmuir isotherm is most successful when it treats adsorption (most often chemisorption) where only a small fraction of the surface is available for adsorption.

IV. A WORKING ISOTHERM

It is apparent that an isotherm equation embracing all the possibilities discussed above would

[10] W. J. C. Orr, Proc. Roy. Soc. **173**, 349 (1939).

be too complex to have utility. On the other hand, many of the data of adsorption have a simplicity that allows them to be fitted to an expression with two parameters.

Equation (9) was developed to provide an expression for condensation of multilayers at a relatively large distance from the surface. Strictly speaking, close to the surface it should be replaced by a series of steps. However, the nonuniform nature of the surface smooths out these steps and makes the equation approximately valid beyond the first layer. At a coverage less than one monolayer, the concept of the field decaying with distance is replaced by the distribution function of adsorption energy that leads to an equivalent isotherm. This distribution corresponds to a strongly heterogeneous surface where the cooperative adsorption implied in the derivation is not distinguishable from noncooperative adsorption.

This situation arises because, in general, when a distribution is wide enough, the functional form of the isotherm for adsorption at a given energy does not influence the form of the isotherm integrated over all values of the adsorption energy.

A considerable adsorption takes place near $p/p_0=0$, giving rise to an "initial" adsorption characteristic of the "Type II" isotherm. If adsorption is measured in multiples of the adsorption at $p/p_0=1/e$ the isotherm takes the form

$$p/p_0=\exp\{-\theta^{-r}\}, \qquad (10)$$

with an inflection at $p/p_0=\exp\{-r+1/r\}$ and $\theta=(r/1+r)^{1/r}$. Equation (10) is plotted in Fig. 3 for various values of r. As r decreases, the point of inflection moves toward the origin, and the isotherms assume the "Type III" form. As r increases, they take on a "Type I" shape.

Using an empirical equation of state for a condensed monolayer, Harkins and Jura[11] have derived the isotherm

$$\log p/p_0=A/v_0^2-B/v^2,$$

where v is the volume of gas adsorbed at p, and v_0 the volume at p_0. In the absence of capillaries, $v_0=\infty$, and the equation becomes $p/p_0=\exp\{-B/V^2\}$. This is a special case of Eq. (10), with $r=2$. Hence, the Harkins-Jura equation of state corresponds to a model in which the attraction of the interface falls off with the second power of the distance. When transformed by the Gibbs adsorption formula, Eq. (10) yields the generalized equation of state

$$\pi=a-b\sigma^{r-1}.$$

For purposes of curve fitting, Eq. (10) is put in the form

$$\log\log(p_0/p)=r\log\theta, \qquad (11)$$

and the constant r evaluated from the slope. In Fig. 4 the data of Harkins and Jura for the adsorption of water on anatase are so plotted. Equation (11) is valid between $p/p_0=0.2$ and 0.98. The fitted isotherm (Fig. 5) shows the extent of the deviation, with $r=2.5$. Figure 6 shows the data for nitrogen on anatase plotted according to Eq. (11), with $r=2.67$. Agreement extends from $p/p_0=0.0026$ to 0.9936.

The data of Boyd and Livingston[12] show a wide variation of the constant r in different isotherms. Estimating from their published curves, r has a value of about 6 for the adsorption of propyl alcohol on anatase, and at least 15 for the same vapor on $BaSO_4$. On the other hand, for the adsorption of water on graphite r is about unity.

If r is very large, the attraction of the solid for the vapor is very specific and does not extend far from the surface. When r is smaller, the forces are more typically van der Waals and are able to act at a greater distance. The magnitude of r characterizes the type of interaction between a vapor and a solid.

Note added in proof: The BET surface area determination has not been discussed here. Despite the unreality of the isotherm equation, the nitrogen areas seem completely satisfactory; the reasons will be discussed elsewhere.

ACKNOWLEDGMENTS

The author is indebted to Dr. J. R. Arnold, Dean Hugh S. Taylor, and Professor G. B. Kistiakowsky for many valuable suggestions.

[11] W. D. Harkins and G. Jura, J. Am. Chem. Soc. 66, 1366 (1944).

[12] G. E. Boyd and H. K. Livingston, J. Am. Chem. Soc. 64, 2383 (1942).

THE JOURNAL OF CHEMICAL PHYSICS VOLUME 16, NUMBER 10 OCTOBER, 1948

Steric Effects. II. General Equations. Application to *Cis*- and *Trans*-2-Butene

TERRELL L. HILL
Department of Chemistry, University of Rochester, Rochester, New York
(Received February 12, 1948)

Steric energy and the semi-empirical method of calculating steric energy are discussed in the language of potential surfaces. Equations are given relating ΔH_0^0 for several types of reactions commonly used to exhibit steric effects experimentally to the steric energy of the molecules involved in the reactions. The equations of Westheimer and Mayer for the calculation of the steric energy of a molecule are generalized in several respects. The difference in ΔH_0^0 (formation) between *cis* and *trans*-2-butene is calculated as a steric effect. Because of various complications the application of the method in its present form to molecules such as H_2O, NH_3, PF_3, etc., is rather unsatisfactory.

I. INTRODUCTION

WESTHEIMER and Mayer[1] and the present author[2] suggested independently a semi-empirical method (method 1, below) for the theoretical investigation of steric effects. The method can be applied without modification to both equilibrium and rate studies, and also to problems in molecular structure without reference to any particular reaction. Westheimer[3] has applied the method in calculating the activation energy for the racemization of 2,2′-dibromo-4,4′-dicarboxydiphenyl.

The purpose of the present series of papers is to investigate this approach to steric effects from as general a point of view as seems profitable at the present time. In paper I of the series[4] a necessary prerequisite study of van der Waals potential energy curves was carried out, and an approximate method of extrapolating our limited knowledge of these curves to new cases was suggested. In this paper (II) we shall discuss the general method and give some applications to molecules. In a proposed third paper, applications to a few chemical reactions will be presented, including some of the cases investigated experimentally by H. C. Brown.[5] The relation between the present point of view and Brown's concepts of *B* and *F* strain will be discussed.

The word "steric" is used generally to refer to van der Waals effects (especially repulsions). In most of the applications we have in mind, van der Waals repulsions indeed play a dominant role, but in some cases electrostatic effects are also involved. For convenience we shall often use the words "steric" or "interaction" to include electrostatic effects. As a matter of fact pure electrostatic effects can also be treated by the present method, with appropriate alteration in the equations. However, structural deformations will be small if not negligible here (they have always been ignored hitherto), because V (see below) varies so slowly with distance.

The Method

Consider a certain molecule A with n atoms and in which, in the equilibrium configuration, there are appreciable steric interactions between two or more non-bonded atoms (or groups). In principle it is possible to calculate from quantum mechanics the shape of the potential surface (potential energy U plotted against $3n-6$ or $3n-5$ vibrational coordinates) in the neighborhood (as extensive as necessary) of the configuration of minimum energy (equilibrium configuration) and also the value of the minimum energy referred to infinite separation of atoms as the zero of energy.[6a] Now suppose the calculation is repeated, omitting the contribution V to the

[1] F. H. Westheimer and J. E. Mayer, J. Chem. Phys. **14**, 733 (1946).
[2] T. L. Hill, J. Chem. Phys. **14**, 465 (1946).
[3] F. H. Westheimer, J. Chem. Phys. **15**, 252 (1947). See also I. Dostrovsky, E. D. Hughes, and C. K. Ingold, J. Chem. Soc. 173 (1946).
[4] T. L. Hill, J. Chem. Phys. **16**, 399 (1948).
[5] See, for example, H. C. Brown, J. Am. Chem. Soc. **69**, 1137 (1947); *ibid.* **67**, 378 (1945).

[6a] If the molecule under discussion happens to be an activated complex it is to be understood that the words "equilibrium" and "minimum" are to be replaced by "saddle-point," and that the reaction coordinate is to be omitted in calculating zero-point vibrational energy and thermodynamic functions.

potential energy caused by the interactions between the atoms (or groups) mentioned above. This will lead to a new potential surface ${}^0U$ corresponding to a hypothetical molecule ${}^0A$. If the normal coordinates of A and ${}^0A$ are now obtained using the shapes of the potential surfaces near their respective minima, the minimum (equilibrium) energies may be corrected for zero-point vibrational energy. The steric energy E associated with the particular interactions omitted in the ${}^0A$ calculation is then defined as the difference between the two equilibrium energies corrected for zero-point vibrational energy (Fig. 1). Let E' be the uncorrected steric energy. It is clear from the definition of steric energy that this energy is, to some extent, (a) arbitrary (it depends on which interactions are chosen) and (b) artificial (in a complete quantum-mechanical calculation for the molecule A the energy E does not enter in a natural way).

The surface V in Fig. 1 represents the potential energy of interaction between the atoms (or groups) being considered, as a function of nuclear configuration. A procedure for obtaining the surface ${}^0U$ may be represented by $U-V\rightarrow{}^0U$. It is also possible to find U from ${}^0U$ and V: ${}^0U+V\rightarrow U$. In fact, these procedures are the basis of the method used here for computing steric energies: although the quantum-mechanical calculations are, with rare exceptions,[6b] not possible in practice, such calculations may be replaced by a semi-empirical calculation based on the procedure (1) ${}^0U+V\rightarrow U$ or on (2) $U-V\rightarrow{}^0U$.

Method 1

In many cases the equilibrium configuration of ${}^0A$ and the shape (but, in general, not the absolute energy) of the potential surface in the immediate neighborhood of the equilibrium configuration of ${}^0A$ can be obtained from experimental data in related compounds. Thus the equilibrium configuration can be deduced from known structures of similar molecules unperturbed by the steric interaction or interactions being studied, and the shape of the potential surface can be calculated using force constants[7a] found for other appropriate molecules. If now for each interaction the interaction energy is available as a function of distance, one can carry out the procedure ${}^0U+V\rightarrow U$, and hence find the steric energy E, provided that the equilibrium configurations of A and ${}^0A$ are not too far apart. For in having to use force constants we obtain information concerning the shape of the potential surface for ${}^0A$ to quadratic terms only.

Physically, the point of view is the following. If the steric interactions are introduced into the hypothetical unperturbed molecule ${}^0A$, the interacting atoms or groups will tend to move apart (for repulsions). But this will generally require the stretching or bending of bonds with a related increase in energy. The final configuration will thus be the result of a compromise between the two types of force, and will be the configuration of minimum energy (the equilibrium configuration of A). An analogous discussion of method 2 can be given.

Method 2

In other cases it may be desirable, assuming the quantum-mechanical calculation is impossible, to use V and the experimental force constants for A itself in order to calculate E by the process $U-V\rightarrow{}^0U$. Again we have to restrict ourselves to cases in which the equilibrium configurations of A and ${}^0A$ are not too different.

Method 1 above is the most useful in connection with steric effects on chemical equilibrium

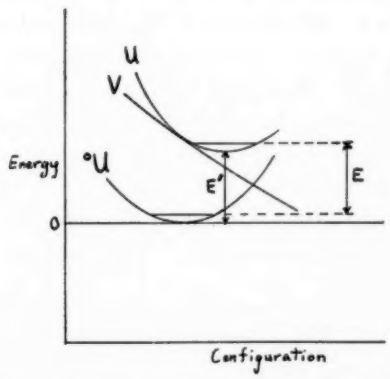

FIG. 1. Plot of energy against configuration.

[6b] An approximate calculation of essentially this type has been carried out for H_2O. See J. H. Van Vleck and P. C. Cross, J. Chem. Phys. **1**, 357 (1934).

[7a] Force constants obtained on the assumption of valence forces (with or without cross products) will be most convenient.

because such effects are usually exhibited experimentally in complicated molecules for which force constants (for the molecule A with the steric interaction) are not yet available. Force constants for the unperturbed molecule ${}^0A$ can usually be taken from simpler molecules. In rate studies method 1 is most convenient to use on the activated complex since force constants will, of course, not be available for this structure.[7b] On the other hand, method 2 is probably the most natural to use for investigations on steric energy and molecular structure in simple molecules for which force constants are available. In the present paper method 1 is emphasized.

In Section II we give a rather formal but necessary discussion of the application of the method to chemical reactions. The problem reduces essentially to the determination of the steric energy of individual molecules. In Section III we consider the calculation of the steric energy of a molecule, and give an application to *cis*- and *trans*-2-butene. Molecules such as H_2O, NH_3, F_2O, etc., are discussed from the present point of view in the appendix.

II. APPLICATION TO REACTIONS

We shall use the language of chemical equilibrium here, but the discussion applies without alteration to reaction rates by considering, in the usual way, the activated complex as a product in a chemical equilibrium.

It involves much less labor to find merely the energy difference between the minima in the potential surfaces for A and ${}^0A$ than to obtain, in addition, the shapes of the potential surfaces and the normal coordinates and vibrational frequencies. We shall confine our interest here to obtaining this energy difference. This restricts our investigation of chemical reactions to steric effects on $\Delta H_0{}^0$ for the reactions, and even here making the approximation of neglecting zero-point vibrational energies[8] (that is, we use E' as an approximation to E; see Fig. 1). It should be emphasized, however, that the calculation of the vibrational frequencies of ${}^0A$ and A is straightforward in principle and hence it is not only possible to correct for zero-point vibrational energy but also to obtain the entropy difference between ${}^0A$ and A at any temperature. This is the way in which steric entropy effects would have to be investigated using the present method.[1]

Experimental studies on steric effects are usually carried out as a comparison method. A related standard molecule A_0 undergoes the same reaction as A. If possible A_0 is chosen so that the steric interaction of interest in A is negligible in A_0. Differences in rate constant, equilibrium constant or ΔH are then attributed to the steric interaction. We shall formulate our equations making use of this procedure. To simplify notation we now let Q stand for $H_0{}^0$. Our object is to relate ΔQ for a given reaction to the steric energies of the substances entering the reaction. Or, where necessary, we take differences in ΔQ values in order to relate the ΔQ's to steric energies.

In the following outline we do not attempt to achieve complete generality; the purpose is simply to include the important cases. Further extensions are rather self-evident.

A. Equilibrium between Rotational or Structural Isomers

This is the simplest type of equilibrium of interest here. By rotational isomers we mean two compounds which can go over into one another by rotation about bonds (e.g., two geometrical isomers, or a substituted diphenyl and the activated complex in the racemization reaction). By structural isomers we mean here (a restricted definition) two compounds which differ only in the location of some substituent (e.g., 2-picoline and 4-picoline).

Let A be the isomer in which the steric interaction (or interactions) is most important. Consider the other isomer as the standard, A_0. Then for the equilibrium $A_0 \rightleftarrows A$ we have

$$\Delta Q = Q_A - Q_{A_0}. \tag{1}$$

We now remove the *same* interactions in A and

[7b] The introduction of the saddle-point property into ${}^0U$ may sometimes be awkward. Because of the special nature of the reaction coordinate in Westheimer's case,[3] this complication did not arise.

[8] In most cases the zero-point vibrational energies should largely cancel. One exception is a reaction involving an activated complex, since one vibrational frequency is missing here. The cancellation is especially effective where one takes first and second differences in $\Delta H_0{}^0$ values in comparing related reactions (see below).

A_0, obtaining ${}^0A$ and ${}^0A_0$ with energies ${}^0Q_A$ and ${}^0Q_{A_0}$. The steric energies (associated with the particular interactions removed) E_A and E_{A_0} are

$$E_A = Q_A - {}^0Q_A, \quad E_{A_0} = Q_{A_0} - {}^0Q_{A_0}. \tag{2}$$

Then

$$\Delta Q = (E_A - E_{A_0}) + ({}^0Q_A - {}^0Q_{A_0}). \tag{3}$$

In general, in deciding which interactions are to be removed in A and A_0, we choose those and only those whose removal are necessary in order to lead to ${}^0A$ and ${}^0A_0$ having all remaining interaction energies the same (to the accuracy desired). In the case of rotational isomers corresponding force constants in ${}^0A$ and ${}^0A_0$ should then be nearly equal and also ${}^0Q_A = {}^0Q_{A_0}$ to a very good approximation (since all bonds are of the same type and all distinguishing interactions have been removed). The normal coordinates and vibrational frequencies of ${}^0A$ and ${}^0A_0$ will, however, be different owing to different geometry. These approximations should also be valid, though somewhat less so, for structural isomers (e.g., resonance and inductive effects may complicate matters, especially in aromatic compounds). Hence, for these cases,

$$\Delta Q = E_A - E_{A_0}. \tag{4}$$

An important special case of the above is the following: the interactions of importance in A cause no appreciable effect on A_0 on their removal from this latter molecule. That is, ${}^0A_0 = A_0$ (structure) and ${}^0Q_{A_0} = Q_{A_0}$. Hence, $E_{A_0} = 0$, and Eq. (4) becomes

$$\Delta Q = E_A. \tag{5}$$

The case studied by Westheimer[3] is of this type.

Another special case: on the removal of the important interactions in A, corresponding force constants in ${}^0A$ and A_0 are taken as being approximately equal, but we do *not* assume ${}^0Q_A = Q_{A_0}$ (this is an approximate method; strictly speaking the two assumptions just mentioned are probably inconsistent in most cases). We use the exact equation

$$\Delta Q = E_A + ({}^0Q_A - Q_{A_0}), \tag{6}$$

but the evaluation of E_A and ${}^0Q_A - Q_{A_0}$ involves approximations. This method is used in Section III in calculating ΔQ for the equilibrium between *cis*- and *trans*-2-butene and will be further discussed there.

B. Other Reactions Involving Rotational and Structural Isomers

Here the same reaction is studied on both isomers for comparison purposes. For example, the addition of $B(CH_3)_3$ to 2-picoline and to 4-picoline, or the rate of esterification of ortho and paramethyl benzoic acid. Let the reactions be (this is sufficiently general for our purposes)

$$\begin{aligned} A + B &\rightleftarrows C + D;\ \Delta Q, \\ A_0 + B &\rightleftarrows C_0 + D;\ \Delta Q_0. \end{aligned} \tag{7}$$

Then

$$\Delta Q - \Delta Q_0 = (Q_C - Q_{C0}) - (Q_A - Q_{A_0}). \tag{8}$$

In analogy with Eq. (3) we have

$$\begin{aligned} \Delta Q - \Delta Q_0 = {} & (E_C - E_{C_0}) - (E_A - E_{A_0}) \\ & + ({}^0Q_C - {}^0Q_{C_0}) - ({}^0Q_A - {}^0Q_{A_0}), \end{aligned} \tag{9}$$

where the interactions used in obtaining E_C and E_{C_0} may be different than those used in obtaining E_A and E_{A_0}. As before, we put ${}^0Q_C - {}^0Q_{C_0} = 0$ and ${}^0Q_A - {}^0Q_{A_0} = 0$[9] so that

$$\Delta Q - \Delta Q_0 = (E_C - E_{C_0}) - (E_A - E_{A_0}). \tag{10}$$

Thus first differences in ΔQ values are necessary in reactions of this type to exhibit a steric effect.

An important special case is $E_A = E_{A_0} = 0$.

C. Reactions Involving Different Substituents

Consider reactions of the type

$$\begin{aligned} AX + B &\rightleftarrows CX + D;\ \Delta Q, \\ AH + B &\rightleftarrows CH + D;\ \Delta Q_0, \end{aligned} \tag{11}$$

where H is a substituent with a small or negligible steric interaction (e.g., hydrogen) for comparison, and X is a substituent with considerable steric interaction. X and H are substituted into identical positions in AX and AH, and in CX and CH. Examples are (a) the rate of esterification of benzoic acid compared to *o*-methyl benzoic acid, (b) the dissociation equilibrium of benzoic acid as an acid compared to *o*-methyl benzoic acid, and (c) the addition of $B(CH_3)_3$ to NH_3 as compared to CH_3NH_2.

---

[9] The two separate assumptions are not necessary. It is obviously sufficient to make the single assumption ${}^0Q_C - {}^0Q_{C_0} = {}^0Q_A - {}^0Q_{A_0}$, which should be even more exact.

Let $A_0=AH$, $A_1=AX$, $C_0=CH$, and $C_1=CX$. Then, as for Eq. (9), we find

$$\Delta Q-\Delta Q_0=(Ec_1-Ec_0)-(E_{A_1}-E_{A_0})+({}^0Qc_1-{}^0Qc_0)-({}^0Q_{A_1}-{}^0Q_{A_0}). \quad (12)$$

Here we cannot assume ${}^0Qc_1={}^0Qc_0$ and ${}^0Q_{A_1}={}^0Q_{A_0}$ because there are different bonds and therefore bond energies involved (the force constants will also be different). However, in many cases it will still be a very good assumption to set ${}^0Qc_1-{}^0Qc_0={}^0Q_{A_1}-{}^0Q_{A_0}$ since the *differences* in bond energies will often be effectively the same in the two pairs of compounds (e.g., in the benzoic acid examples above, except for small resonance and inductive effects). In these cases

$$\Delta Q-\Delta Q_0=(Ec_1-Ec_0)-(E_{A_1}-E_{A_0}). \quad (13)$$

First differences in ΔQ values are thus sufficient here.

In other reactions, as, for example, the addition of $B(CH_3)_3$ to NH_3 and to CH_3NH_2, it would not be safe to assume that Eq. (12) reduces approximately to Eq. (13). In this case the *type* of bond is different in A_0 and A_1 as compared to C_0 and C_1, and hence the energy differences ${}^0Qc_1-{}^0Qc_0$ and ${}^0Q_{A_1}-{}^0Q_{A_0}$ may be appreciably different. It is necessary in this case and related cases to use *second* differences in ΔQ values. Thus, Brown[5] has studied

$$\begin{aligned} &NH_3(A_0)+B(CH_3)_3(B)\rightleftarrows H_3N{:}B(CH_3)_3(C_0);\ \Delta Q_0\\ &CH_3NH_2(A_1)+B(CH_3)_3(B)\rightleftarrows CH_3H_2N{:}B(CH_3)_3(C_1);\ \Delta Q_1\\ &(CH_3)_2NH(A_2)+B(CH_3)_3(B)\rightleftarrows (CH_3)_2HN{:}B(CH_3)_3(C_2);\ \Delta Q_2. \end{aligned} \quad (14)$$

We have

$$\begin{aligned} &(\Delta Q_2-\Delta Q_1)-(\Delta Q_1-\Delta Q_0)\\ &\quad=[(Ec_2-Ec_1)-(Ec_1-Ec_0)]\\ &\qquad-[(E_{A_2}-E_{A_1})-(E_{A_1}-E_{A_0})]\\ &\qquad+\{[({}^0Qc_2-{}^0Qc_1)-({}^0Qc_1-{}^0Qc_0)]\\ &\qquad-[({}^0Q_{A_2}-{}^0Q_{A_1})-({}^0Q_{A_1}-{}^0Q_{A_0})]\}. \end{aligned} \quad (15)$$

It is now a good approximation to set $\{\ \}=0$ in Eq. (15), for even the separate expressions in square brackets in $\{\ \}$ should be approximately equal to zero.

In all of the above reactions the problem has thus been reduced to the calculation of the steric energy in individual molecules. This calculation has been discussed in Section I and will be discussed further in Section III. It will be noted that the question of *method 1-vs.-method 2* examined in Section I has not arisen in the present section since we have been interested in formal relations between ΔQ values and steric energies without considering methods of calculating these steric energies.

We have ignored solvent effects above, and we do so throughout the paper. The equations derived are therefore most appropriate for gaseous reactions, but they should also apply, to varying degrees of approximation, to reactions in solution. Van der Waals interactions are presumably relatively insensitive to solvent effects compared to electrostatic interactions. Also, in most cases, the solvent should have only a small perturbing effect on internal molecular vibrations. In any case, practically nothing fundamental is known about solvent effects, so there is little choice here but to ignore them.

In most actual cases the experimental data are at best in the form of ΔH^0 values and not ΔQ.[10] The usually difficult calculation of ΔH^0 from ΔQ can in principle be carried out using the potential surfaces. The alternative is to assume that differences between ΔH^0 and ΔQ values cancel. We illustrate this for only one case: Referring to Eq. (10) we have [11]

$$\Delta H^0-(\Delta H^0)_0=(\Delta Q-\Delta Q_0)+\{(\Delta H^0-\Delta Q)-[(\Delta H^0)_0-\Delta Q_0]\}. \quad (16)$$

Although $\Delta H^0\neq\Delta Q$ and $(\Delta H^0)_0\neq\Delta Q_0$, in most cases it is probably a good approximation to write

$$\Delta H^0-\Delta Q=(\Delta H^0)_0-\Delta Q_0.$$

Then

$$\Delta H^0-(\Delta H^0)_0=\Delta Q-\Delta Q_0=(E_C-Ec_0)-(E_A-E_{A_0}). \quad (17)$$

Thus, when first, or especially when second,

[10] In rate studies there is ordinarily available the experimental activation energy E_{exp} defined by $d\ln k/dT=E_{exp}/RT^2$. See Glasstone, Laidler, and Eyring, *Theory of Rate Processes* (McGraw-Hill Book Company, Inc., New York, 1941), pp. 197–199. See also footnote 12 of paper I.

[11] In these equations the symbol $(\Delta H^0)_0$ represents the value of ΔH^0 for the reference reaction, in conformity with our notation. It is *not* to be confused with ΔH_0^0.

differences in ΔQ values are used the above approximation may be a good one (see also footnote 8).

III. APPLICATION TO MOLECULES

The principal point of this section is to generalize somewhat the equations of Westheimer and Mayer[1] and to apply the results to *cis*- and *trans*-2-butene as an example. We follow the notation of Westheimer and Mayer as closely as possible.

Let a set of $3n-6$ or $3n-5$ coordinates q_i represent displacements from the equilibrium configuration of ${}^0A$. If we choose the zero of energy as the bottom of the ${}^0A$ potential surface (Fig. 1), we have

$$U(q)=\tfrac{1}{2}\sum a_{ij}q_iq_j+V(q) \quad (a_{ij}=a_{ji}) \quad (18)$$

as the expression giving the shape of the potential surface for A, provided the equilibrium configurations of A and ${}^0A$ are not too different, where $V(q)$ is the steric interaction energy and the a_{ij} are unperturbed force constants. V depends on one or more interatomic or intergroup distances, and these in turn depend on the q_i. The minimum in U is determined by setting $\partial U/\partial q_i=0$ $(i=1, 2, \cdots)$. Suppose the minimum occurs at $q_i=q_i^0$ $(i=1, 2, \cdots)$. Then

$$E'=U(q^0)=\tfrac{1}{2}\sum a_{ij}q_i^0q_j^0+V(q^0). \quad (19)$$

Let another set of coordinates η_i represent displacements from the equilibrium configuration of A. Let ${}^0U$ be the potential energy of ${}^0A$. Then

$${}^0U(\eta)=E'+\tfrac{1}{2}\sum\alpha_{ij}\eta_i\eta_j-V(\eta) \quad (\alpha_{ij}=\alpha_{ji}), \quad (20)$$

where the α_{ij} are perturbed force constants. The minimum in ${}^0U$ is determined by $\partial{}^0U/\partial\eta_i=0$ $(i=1, 2, \cdots)$. Suppose the minimum occurs at $\eta_i=\eta_i^0$ $(i=1, 2, \cdots)$. Then ${}^0U(\eta^0)=0$ (our choice of the zero of energy) and

$$-E'=\tfrac{1}{2}\sum\alpha_{ij}\eta_i^0\eta_j^0-V(\eta)^0. \quad (21)$$

Equations (19) and (21) show how to calculate E' by methods (1) and (2), respectively. On adding these two equations one gets

$$V(\eta^0)-V(q^0)=\tfrac{1}{2}(\sum\alpha_{ij}\eta_i^0\eta_j^0+\sum a_{ij}q_i^0q_j^0), \quad (22)$$

a relation which might be used to obtain some information about V if both equilibrium configurations and both sets of force constants are known.

The general relationship of U to ${}^0U$ is summarized by:

$$\begin{aligned} U(q)&=\tfrac{1}{2}\sum a_{ij}q_iq_j+V(q)=E'+\tfrac{1}{2}\sum\alpha_{ij}\eta_i\eta_j,\\ {}^0U(q)&=E'+\tfrac{1}{2}\sum\alpha_{ij}\eta_i\eta_j-V(\eta)=\tfrac{1}{2}\sum a_{ij}q_iq_j. \end{aligned} \quad (23)$$

We now give explicit equations for calculating E' based on Eq. (19) (method 1). In the treatment of Westheimer and Mayer[1] cross products were not allowed in the potential function. They pointed out that although the coordinates chosen were to be such that cross products did not appear, for the calculation of E' these coordinates need not be normal coordinates (i.e., the kinetic energy need not be diagonalized). We shall derive the slightly more complicated equations here for the case where cross products in the potential energy are permitted. The use of these more complicated equations entails much less labor in many cases (e.g., the application treated at the end of this section) than would be involved in the diagonalization of the potential energy.

Westheimer and Mayer[1] included only a repulsive term of the form $P\exp(-d/\rho)$ in $V(q)$, where d is an interatomic or intergroup distance. In paper I an attractive term was introduced. Let us consider first the case where there is just one steric interaction and

$$V=P\exp(-d/\rho)-(\mu/d^6), \quad (24)$$

so that

$$U(q)=\tfrac{1}{2}\sum a_{ij}q_iq_j+P\exp(-d/\rho)-(\mu/d^6). \quad (25)$$

Here P, ρ, and μ are parameters discussed in detail in paper I. Let d_0 be the distance between the interacting atoms or groups in the equilibrium configuration of ${}^0A$. We are already restricted to cases where there is a small change in configuration on the introduction of the steric interaction into ${}^0A$ (because of the inclusion of only quadratic terms in Eq. (19)), so we include only linear terms in the expansion of d about d_0:

$$d=d_0+\sum b_iq_i. \quad (26)$$

Let $P\exp(-d_0/\rho)=Ed_0$. Then

$$\frac{\partial U}{\partial q_k}=-\frac{b_k}{\rho}Ed_0\exp\left(-\frac{1}{\rho}\sum b_iq_i^0\right)+\frac{6\mu b_k}{(d_0+\sum b_iq_i^0)^7}+\sum_j a_{jk}q_j^0=0 \quad (k=1, 2, \cdots). \quad (27)$$

Define

$$Z=E_{d_0}\exp\left(-\frac{1}{\rho}\sum b_i q_i^0\right)-\frac{6\mu\rho}{(d_0+\sum b_i q_i^0)^7}. \quad (28)$$

Eq. (27) becomes

$$\sum_i a_{jk}q_j^0=\frac{b_k}{\rho}Z \quad (k=1, 2, \cdots). \quad (29)$$

On solving this set of linear equations for q_k^0 we get

$$q_k^0=\frac{Z}{\rho}\frac{D_k}{D}, \quad (30)$$

where

$$D=|a_{ij}|=\begin{vmatrix} a_{11} & a_{21} & \cdots \\ a_{12} & a_{22} & \cdots \\ \cdot & & \\ \cdot & & \\ \cdot & \cdot & \cdots \end{vmatrix}, \quad (31)$$

and D_k is the determinant obtained by replacing the k-th column $a_{k1}, a_{k2}, \cdots$ in D by $b_1, b_2, \cdots$. On substituting Eq. (30) into Eq. (28) we have

$$Z=E_{d_0}\exp\left(-\frac{Z}{\rho^2 D}\sum b_i D_i\right) - \frac{6\mu\rho}{\left(d_0+\frac{Z}{\rho D}\sum b_i D_i\right)^7}. \quad (32)$$

This equation can be solved numerically for Z. Finally, from Eqs. (25) and (30),

$$E'=E_{d_0}\exp\left(-\frac{Z}{\rho^2 D}\sum b_i D_i\right)-\frac{\mu}{\left(d_0+\frac{Z}{\rho D}\sum b_i D_i\right)^6} +\tfrac{1}{2}\frac{Z^2}{\rho^2 D^2}\sum a_{ij}D_i D_j. \quad (33)$$

Two or more interactions. If there are two interactions of the above type in the molecule, we have

$$U(q)=\tfrac{1}{2}\sum a_{ij}q_i q_j+P\exp(-d/\rho) -\frac{\mu}{d^6}+P'\exp(-d'/\rho')-\frac{\mu'}{d'^6}, \quad (34)$$

where $d'=d_0'+\sum b_i' q_i$. On setting $\partial U/\partial q_k=0$ $(k=1, 2, \cdots)$, one finds

$$q_k^0=\frac{Z}{\rho}\frac{D_k}{D}+\frac{Z'}{\rho'}\frac{D_k'}{D}, \quad (35)$$

where

$$Z'=E_{d_0'}\exp\left(-\frac{1}{\rho'}\sum b_i' q_i^0\right) -\frac{6\mu'\rho'}{(d_0'+\sum b_i' q_i^0)^7}, \quad (36)$$

and D_k' is obtained from D by using the b_i' instead of the b_i. Putting Eq. (35) into Eqs. (28) and (36) one obtains

$$Z=E_{d_0}\exp\left(-\frac{Z}{\rho^2 D}\sum b_i D_i\right) \times\exp\left(-\frac{Z'}{\rho\rho' D}\sum b_i D_i'\right) -\frac{6\mu\rho}{\left(d_0+\frac{Z}{\rho D}\sum b_i D_i+\frac{Z'}{\rho' D}\sum b_i D_i'\right)^7}, \quad (37)$$

$$Z'=E_{d_0'}\exp\left(-\frac{Z'}{\rho'^2 D}\sum b_i' D_i'\right) \times\exp\left(-\frac{Z}{\rho\rho' D}\sum b_i' D_i\right) -\frac{6\mu'\rho'}{\left(d_0'+\frac{Z'}{\rho' D}\sum b_i' D_i'+\frac{Z}{\rho D}\sum b_i' D_i\right)^7}. \quad (38)$$

These two equations must be solved numerically and simultaneously for Z and Z'. Finally, one

finds

$$E' = E_{d_0} \exp\left(-\frac{Z}{\rho^2 D}\sum b_i D_i\right) \times \exp\left(-\frac{Z'}{\rho\rho' D}\sum b_i D_i'\right) - \frac{\mu}{\left(d_0+\frac{Z}{\rho D}\sum b_i D_i+\frac{Z'}{\rho' D}\sum b_i D_i'\right)^6} + E_{d_0'} \exp\left(-\frac{Z'}{\rho'^2 D}\sum b_i' D_i'\right) \times \exp\left(-\frac{Z}{\rho\rho' D}\sum b_i' D_i\right) - \frac{\mu'}{\left(d_0'+\frac{Z'}{\rho' D}\sum b_i' D_i'+\frac{Z}{\rho D}\sum b_i' D_i\right)^6} + \tfrac{1}{2}\sum a_{ij}\left(\frac{Z}{\rho}\frac{D_i}{D}+\frac{Z'}{\rho'}\frac{D_i'}{D}\right) \times \left(\frac{Z}{\rho}\frac{D_j}{D}+\frac{Z'}{\rho'}\frac{D_j'}{D}\right). \quad (39)$$

It is obvious that any number of interactions can be taken into account in this way, but the numerical solution for Z, Z', Z'', $\cdots$ would become quite difficult. It is also obvious that there would be no difficulty in including any term or terms of the form $1/d^n$ $(n \geqslant 1)$ in Eq. (24) (see, for example, Eq. (44)).

The above equations apply to method 1. They also apply to method 2 if we make the appropriate change in the meaning (replace ${}^0A$ by A) of d_0, the q_i, the a_{ij}, and the b_i, and substitute everywhere $-P$ for P, $-\mu$ for μ, and $-E'$ for E' (Eq. (21)).

In summary, the generalizations included here and in paper I over the treatment of Westheimer and Mayer are: (a) the inclusion of terms of the form $1/d^n$ $(n \geqslant 1)$ in V; (b) the inclusion of two or more different steric interactions; (c) the introduction of cross products; and (d) the introduction of method 2.

Cis- and *Trans*-2-Butene

Consider the equilibrium

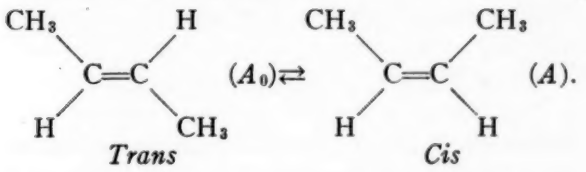

ΔQ for this reaction is available from the heats of formation:[12] $\Delta Q = 1.288$ kcal./mole. A is less stable energetically than A_0, presumably primarily as a result of the van der Waals repulsion between the methyl groups in A.

In addition to the CH_3-CH_3 van der Waals interactions, there are also to be considered the $H-CH_3$ van der Waals interactions, the $H-H$ van der Waals interactions, and the interactions between the CH dipoles (we assume no CCH_3 dipole). The force constants for A and A_0 are not available, but a set of force constants has been determined for propylene.[13] Hence the way to proceed in order to use Eq. (4) in this case would be to: (a) take into account in propylene all interactions of the type mentioned above and obtain for this molecule the unperturbed potential surface by method 2; (b) the valence force constants (with cross products) associated with this surface should be very nearly the same as the corresponding force constants for ${}^0A_0$ and ${}^0A$ above, again omitting, in obtaining ${}^0A_0$ and ${}^0A$, interactions of the sort mentioned; (c) then using method 1 and these unperturbed force constants, E_A and E_{A_0} could be calculated. In view of various uncertainties mentioned below this tedious program hardly seems worth while for the present.

We content ourselves with the approximate treatment discussed in connection with Eq. (6). Also, we treat the methyl group as an atom. The most important interaction is the CH_3-CH_3 interaction in A. We therefore remove only this interaction from A in forming ${}^0A$. We then assume as an approximation that corresponding bond angles, bond distances, and valence force constants are the same in ${}^0A$, A_0, and propylene.

[12] A. P. I. Research Project 44, National Bureau of Standards. Selected Values of Properties of Hydrocarbons. Table 8w (Part 1), 1944–1946.

[13] E. B. Wilson, Jr. and A. J. Wells, J. Chem. Phys. 9, 319 (1941).

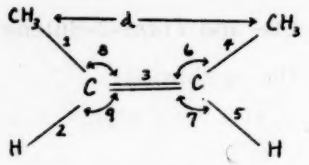

FIG. 2. Coordinates of *cis*-2-butene.

When the CH_3-CH_3 interaction is introduced into ${}^0A$, the observed deformations will result from a compromise between this interaction and the force constants. The effect of other interactions on the deformations is automatically included, approximately, in the force constants (i.e., these are not the completely unperturbed force constants mentioned in the preceding paragraph).

We do not assume that ${}^0Q_A = Q_{A_0}$. We can estimate ${}^0Q_A - Q_{A_0}$ by calculating (a) the interaction energy in the equilibrium configuration of ${}^0A$ due to all interactions other than CH_3-CH_3 and (b) the interaction energy in the equilibrium configuration of A_0 due to *all* interactions, and assuming that ${}^0Q_A - Q_{A_0}$ is equal to the difference in these interaction energies. Here again we are neglecting zero-point vibrational energies, and this could be serious here.

The $3n-6=12$ internal coordinates for ${}^0A$ suggested by the force constants given for propylene by Wilson and Wells[13] are shown in Fig. 2. The q_i are valence displacement coordinates. Let q_{10} be the angle between one

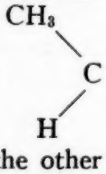

plane and the C=C axis and q_{11} be the other similar angle. Let q_{12} be the angle of torsion between these two planes. The deformation potential function suggested by the propylene force constants is[14]

$$\begin{aligned}\tfrac{1}{2}\textstyle\sum a_{ij}q_iq_j &= \tfrac{1}{2}a_{11}(q_1^2+q_4^2)+\tfrac{1}{2}a_{22}(q_2^2+q_5^2)\\ &+\tfrac{1}{2}a_{33}q_3^2+\tfrac{1}{2}a_{66}(q_6^2+q_8^2)\\ &+\tfrac{1}{2}a_{77}(q_7^2+q_9^2)+\tfrac{1}{2}a_{10,10}(q_{10}^2+q_{11}^2)\\ &+\tfrac{1}{2}a_{12,12}q_{12}^2+a_{37}(q_3q_7+q_3q_9)\\ &+a_{36}(q_3q_6+q_3q_8)+a_{67}(q_6q_7+q_8q_9)\\ &+a_{10,11}q_{10}q_{11}. \qquad (40)\end{aligned}$$

[14] For an excellent discussion of valence force constants and generalizations, see G. Herzberg, *Infrared and Raman Spectra* (D. Van Nostrand Company, Inc., New York, 1945), pp. 168–191.

We have $d=d_0+\sum b_iq_i$. Let ${}^0\alpha_i$ and ${}^0r_j$ be the equilibrium bond angle and bond distance in ${}^0A$ associated with $q_i=0$ and $q_j=0$, respectively. Then it is easy to see that

$$\begin{aligned}b_1&=b_4=\sin\left({}^0\alpha_6-\frac{\pi}{2}\right),\\ b_2&=b_5=b_7=b_9=0,\\ b_3&=1,\\ b_6&=b_8={}^0r_4\cos\left({}^0\alpha_6-\frac{\pi}{2}\right),\\ b_{10}&=b_{11}=b_{12}=0.\end{aligned} \qquad (41)$$

Clearly d is affected by changes in q_{10}, q_{11}, and q_{12}, but *not* to linear terms. So $b_{10}=b_{11}=b_{12}=0$.

It follows from Eq. (30) (or on physical grounds) that if $b_i=0$ and q_i appears in Eq. (40) only in a squared term (i.e., no cross products involve q_i), then $q_i^0=0$. Hence we can ignore q_i from the outset without loss of generality. This applies to q_2, q_5, and q_{12}. Also, if $b_j=b_k=0$ and the only cross product which involves either q_j or q_k is $a_{jk}q_jq_k$, then $q_j^0=q_k^0=0$. Hence we also ignore q_{10} and q_{11}. Equation (40) reduces to

$$\begin{aligned}\tfrac{1}{2}\textstyle\sum a_{ij}q_iq_j &= \tfrac{1}{2}a_{11}(q_1^2+q_4^2)+\tfrac{1}{2}a_{33}q_3^2\\ &+\tfrac{1}{2}a_{66}(q_6^2+q_8^2)+\tfrac{1}{2}a_{77}(q_7^2+q_9^2)\\ &+a_{37}(q_3q_7+q_3q_9)+a_{36}(q_3q_6+q_3q_8)\\ &+a_{67}(q_6q_7+q_8q_9). \qquad (42)\end{aligned}$$

The determinants D and D_i to be evaluated are thus of order seven. However they can be reduced readily to order 2×3. Let

$$J=\begin{vmatrix}a_{77} & a_{67}\\ a_{67} & a_{66}\end{vmatrix}, \qquad K=\begin{vmatrix}a_{37} & a_{67} & a_{77}\\ a_{36} & a_{66} & a_{67}\\ a_{33} & 2a_{36} & 2a_{37}\end{vmatrix},$$

$$K_1=\begin{vmatrix}0 & a_{67} & a_{77}\\ b_6 & a_{66} & a_{67}\\ b_3 & 2a_{36} & 2a_{37}\end{vmatrix}, \qquad K_2=\begin{vmatrix}a_{37} & 0 & a_{77}\\ a_{36} & b_6 & a_{67}\\ a_{33} & b_3 & 2a_{37}\end{vmatrix},$$

and

$$K_3=\begin{vmatrix}a_{37} & a_{67} & 0\\ a_{36} & a_{66} & b_6\\ a_{33} & 2a_{36} & b_3\end{vmatrix}.$$

Then one finds

$$D=-a_{11}^2JK, \qquad D_6=D_8=-a_{11}^2JK_2,$$
$$D_1=D_4=-a_{11}b_1JK, \quad D_7=D_9=-a_{11}^2JK_3. \quad (43)$$
$$D_3=-a_{11}^2JK_1,$$

The structure of propylene, which we need for ${}^0A$ and A_0, has apparently not been determined by electron diffraction. The structures of *cis*- and *trans*-2-butene are not known accurately.[15] So we take the following reasonable structure parameters for ${}^0A$ and A_0: from ethylene,[16a]

$${}^0\alpha_6={}^0\alpha_7={}^0\alpha_8={}^0\alpha_9=122°; \quad {}^0r_1={}^0r_4=1.54\text{A};$$
$${}^0r_2={}^0r_5=1.09\text{A}; \quad \text{and} \quad {}^0r_3=1.34\text{A}.$$

In Table I we give the force constants[13] used and the values of b_i and D_i calculated from Eqs. (41) and (43).

We must now make some assumptions about interactions. The van der Waals parameters are uncertain. We refer to paper I for a detailed discussion. Using the method described there we take for the CH_3-CH_3 interaction $r^*=4.0$A and $\epsilon=16.0\times10^{-15}$ erg, and for the H−H interaction[16b] $r^*=2.4$A and $\epsilon=2.92\times10^{-15}$ erg. These automatically determine r^* and ϵ for the CH_3-H interaction and then P, ρ, and μ for all three interactions. We assume that the CH dipole is located in the middle of the CH bond and that the bond moment is $\mu=0.4\times10^{-18}$ e.s.u.[17a] The dipole-dipole interaction energy is then given by $2\mu^2\cos^2\theta/r^3$, where $\theta=58°$ in ${}^0A$ and $\theta=32°\,16'$ in A_0. r is the dipole-dipole distance.

Using the unperturbed structure parameters and the above energy parameters, interatomic distances and interaction energies can be calculated and ${}^0Q_A-Q_{A_0}$ estimated as discussed above. One finds, with these parameters, ${}^0Q_A-Q_{A_0}=-0.365$ kcal./mole. Equations (32) and (33) may now be used to calculate $E_A\cong E_A'$. The result is $E_A'=2.217$ kcal./mole. Hence, from Eq. (6), $\Delta Q\cong E_A'+({}^0Q_A-Q_{A_0})=1.852$ kcal./mole, compared to the known value 1.288 kcal./mole. This is certainly satisfactory agreement considering all the uncertainties involved in the calculation (e.g., structure, force constants, van der Waals parameters, bond dipole moment, and especially zero-point vibrational energy).

It is hoped that the zero-point vibrational energy correction can be made in a future calculation. G. W. Wheland has suggested[17b] a perturbation procedure which may be useful for this purpose. Of course the fact that a quite satisfactory result is obtained, ignoring zero-point vibrational energy, implies that the large zero-point energies in ${}^0A$ and A must almost cancel.

If we take $\epsilon=10.0\times10^{-15}$ erg for the CH_3-CH_3 interaction, and make the corresponding change in ϵ for CH_3-H, but make no other changes in the fundamental parameters, one gets ${}^0Q_A-Q_{A_0}=-0.373$ kcal./mole, $E_A'=1.674$ kcal./mole, and $\Delta Q\cong1.301$ kcal./mole, in virtual agreement with 1.288 kcal./mole. However, the present calculation is certainly not accurate enough to conclude from these results that $\epsilon<16.0\times10^{-5}$ erg. We give a few more

TABLE I.

i	a_{ii}	b_i	D_i(c.g.s., rad.)	$q_i^0(\epsilon=10)$
1 or 4	4.50×10^5 dyne/cm	0.5299	6.57×10^{-34}	0.0045A
3	9.72×10^5 dyne/cm	1.000	0.763×10^{-34}	0.00052A
6 or 8	1.20×10^{-11} dyne cm/rad.^{2}	1.306×10^{-8} cm/rad.	121.0×10^{-26}	0.0830 rad. $=4.8°$
7 or 9	0.939×10^{-11} dyne cm/rad.^{2}	0.000	-97.2×10^{-26}	-0.0667 rad. $=-3.8°$
	$a_{37}=0.66\times10^{-8}$ dyne/rad.		$D=55.8\times10^{-29}$	
	$a_{36}=0.73\times10^{-8}$ dyne/rad.			
	$a_{67}=0.75\times10^{-11}$ dyne cm/rad.^{2}			

[15] L. O. Brockway and P. C. Cross, J. Am. Chem. Soc. **58**, 2407 (1936).
[16a] E. H. Eyster, J. Chem. Phys. **6**, 580 (1938).
[16b] Strictly speaking, the H−H van der Waals interaction chosen includes already some dipole interaction. However, this van der Waals curve does not give any angular dependence to the dipole interaction as it properly should. Also, since the van der Waals parameters are in any case very uncertain for this interaction, we ignore this complication in the present case.
[17a] L. Pauling, *Nature of the Chemical Bond* (Cornell University Press, Ithaca, 1945).
[17b] Personal communication to F. H. Westheimer.

TABLE II. ($\epsilon=10$.)

Interaction	${}^0A$	A_0
$2\times(CH_3-H)$	-0.155 kcal./mole	0.197 kcal./mole
$H-H$	-0.050	-0.019
dipole-dipole	0.183	0.341
$CH_3—CH_3$	—	-0.168
Total	-0.022 kcal./mole	0.351 kcal./mole

details below concerning the second calculation ($\epsilon=10$).

In Table II we list the individual interaction energies found in computing ${}^0Q_A-Q_{A_0}$ ($\epsilon=10$). The contributions to E_A' are the following: van der Waals repulsion, 2.312 kcal./mole; van der Waals attraction, -1.250 kcal./mole; and deformations, 0.612 kcal./mole. Also, $d_0=2.972$A and d (equilibrium configuration of A) $=3.194$A. The net CH_3-CH_3 van der Waals energy corresponding to a distance of 2.972A between methyl groups amounts to 2.993 kcal./mole compared to 1.062 kcal./mole for a distance of 3.194A. The deformations are given in Table I (q_i^0). It is seen that bond stretching is negligible but that there are small but appreciable changes predicted in bond angles: in A, $\alpha_6=\alpha_8=126.8°$ and $\alpha_7=\alpha_9=118.2°$. The $H-C-CH_3$ angle is then 115°. It is interesting that the angles α_7 and α_9 play an important role in the calculation even though $b_7=b_9=0$. This is, of course, a result of the inclusion of cross-products in the potential function.

It is gratifying that reasonable results have now been obtained by this type of calculation in a case[3] where there is a large steric effect (about 20 kcal./mole) and also in a case (the above) where the steric effect is small (about 2 kcal./mole).

It might be remarked that this semi-empirical approach to steric effects provides, in principle, a method of explaining differences in vibrational frequencies, deduced from infra-red and Raman spectra, in a pair of molecules such as *cis*- and *trans*-2-butene.

Another conceivable application is that the present method might in the future be useful in estimating the rate of a reaction involving a substrate molecule or molecules in the presence of an enzyme,[18] in accordance with a recent proposal of Pauling in his Silliman lecture.[19] Pauling suggested that an enzyme has a structure closely complementary to the activated complex for the reaction that is catalyzed by the enzyme. The present method would apply in principle as follows: consider the activated complex for the reaction in the absence of the enzyme as the unperturbed molecule ${}^0A$, with coordinates q_i and force constants a_{ij}, as in connection with Eq. (18). It might be necessary to find the a_{ij} by applying method 1 to a molecule ${}^0({}^0A)$ with internal steric interactions removed. Let $V(q)$ be the (perturbing) energy of interaction between the enzyme and the activated complex as a function of the q_i. Then Eq. (18) gives the potential energy U of the perturbed molecule A in the presence of the enzyme surface. Eq. (19) also applies. If the enzyme surface fits the activated complex ${}^0A$ "perfectly" (i.e., if $(\partial V/\partial q_i)=0$ $(i=1, 2, \cdots)$ at $q_1=q_2=\cdots=0$), then $q_i^0=0$ $(i=1, 2, \cdots)$, $A={}^0A$ (structure) and $E'=U(0)=V(0)$. In this case the energy of the activated complex is lowered ($E'=V(0)$ is negative) in the presence of the enzyme by just the energy of interaction $V(0)$ between the enzyme and the unperturbed activated complex ${}^0A$. In general, though, the fit will not be "perfect:" $q_i^0\neq 0$ $(i=1, 2, \cdots)$ and $E'<V(0)$. In any case, to find the free energy of activation and hence the rate of the reaction, the shape of the potential energy surface U must be studied (normal coordinates) in the neighborhood of its saddle point.

APPENDIX

In the absence of any interaction between the hydrogen atoms in a molecule such as H_2O, we would expect a 90° $H-O-H$ angle owing to directed valence considerations.[17a] The observed angle in H_2O is 104° 31′, the increase presumably being due to $H-H$ repulsion. It is clearly of interest to try to apply the present method to this problem.

The results obtained are, on the whole, rather unsatisfactory. The principal sources of difficulty which arise in trying to fit these molecules into the semi-empirical method being used here seem to be: (a) the treatment of the large electrostatic effects (see below); (b) the probability

[18] The same possibility exists and is, of course, more practical in connection with ordinary catalysts and smaller molecules.

[19] L. Pauling, American Scientist **36**, 51 (1948).

that van der Waals parameters for a given type of interaction, say H−H, are not constant from case to case when both interacting atoms or groups are bonded to the same atom (see reference 17a, pp. 192–193); (c) uncertainty concerning the extent of hybridization which would tend to increase appreciably the unperturbed bond angle over 90° in some cases (see reference 17a, pp. 86–88); and (d) the treatment of a group, such as a methyl group, as an atom will introduce a relatively large error in a small molecule as compared to a large molecule. In connection with (a), the bond dipoles are so close together that one is hardly justified in treating the electrostatic interaction as a dipole-dipole interaction as in Section III. In the calculations carried out we have gone to the opposite extreme by finding the charge on the terminal atom (H in H_2O) from the equation *bond moment = charge × bond length*, and then calculating the electrostatic repulsion between the terminal atoms from (charge)²/(interatomic distance). The results (ϵ; see below) obtained for a given interaction (H−H, Cl−Cl or F−F) show an unexplained systematic trend with charge which probably (other parameters vary concomitantly so this is not certain) indicates that this assumption is not good. Actually, of course, one would expect that only a detailed quantum-mechanical treatment could correctly take into account a large, short range electrostatic interaction of this type.

The above difficulties are in addition to uncertainties in the actual numerical values of force constants, van der Waals parameters, and bond dipole moments.

The procedure used is the following:

(a) We ignore bond stretching. Since many of the increases, $\alpha-90°$, in bond angle over 90° are considerable, we do not assume a linear relation between interatomic distance r and $\alpha-90°$ in analogy with $d=d_0+\sum b_i q_i$ in Section III, but use the general expression $r(\alpha)$. However, we must still assume that Hooke's law holds, for very large displacements in some cases; this will certainly be an important source of error.

(b) We use method 1.[20] For a triatomic symmetrical molecule such as H_2O, let r_0 be the fixed bond distance, e the charge on the terminal atom, α the bond angle, a the force constant in ${}^0A$, f the force constant in A, let $\alpha=\alpha_0$ in ${}^0A$ (equilibrium configuration) and let $\alpha=\beta$ in A (equilibrium configuration). Then (Eq. (18))

$$U(\alpha)=P\exp(-r/\rho)-(\mu/r^6)+(e^2/r)+(1/2)a(\alpha-\alpha_0)^2, \quad (44)$$

where $r=2r_0\sin(\alpha/2)$. The equation for a tetratomic symmetrical molecule such as NH_3 is similar.

(c) We set $(dU/d\alpha)_{\alpha=\beta}=0$, solve for a, and substitute the expression for a into $(d^2U/d\alpha^2)_{\alpha=\beta}=f$. If we now put[4] $\mu=17.1P\rho^6$, the resulting equation can be regarded as giving $P(\rho)$ (or, the equivalent,[4] $\epsilon(r^*)$) in terms of the known quantities f, e, r_0, β, and α_0. We then choose a reasonable value of r^* (the same value for a given interaction in different molecules) and calculate ϵ. It should be remarked that ϵ is very sensitive to the choice of r^*.

The above calculation was carried out on every suitable molecule (taking $\alpha_0=90°$ in each case; see above) for which r_0, f, β, and the bond dipole moment (or the molecular dipole moment) are available. On the basis of the results found in paper I, the values of ϵ obtained for the interactions in H_2O, NH_3, H_2S, Cl_2O, PCl_3, and F_2O are quite reasonable. However, the values found for PH_3, $AsCl_3$, $SbCl_3$, PF_3, AsF_3, $(CH_3)_2O$, $(CH_3)_3N$ and PBr_3 are not reasonable.[21] In view of this inconsistency one must conclude that the semi-empirical method in its present form is not generally well suited to these small molecules with large electrostatic effects. For this reason we have refrained from giving detailed equations, data, and results here.

[20] Method 2 leads to essentially the same results.

[21] One is tempted to make the following classification: the reasonable result for PCl_3 is probably fortuitous; for some reason P, As, and Sb compounds are anomolous; methyl compounds are not expected to give good results in view of difficulties (b) and (e) listed above.

THE JOURNAL OF CHEMICAL PHYSICS VOLUME 16, NUMBER 10 OCTOBER, 1948

Force Constants and Frequency Assignments for Some Substituted Methylacetylenes

ARNOLD G. MEISTER
Department of Physics, Illinois Institute of Technology, Chicago 16, Illinois
(Received May 5, 1948)

Force constants have been determined for methylacetylene using the Wilson FG matrix method. It was found that of the thirteen force constants required for the potential energy function for methylchloroacetylene, methylbromoacetylene, and methyliodoacetylene, eight could be transferred from the set obtained for methylacetylene. Since only four of the ten fundamental frequencies of the methylhaloacetylenes were used in establishing the force constants, all the frequencies were calculated to see if the sets of force constants for the methylhaloacetylenes were reasonable. With the exception of one frequency, the agreement between the calculated and observed values was within two percent. As the calculations served to identify the fundamental frequencies for the methylhaloacetylenes, it was found that previous assignments by Cleveland and Murray of the observed Raman frequencies for methylbromoacetylene and methyliodoacetylene had to be modified. New assignments are given for some of their observed values for these two molecules and assignments also are given for their observed Raman frequencies for a solution of methylchloroacetylene in ethylbromide for which they made no assignments. The fundamental frequencies for methyldeuteroacetylene also were calculated using the same force constants, interbond angles, and equilibrium values for the bond distances as for methylacetylene, in order to determine how a pure mass change affects the frequencies of methylacetylene. As a result of this investigation the C−C and C≡C stretching frequencies were found to be greater for the methylhaloacetylenes than for methylacetylene or methyldeuteroacetylene. The C−X (X = halogen atom) stretching frequencies for the methylhaloacetylenes were found to be less than for the corresponding methyl halides despite the fact that the C−X stretching force constant for the methylhaloacetylenes always was greater than for the corresponding methyl halides.

INTRODUCTION

RAMAN spectra of methylchloroacetylene, methylbromoacetylene, and methyliodoacetylene were obtained by Cleveland and Murray.[1] These investigators made frequency assignments for the last two molecules but they were unable to do so for methylchloroacetylene because of the presence of solvent lines. In order to check their assignments and to see if assignments for the Raman frequencies of methylchloroacetylene could be made, force constants were determined for methylacetylene and as many as possible were transferred to the methylhaloacetylenes. Some of the force constants used for methylacetylene were obtained from a previous investigation of dimethylacetylene.[2] The remaining force constants were determined from some of the observed frequencies and, finally, all of the frequencies were calculated in order to see if the force constants so obtained would give reasonable frequency values.

Such a study of a series of molecules in which only one of the atoms (the acetylenic hydrogen atom) is changed, so that most of the force constants can be kept the same, should furnish information about the behavior of the fundamental frequencies. For the molecules concerned in this study, one would not expect the methyl group frequencies to change much as the acetylenic hydrogen atom is replaced by a halogen atom. On the other hand, one would expect the values of C−X stretching and C≡C−X bending frequencies to change considerably and also smaller changes would be expected to occur in the values of the C≡C and C−C stretching frequencies and the C−C≡C bending frequency. Also, since it should be possible to transfer all of the force constants for methylacetylene to methyldeuteroacetylene, it should be interesting to calculate the fundamental frequencies for this molecule in order to see how a pure mass change affects the fundamental frequencies.

The Wilson FG matrix method[3] was used in all of the calculations. For the methylhaloacetylenes investigated, as a further simplification, the nondegenerate and doubly degenerate C−H vibrations of the methyl group near 3000 cm^{-1} were "split out" from the rest of the frequencies.[3] The

[1] F. F. Cleveland and M. J. Murray, J. Chem. Phys. **11**, 450 (1943); **12**, 320 (1944).
[2] A. G. Meister and F. F. Cleveland, J. Chem. Phys. **15**, 349 (1947).
[3] E. B. Wilson, Jr., J. Chem. Phys. **7**, 1047 (1939); **9**, 76 (1941).

same method was used for the doubly degenerate vibrations of methylacetylene and methyldeuteroacetylene. The method of "splitting out" frequencies which was used for the non-degenerate vibrations of these two molecules will be discussed in connection with the normal coordinate treatment.

NORMAL COORDINATE TREATMENT

Although Crawford[4] has calculated the fundamental frequencies for methylacetylene, it seems that the force constants should be redetermined since he was interested only in establishing approximate values for the fundamental frequencies. For this reason, he transferred most of the necessary force constants from ethane, acetylene, and dimethylacetylene, so that he had to determine only one force constant. Since he made no attempt to modify the transferred force constants in order to obtain better agreement between the observed and calculated values of the frequencies, it seemed that in the present investigation such a modification should be made. Following Crawford,[4] the methylacetylene molecule and the substituted methylacetylenes were assumed to have the symmetry C_{3v}. Such a symmetry permits only five type A_1 non-degenerate vibrations and five type E doubly degenerate vibrations. The various bond distances and interbond angles used to determine the internal coordinates are shown in Fig. 1.

From the internal coordinates the following symmetry coordinates were formed: for the A_1 vibrations

$$R_1=(\Delta r_1+\Delta r_2+\Delta r_3)/(3)^{\frac{1}{2}},$$
$$R_2=\Delta r_a,$$
$$R_3=\Delta r_C,$$
$$R_4=\Delta r_X,$$
$$R_5=(\Delta\alpha_{12}+\Delta\alpha_{23}+\Delta\alpha_{13}-\Delta\beta_1-\Delta\beta_2-\Delta\beta_3)/(6)^{\frac{1}{2}},$$
$$R_6=(\Delta\alpha_{12}+\Delta\alpha_{23}+\Delta\alpha_{13}+\Delta\beta_1+\Delta\beta_2+\Delta\beta_3)/(6)^{\frac{1}{2}}\equiv 0$$
(redundant coordinate);

and for the E vibrations

$$R_{1a}=(2\Delta r_1-\Delta r_2-\Delta r_3)/(6)^{\frac{1}{2}},$$
$$R_{1b}=(\Delta r_2-\Delta r_3)/(2)^{\frac{1}{2}},$$
$$R_{2a}=(2\Delta\beta_1-\Delta\beta_2-\Delta\beta_3)/(6)^{\frac{1}{2}},$$
$$R_{2b}=(\Delta\beta_2-\Delta\beta_3)/(2)^{\frac{1}{2}},$$
$$R_{3a}=(2\Delta\alpha_{23}-\Delta\alpha_{12}-\Delta\alpha_{13})/(6)^{\frac{1}{2}},$$
$$R_{3b}=(\Delta\alpha_{13}-\Delta\alpha_{12})/(2)^{\frac{1}{2}},$$
$$R_{4a}=\Delta\varphi_a,$$
$$R_{4b}=\Delta\varphi_b,$$
$$R_{5a}=\Delta\theta_a,$$
$$R_{5b}=\Delta\theta_b.$$

Since there are sixteen internal coordinates and only fifteen fundamental vibrations, one internal coordinate can be expressed in terms of the others. Instead of ignoring this coordinate and thus destroying the symmetry, another A_1 symmetry coordinate was chosen which was identically zero and all the other symmetry coordinates were made orthogonal to this redundant symmetry coordinate. The symmetry coordinates also were normalized and made orthogonal to one another.

The potential energy function used in this investigation was the same as the one used by Crawford.[4] It was

$$\begin{aligned}2V=&k_H[(\Delta r_1)^2+(\Delta r_2)^2+(\Delta r_3)^2]\\&+k_a(\Delta r_a)^2+k_C(\Delta r_C)^2+k_X(\Delta r_X)^2\\&+2k_{Ca}(\Delta r_C)(\Delta r_a)+2k_{Xa}(\Delta r_X)(\Delta r_a)\\&+k_\alpha r_1^2[(\Delta\alpha_{12})^2+(\Delta\alpha_{23})^2+(\Delta\alpha_{13})^2]\\&+k_\beta r_1^2[(\Delta\beta_1)^2+(\Delta\beta_2)^2+(\Delta\beta_3)^2]\\&+2k_{\alpha\beta}r_1^2[(\Delta\beta_1)(\Delta\alpha_{12}+\Delta\alpha_{13})\\&+(\Delta\beta_2)(\Delta\alpha_{23}+\Delta\alpha_{12})+(\Delta\beta_3)(\Delta\alpha_{23}+\Delta\alpha_{13})]\\&+2k_{C\alpha}r_1[(\Delta r_C)(\Delta\alpha_{12}+\Delta\alpha_{23}+\Delta\alpha_{13})]\\&+2k_{C\beta}r_1[(\Delta r_C)(\Delta\beta_1+\Delta\beta_2+\Delta\beta_3)]\\&+k_\varphi r_C^2[(\Delta\varphi_a)^2+(\Delta\varphi_b)^2]\\&+k_\theta r_X^2[(\Delta\theta_a)^2+(\Delta\theta_b)^2]\\&+2k_{\varphi\theta}r_Cr_X[(\Delta\varphi_a)(\Delta\theta_a)+(\Delta\varphi_b)(\Delta\theta_b)],\end{aligned}$$

where r_1, r_C, and r_X represent the equilibrium

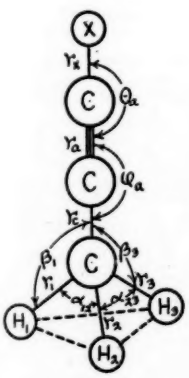

FIG. 1. Bond distances and interbond angles for a substituted methylacetylene.

[4] B. L. Crawford, Jr., J. Chem. Phys. 8, 526 (1940).

values of the C−H, C−C, and C−X bond distances, respectively.

From the potential energy matrix and the matrix formed from the coefficients of the internal coordinates, as obtained from the symmetry coordinates, one gets the following F matrices: for the A_1 vibrations

$$A_1 \qquad F = \begin{vmatrix} k_H & 0 & 0 & 0 & 0 \\ 0 & k_a & k_{Ca} & k_{Xa} & 0 \\ 0 & k_{Ca} & k_C & 0 & (3r_1k_{C\gamma})/(6)^{\frac{1}{2}} \\ 0 & k_{Xa} & 0 & k_X & 0 \\ 0 & 0 & (3r_1k_{C\gamma})/(6)^{\frac{1}{2}} & 0 & (r_1^2K_{\alpha\beta})/2 \end{vmatrix};$$

and for the E vibrations

$$E \qquad F = \begin{vmatrix} k_H & 0 & 0 & 0 & 0 \\ 0 & r_1^2k_\beta & -r_1^2k_{\alpha\beta} & 0 & 0 \\ 0 & -r_1^2k_{\alpha\beta} & r_1^2k_\alpha & 0 & 0 \\ 0 & 0 & 0 & r_C^2k_\varphi & r_Cr_Xk_{\varphi\theta} \\ 0 & 0 & 0 & r_Cr_Xk_{\varphi\theta} & r_X^2k_\theta \end{vmatrix},$$

where $k_{C\gamma}=k_{C\alpha}-k_{C\beta}$ and $K_{\alpha\beta}=k_\alpha+k_\beta-4k_{\alpha\beta}$.

The G matrices were obtained from relations given by Wilson.[3] They were the following, assuming tetrahedral angles for the methyl group: for the A_1 vibrations

$$A_1 \qquad G = \begin{vmatrix} \mu_H+(\mu_C)/3 & 0 & (-(3)^{\frac{1}{2}}\mu_C)/3 & 0 & (-4a\mu_C)/3 \\ 0 & 2\mu_C & -\mu_C & -\mu_C & 0 \\ (-(3)^{\frac{1}{2}}\mu_C)/3 & -\mu_C & 2\mu_C & 0 & (4(3)^{\frac{1}{2}}a\mu_C)/3 \\ 0 & -\mu_C & 0 & \mu_C+\mu_X & 0 \\ (-4a\mu_C)/3 & 0 & (4(3)^{\frac{1}{2}}a\mu_C)/3 & 0 & 2a^2[\mu_H+(8\mu_C)/3] \end{vmatrix};$$

and for the E vibrations

$$E \qquad G = \begin{vmatrix} \mu_H+4\mu_C/3 & -(2)^{\frac{1}{2}}\mu_C(b+a/3) & G_{31} & G_{41} & 0 \\ -(2)^{\frac{1}{2}}\mu_C(b+a/3) & a^2\mu_H+(3\mu_C/2)[b^2+(b+a/3)^2] & G_{32} & G_{42} & G_{52} \\ (4(2)^{\frac{1}{2}}a\mu_C)/3 & (a^2\mu_H)/2-2a(b+a/3)\mu_C & (5a^2\mu_H)/2+(8a^2\mu_C)/3 & G_{43} & 0 \\ (-(3)^{\frac{1}{2}}b\mu_C)/3 & ((6)^{\frac{1}{2}}b/4)(2b+c+a/3)\mu_C & (-(6)^{\frac{1}{2}}ab\mu_C)/3 & 2(\mu_C)(b^2+c^2+bc) & -c(b+2c+d)\mu_C \\ 0 & (-(6)^{\frac{1}{2}}bc\mu_C)/4 & 0 & G_{45} & d^2\mu_X+[c^2+(c+d)^2]\mu_C \end{vmatrix},$$

where $a=1/r_1$, $b=1/r_C$, $c=1/r_a$, $d=1/r_X$ and μ_H, μ_C, and μ_X represent the reciprocals of the masses of the H, C, and X atoms, respectively.

In order to obtain force constants for methylacetylene values of k_a, k_β, $k_{\alpha\beta}$, $k_{C\gamma}$, k_a, k_{Ca} and k_φ were transferred from previous work on dimethylacetylene.[2] The values of k_H, k_C, and k_X were

TABLE I. Force constants for methylacetylene (10^5 dynes/cm).

Force constant	Set I	Set II	Crawford's value
k_α	(0.45342)*	same	0.46
k_β	(0.56207)	same	0.55
$k_{\alpha\beta}$	(0.01285)	same	0.01
$k_{C\gamma}$	(−0.26186)	same	−0.235
k_H	4.9967	same	4.79
k_C	5.1266	(5.1296)	5.183
k_a	(16.312)	15.799	15.587
k_X	6.4415	same	5.850
k_{Ca}	(0.47059)	same	0.22
k_{Xa}	0.00000	same	0.028
k_φ	(0.12714)	same	0.155
k_θ	0.18970	same	0.2096
$k_{\varphi\theta}$	0.03390	same	0.0725

* Force constants enclosed in parentheses were transferred from dimethylacetylene.

TABLE II. Calculated and observed values (cm^{-1}) for the fundamental frequencies of methylacetylene and the calculated values for the fundamental frequencies of methyldeuteroacetylene.

		$CH_3C\equiv C-H$				$CH_3C\equiv C-D$	
Type	Designation	Set I	Set II*	Crawford's values	Observed values	Calculated values	
A_1	ν_1	2941	2941	2905	2941	2941*	2940
	ν_2	2178	2146	2137	2146	2009	1925
	ν_3	1379	1380	1402	1382	1376	1380
	ν_4	928	927	925	928	914	954
	ν_5	3429	3429	3331	3429	2674	2674
E	ν_1	3059	3059	3021	2982	3059	3059
	ν_2	1454	1454	1475	1448	1454	1454
	ν_3	1037	1037	1040	1038	1037	1037
	ν_4	329	329	332	336	309	309
	ν_5	644	644	656	642	518	518

* Best set.

TABLE III. Force constants for some methylacetylenes (10^5 dynes/cm).

Force constant	$CH_3C\equiv C-Cl$	$CH_3C\equiv C-Br$				$CH_3C\equiv C-I$			$CH_3C\equiv C-H$
	Set I	Set I	Set II	Set III	Set IV*	Set I	Set II	Set III*	Set II
k_α	0.45342	same	same	same	same	same	same	same	0.45342
k_β	0.56207	same	same	same	same	same	same	same	0.56207
$k_{\alpha\beta}$	0.01285	same	same	same	same	same	same	same	0.01285
$k_{C\gamma}$	−0.26186	same	same	same	same	same	same	same	−0.26186
k_H	4.8384	same	same	same	same	same	same	same	4.9967
k_C	5.1296	same	same	same	same	same	same	same	5.1296
k_a	15.799	16.312	15.799	15.588	15.799	15.799	15.271	15.799	15.799
k_X	5.3008	4.0998	4.3525	4.3627	4.3525	3.5707	3.5844	3.5707	6.4415
k_{Ca}	0.47059	same	same	same	same	same	same	same	0.47059
k_{Xa}	0.00000	0.6585	0.00000	0.00000	0.2075	0.00000	0.00000	0.5320	0.00000
k_φ	0.12714	same	same	same	same	same	same	same	0.12714
k_θ	0.097298	0.074506	same	same	same	0.059671	same	same	0.18970
$k_{\varphi\theta}$	0.045303	0.040290	same	same	same	0.036945	same	same	0.03390

* Best set.

obtained from the observed values of ν_1, ν_4, and ν_5 of the A_1 vibrations while the values of k_θ and $k_{\varphi\theta}$ were determined from the observed values of ν_4 and ν_5 of the E vibrations. The force constants obtained in this manner are given as set I in Table I. The value of k_{Xa} was taken to be zero since when the ν_1 and ν_2 frequencies are split out from the rest of the A_1 frequencies, as was done in this investigation, this force constant does not occur in the calculations. Also, as can be seen from Table I, the value of this force constant as determined by Crawford[4] is very small.

When the frequencies for methylacetylene were calculated using the force constants of set I of Table I, it was found that the calculated value of ν_2 for the A_1 vibrations did not agree very well with the observed value. Since ν_2 is the C≡C stretching frequency, it seemed that the value of k_a should be modified using the observed value of ν_2. Also, since the value obtained for k_C was so close to that obtained for the same constant for dimethylacetylene, its value was transferred from dimethylacetylene. The force constants obtained in this manner are given as set II in Table I. For comparison, Crawford's values[4] for these force constants are given in the last column of Table I.

It will be noted that most of the force constants are given to five significant figures, which is greater than the number of significant figures occurring in the frequencies used to determine the force constants. This greater number of significant figures was retained in order to insure agreement between observed and calculated frequencies to the nearest cm^{-1} for those observed frequencies used in establishing the force constants. Since the error in the observed frequencies may be greater than one cm^{-1}, the force constants cannot, of course, be considered as having been reliably established to five significant figures.

The values of the fundamental frequencies for methylacetylene calculated from these two sets of force constants are given in Table II. Also, for comparison the calculated values for the fundamental frequencies of methyldeuteroacetylene and Crawford's calculated values[4] for methylacetylene are given. In the sixth column are given the observed values for the fundamental frequencies of methylacetylene according to Herzberg,[5] which are based on the investigations of Glockler and Davis,[6] Glockler and Wall,[7] and Crawford.[4] For methylacetylene the poorer agreement, in some cases, between Crawford's calculated values and the present calculated values and the observed values occurs because he did not attempt to modify his force constants, or else because he used different observed values for the fundamental frequencies in obtaining his force constants.

It will be noted that two sets of calculated values for the fundamental frequencies of methyldeuteroacetylene have been given in Table II. This was necessary since in using the "splitting out" method to separate ν_1 from the rest of the

[5] G. Herzberg, *Infrared and Raman Spectra of Polyatomic Molecules* (D. Van Nostrand Company, Inc. New York, 1945), p. 338.

[6] G. Glockler and H. M. Davis, J. Chem. Phys. **2**, 881 (1934).

[7] G. Glockler and F. T. Wall, Phys. Rev. **51**, 529 (1937).

TABLE IV. Fundamental frequencies for some methylacetylenes (cm^{-1}).

Type	Designation	$CH_3C{\equiv}C-Cl$ Calc.	$CH_3C{\equiv}C-Cl$ Obs.	$CH_3C{\equiv}C-Br$ Set I	Set II	Set III	Set IV*	Obs.	$CH_3C{\equiv}C-I$ Set I	Set II	Set III*	Obs.	$CH_3C{\equiv}C-D$ Calc.	$CH_3C{\equiv}C-H$ Calc.	Obs.
A_1	ν_1	2894	2926	2894	2894	2894	2894	2921	2894	2894	2894	2913	2941	2941	2941
	ν_2	2261	2263	2230	2243	2230	2230	2230	2230	2197	2197	2197	2009	2146	2146
	ν_3	1391	1380	1389	1389	1391	1389	1375	1388	1389	1389	1375	1376	1380	1382
	ν_4	1078	—	1024	1036	1034	1034	—	1014	1013	1008	—	914	927	928
	ν_5	579	—	464	464	464	467	464	405	405	412	405	2674	3429	3429
E	ν_1	3010	2971	3010	3010	3010	3010	2968	3010	3010	3010	2958	3059	3059	2982
	ν_2	1456	1449	1455	1455	1455	1455	1443	1455	1455	1455	1438	1454	1454	1448
	ν_3	1036	1029	1036	1036	1036	1036	1026	1036	1036	1036	1021	1037	1037	1038
	ν_4	353	353	343	343	343	343	343	343	343	343	343	309	329	336
	ν_5	184	184	171	171	171	171	171	163	163	163	163	518	644	642

* Best set.

A_1 frequencies, the calculated value of ν_5 fell close to that of ν_1. In order to be more certain of the value of ν_5 the "splitting out" method was used again, only this time ν_1, ν_2, and ν_5 were "split out" from the rest of the A_1 frequencies. The results of these two calculations are given in columns seven and eight of Table II, respectively. Since the value obtained for ν_5 was the same in both cases and because more interaction constants were involved in the calculations leading to the fundamental frequencies given in column seven, it seems that this set of frequencies represents the most likely set of values for the fundamental frequencies of methyldeuteroacetylene. For both cases, in the calculation of these frequencies, the force constants of set II for methylacetylene were used. Also, the following equilibrium values[4] for the bond distances were used:

$$r_1 = 1.093\text{A},$$
$$r_C = 1.462\text{A},$$
$$r_X = 1.057\text{Å},$$
$$r_a = 1.204\text{A}.$$

Other constants used in the calculations were

$$\mu_C = 5.0183\times10^{22}\ g^{-1},$$
$$\mu_H = 5.9742\times10^{23}\ g^{-1},$$
$$\mu_D = 3.0110\times10^{23}\ g^{-1}.$$

For the remaining molecules investigated (methylchloroacetylene, methylbromoacetylene, and methyliodoacetylene) all force constants with the exception of k_X, k_{Xa}, k_H, k_θ, and $k_{\varphi\theta}$ were transferred from methylacetylene. Values for k_X and k_{Xa} were obtained using observed values of ν_2 and ν_5 for the A_1 vibration type of each molecule and in cases where k_{Xa} was made zero the observed value of ν_5 was used to obtain a value of k_X. This procedure was not possible for methylchloroacetylene since no observed value of ν_5 could be obtained, so the observed value of ν_2 was used to determine a value of k_X. Also, because the calculated value of ν_1 for the type E vibrations of methylacetylene is considerably greater than the observed value, the value of k_H for the methylhaloacetylenes was modified to get better agreement, since only this force constant is used in determining the frequency. The values of k_θ and $k_{\varphi\theta}$ for each molecule were obtained using observed values of ν_4 and ν_5 for the E vibration type. The various sets of force constants which were determined are given in Table III. Also, in the last column of Table III the force constants of set II for methylacetylene are given for comparison.

In all of the calculations, besides the constants already given, the following were used:

$$\mu_{Cl} = 1.6984\times10^{22}\ g^{-1},$$
$$\mu_{Br} = 7.5354\times10^{21}\ g^{-1},$$
$$\mu_{I} = 4.7447\times10^{21}\ g^{-1},$$
$$r_{C-Cl} = 1.68\text{A},$$
$$r_{C-Br} = 1.80\text{A},$$
$$r_{C-I} = 2.03\text{A},$$
$$r_{C\equiv C} = 1.21\text{A (for methylchloroacetylene)},$$
$$r_{C\equiv C} = 1.204\text{A (for methylbromoacetylene)},$$
$$r_{C\equiv C} = 1.18\text{A (for methyliodoacetylene)}.$$

TABLE V. Carbon-halogen stretching frequencies, stretching force constants, and bond distances for some methyl halides and for the corresponding methylhaloacetylenes.

Quantity	CH_3Cl	$CH_3C{\equiv}C-Cl$	CH_3Br	$CH_3C{\equiv}C-Br$	CH_3I	$CH_3C{\equiv}C-I$
ν_{C-X} (cm^{-1})	732	579	610	464	532	405
k_X (10^5 dynes/cm)	3.64	5.3008	3.129	4.3525	2.648	3.5707
r_{C-X} (A)	1.779	1.68	1.940	1.80	2.136	2.03

TABLE VI. A revised assignment of the observed Raman frequencies of methylbromoacetylene.*

$\Delta\nu$	I	ρ	Assignment and symmetry
171	1	—	E Fundamental
±343	50	6/7	E Fundamental
464	6	0.3	A_1 Fundamental
692	1	P	$2(343)=686$; A_1+E
1026	1	D	E Fundamental
1034	(not observed)		A_1 Fundamental
1154	*vw*	—	2921 excited by Hg 4047
1375	9	0.6	A_1 Fundamental
1443	2	D	E Fundamental
2060	*vw*	—	$2(1034)=2068$; A_1 $2(1026)=2052$; A_1+E $1026+1034=2060$; E
2213	(16)	(0.3)	$2921-2(343)=2235$; A_1+E $(2230+343)-343$; A_1+A_2+E
2230	80	0.35	A_1 Fundamental
2853	5	0.2	$2(1443)=2886$; A_1+E
2921	100	0.15	A_1 Fundamental
2968	8	6/7	E Fundamental

* $\Delta\nu$ = Raman displacement in cm^{-1}; I = relative intensity on the basis of 100 for the strongest Raman line; ρ = depolarization factor; ± = Stokes and anti-Stokes lines, respectively; data in regard to which there is some uncertainty are enclosed in parentheses; *vw* = very weak; D = depolarized; P = polarized.

TABLE VII. A revised assignment of the observed Raman frequencies of methyliodoacetylene.*

$\Delta\nu$	I	ρ	Assignment and symmetry
163	2	(0.8)	E Fundamental
±343	60	0.8	E Fundamental
±405	10	0.3	A_1 Fundamental
497	1	—	$163+343=506$; A_1+A_2+E
691	1	P	$2(343)=686$; A_1+E
1008	(not observed)		A_1 Fundamental
1021	1	D	E Fundamental
1150	*vw*	(D)	2913 excited by Hg 4047
1375	10	0.7	A_1 Fundamental
1438	1	0.9	E Fundamental
2011	*vw*	—	$2(1008)=2016$; A_1 $2(1021)=2042$; A_1+E $1021+1008=2029$; E
2182	*vw*	—	$2913-2(343)=2227$; A_1+E $(2197+343)-343$; A_1+A_2+E
2197	100	0.4	A_1 Fundamental
2730	*vw*	—	$2(1375)=2750$; A_1
2851	2	0.3	$2(1438)=2876$; A_1+E
2913	100	0.2	A_1 Fundamental
2958	3	0.9	E Fundamental

* The symbols used in this table have the same meaning as those used in Table VI.

The equilibrium values for the bond distances given above were taken from Maxwell.[8]

From Table III it can be seen that for the force constants given as set I for methylbromoacetylene (which was the first molecule to be investigated) the interaction constant k_{Xa} has a fairly large value. Since the larger value of k_a was used in determining this value of k_{Xa}, it seemed that the smaller value of k_a should be transferred from methylacetylene and the value of k_{Xa} should be taken as zero in order to determine the importance of k_{Xa} in the calculations. This led to the force constants of set II, and since the calculated value of ν_2 of the A_1 vibrations was about one percent greater than the observed value, the observed value was used to modify k_a in order to get better agreement between the calculated and observed values of ν_2. This resulted in set III. In set IV an attempt was made to use k_a of set II and to obtain a value of k_{Xa} from the observed value of ν_2 so that a better calculated value of ν_2 would result. Since the value given for k_{Xa} in set IV is about one-third the value obtained in set I, it seems that the force constants of set IV are to be preferred over those of the other sets.

No attempt was made to use the larger value of k_a (16.312×10^5 dynes/cm) in the subsequent calculations for methyliodoacetylene and methylchloroacetylene because a greater value of k_{Xa} results when this value of k_a is used. Instead, a set of force constants was obtained using the k_a (15.799×10^5 dynes/cm) of the second set for methylacetylene. Since for methyliodoacetylene the calculated value of ν_2 for the A_1 vibrations obtained in this manner was about 1.5 percent greater than the observed value, the values of k_a and k_X were modified using the observed values of ν_2 and ν_5 in order to obtain better agreement between the calculated and observed values of ν_2. This procedure led to the force constants given in set II. The force constants given in set III (the best set) resulted when the values of k_a and k_X of set I were used with the observed value of ν_2 for the A_1 vibrations in order to determine a value of k_{Xa} different from zero. For methylchloroacetylene only one set of force constants was determined since the value of ν_5 for the A_1 vibrations had not been observed.

In Table IV the calculated values for the fundamental frequencies are given for methylchloroacetylene, methylbromoacetylene, methyliodoacetylene, methyldeuteroacetylene, and methylacetylene. For the methylhaloacetylenes, calculated frequency values are given for the various sets of force constants in Table III, and the calculated frequency values for methyldeutero-

[8] L. R. Maxwell, J. Opt. Soc. Am. **30**, 390 (1940).

acetylene and methylacetylene are given for comparison. Observed values for the fundamental frequencies also are given in Table IV for all the compounds, with the exception of methyldeuteroacetylene for which neither the Raman nor the infra-red spectrum could be found in the literature. The observed values for the methylhaloacetylenes are those given by Cleveland and Murray,[1] while those given for methylacetylene were taken from Table II.

As a result of these calculations, one comes to several interesting conclusions. First, it appears that if one desires reasonable calculated values for the fundamental frequencies of the methylhaloacetylenes, the force constant k_{Xa} need not be used in the calculations. The influence of this force constant seems to increase with increasing atomic weight of the X atom, since this constant had its greatest value for methyliodoacetylene and was zero for methylacetylene. Secondly, in the series of molecules studied in this investigation, in which only one atom is changed from compound to compound, it is possible to transfer most of the force constants from one molecule to another of the series, for of the thirteen force constants required for the potential energy function, eight could be transferred directly from methylacetylene. Furthermore, it is interesting to note that the value of k_a determined for methylacetylene (15.799×10^5 dynes/cm) is almost the same as the mean value (15.785×10^5 dynes/cm) for this constant obtained from the values given by Herzberg[9] for C_2H_2 and C_2D_2.

Also, one can observe the behavior of the fundamental frequencies as the X atom is changed. The methyl group frequencies ν_1 and ν_3 of the A_1 type vibrations and ν_1, ν_2, and ν_3 of the E type vibrations do not change much in going from one molecule to another in the series. This is true of the calculated values as well as for the observed values for these frequencies. The C≡C stretching frequency (ν_2 of type A_1) shows a peculiar behavior; starting with a value of 2146 cm^{-1} for methylacetylene it falls to 2009 cm^{-1} for methyldeuteroacetylene and then, despite the increased mass, jumps to 2261 cm^{-1} for methylchloroacetylene, after which it gradually falls off again, as the mass is increased, from this value to 2197 cm^{-1} for methyliodoacetylene. The effect of replacing the acetylenic hydrogen atom with a deuterium atom is to lower this frequency about 137 cm^{-1} and this shift is due solely to a change in mass since the same force constants, bond distances, and bond angles were used for methylacetylene and methyldeuteroacetylene. It had been hoped that the fundamental frequencies for methylfluoroacetylene could be calculated, but because of considerable uncertainty as to the value of the C−F stretching force constant (k_X) and since data for both the Raman and the infra-red spectrum of this molecule could not be found in the literature, no calculations were made for this molecule. This was unfortunate since the value of the C≡C stretching frequency for this molecule should be very interesting because of the 254 cm^{-1} increase in this frequency in going from methyldeuteroacetylene to methylchloroacetylene. The C−C stretching frequency (ν_4 of type A_1) also exhibits interesting behavior. While the calculated value of this frequency for methyldeuteroacetylene is somewhat less than the observed value for methylacetylene, the calculations for methyl-

TABLE VIII. A tentative assignment of the observed Raman frequencies of a solution of methylchloroacetylene in ethylbromide.*

Solution		C_2H_5Br		
$\Delta\nu$	I	$\Delta\nu$	I	Assignment and symmetry
184	3			E Fundamental
±293	4	292	30	C_2H_5Br line
±353	35			E Fundamental
439	2			1029 − 579 = 450; E
564	40	560	100	C_2H_5Br line
579	(not observed)			A_1 Fundamental
842	*vw*			1029 − 184 = 845; A_1+A_2+E 293 + 564 = 857; C_2H_5Br line
955	*vw*	960	10*b*	C_2H_5Br line
1029	*vw*	1027	00	E Fundamental C_2H_5Br line
(1068)	*vw*	1069	10	C_2H_5Br line
1078	(not observed)			A_1 Fundamental
1152	2			2926 excited by Hg 4047
1246	3	1248	20*b*	C_2H_5Br line
1380	7			A_1 Fundamental
1449	7	1442	20*b*	E Fundamental C_2H_5Br line
1637	2			due to olefinic impurity
2102	1			1029 + 1068 = 2097; C_2H_5Br line 1029 + 1078 = 2107; E
2134	2			2(1078) = 2156; A_1 2(1068) = 2136; C_2H_5Br line
2235	11			2926 − 2(353) = 2220; A_1+E (2263 + 353) − 353; A_1+A_2+E
2263	20			A_1 Fundamental
2733	2			2(1380) = 2760; A_1
2864	18	2866	30	2(1449) = 2898; A_1+E C_2H_5Br line
2926	100	2924	50	A_1 Fundamental C_2H_5Br line
2971	35	2960 2980	40 30*b*	E Fundamental C_2H_5Br line

* The symbols used in this table have the same meaning as those used in Table VI.

[9] Reference 5, p. 189.

chloroacetylene indicate a large increase in the value for this frequency, 914 to 1078 cm^{-1}, in going from methyldeuteroacetylene to methylchloroacetylene. Again, the behavior of this frequency for methylfluoroacetylene should prove to be interesting. This frequency appears to decrease for the other methylhaloacetylenes investigated since for methylbromoacetylene and methyliodoacetylene the calculated values are 1034 and 1008 cm^{-1}, respectively. However, for all the methylhaloacetylenes studied the calculated value of this frequency was greater than the observed value for methylacetylene. Unfortunately, for reasons given in the next section in connection with the frequency assignments, one does not have good observed values for this frequency for the methylhaloacetylenes to compare with the calculated values, so one cannot be certain as to how much of this variation is due to deviations of the calculated values from the actual values.

The type E bending frequencies (ν_4 and ν_5) do not exhibit very unusual behavior for the methylhaloacetylenes. After a sudden change from methylacetylene to methyldeuteroacetylene, the value of ν_5 changes slowly and has its lowest value for methyliodoacetylene. Although ν_4 appears to remain fairly constant for all of the molecules considered, the calculated value of this frequency for methyldeuteroacetylene seems to indicate a lower value than for methylacetylene.

No unusual behavior is shown by the type A_1, C−X stretching frequency ν_5, since it has its greatest value (3429 cm^{-1}) for methylacetylene when the X atom is the lightest, and its lowest value (163 cm^{-1}) for methyliodoacetylene when the X atom is the heaviest. As a final comparison, the values of the C−X stretching frequencies for the methyl halides are compared with the corresponding frequencies for the methylhaloacetylenes in Table V. Also given in Table V are the equilibrium values for the C−X bond distances and the C−X stretching force constants (k_X) for the methyl halides and the corresponding methylhaloacetylenes. The values of the C−X stretching frequencies and force constants for the methyl halides were obtained from Crawford and Brinkley,[10] while the equilibrium values for the C−X bond distances for the methyl halides were taken from Simmons, Gordy, and Smith.[11] It is seen that for all the methylhaloacetylenes investigated, the C−X stretching force constant is much greater than for the corresponding methyl halide. This would indicate smaller C−X bond distances for the methylhaloacetylenes and such is indeed the case for all the methylhaloacetylenes studied. Finally, in every case investigated, the C−X stretching frequency for the methyl halides is greater than the corresponding frequency for the methylhaloacetylenes, despite the fact that the C−X stretching force constant for the methylhaloacetylenes is always considerably greater than the corresponding force constant for the methyl halides.

ASSIGNMENTS OF THE FREQUENCIES

After the values for the fundamental frequencies of the methylhaloacetylenes had been established by the calculations, it was possible to check the assignments of Cleveland and Murray[1] for methylbromoacetylene and methyliodoacetylene and also to make tentative assignments for the observed Raman frequencies of methylchloroacetylene. In their assignments Cleveland and Murray chose the Raman frequency near 690 cm^{-1} as the type A_1, C−C stretching frequency. However, the calculations indicate that this frequency is near 1000 cm^{-1} for both of the molecules and that the 690 cm^{-1} frequency is more likely to be the first overtone of the strong 343 cm^{-1}, type E, bending frequency. A few other changes in their assignments are necessary since a new value for ν_4 of the A_1 vibration type can now be used. Hence, in Tables VI and VII new assignments are given of their observed Raman frequencies for methylbromoacetylene and methyliodoacetylene. Also, a knowledge of the calculated values for the fundamental frequencies of methylchloroacetylene made it possible to arrive at the tentative assignments of the observed Raman frequencies for this molecule given in Table VIII. Since the Raman spectrum of methylchloroacetylene was obtained in ethylbromide solution, the observed Raman frequencies for ethylbromide also are given in Table VIII so that the solvent lines

[10] B. L. Crawford, Jr., and S. R. Brinkley, Jr., J. Chem. Phys. **9**, 69 (1941).

[11] J. W. Simmons, W. Gordy, and A. G. Smith, Phys. Rev. **74**, 243 (1948).

can be identified. The observed values for the Raman frequencies of ethylbromide were taken from Kohlrausch.[12]

It appears from Tables VI–VIII that there were good reasons for not observing the type A_1, C−C stretching frequency for all of the methylhaloacetylenes considered in this investigation. For methylbromoacetylene and methyliodoacetylene the calculated value of this frequency falls close to the observed value of the type E methyl group frequency at about 1025 cm^{-1}. Hence, it is possible that the two frequencies were not resolved so that the type A_1, C−C stretching, frequency was not reported. In the case of methylchloroacetylene the calculated value of this frequency (1078 cm^{-1}) lies very close to the 1068 cm^{-1} line of the solvent. Again, it is possible that the two lines were not resolved so that the C−C stretching frequency was not observed. For a similar reason the 579 cm^{-1} type A_1, C−Cl stretching frequency may not have been reported because this calculated value is near the observed value for the second strongest line (564 cm^{-1}) of ethylbromide.

It will be noticed that in Tables VI–VIII several assignments are given for some of the lines. This was necessary because for a given line each assignment seemed reasonable and there was no way of eliminating any of the extra assignments. Also, for methylchloroacetylene one has to consider possible solvent lines so that even more assignments result for a given line.

For all of the methylhaloacetylenes investigated, the type A_1 methyl group frequency at about 2920 cm^{-1} seems to be undergoing a Fermi resonance interaction with the first overtone of the 1440 cm^{-1}, type E, methyl group frequency. Similar behavior of this A_1 fundamental frequency also was reported by Crawford[4] for methylacetylene. If an attempt is made to correct the observed value of this A_1 fundamental frequency using the observed values of the relative intensities for the two lines, one finds only a small correction is necessary. Hence, no correction of ν_1 for the type A_1 vibrations was made for any of the methylhaloacetylenes. Although the intensity of the overtone is increased somewhat as a result of the Fermi resonance, the A_1 fundamental is so strong that only a small shift in the value of the A_1 fundamental results. For methylchloroacetylene the intensity of the overtone is much greater than for the other methylhaloacetylenes investigated, but one must remember that some of this increased intensity may be due to a solvent line which also is found in the same region as the overtone. So for this reason it is hard to determine how much the A_1 fundamental has been shifted by Fermi resonance for this molecule.

The second line observed in the triple bond region (*ca.* 2200 cm^{-1}), which is always lower than the C≡C, type A_1, stretching frequency for the methylhaloacetylenes, has been given two possible assignments. One explanation is that this line results from a difference tone which involves the type A_1 methyl group frequency at about 2920 cm^{-1} and the first overtone of the 345 cm^{-1} type E bending frequency. Otherwise, this line might result from a $(\nu_i+\nu_k)-\nu_k$ type of difference tone. In this case ν_i would be the 2200 cm^{-1} type A_1 C≡C stretching frequency and ν_k would be the type E bending frequency at about 345 cm^{-1}. Such an assignment for a similar line in the triple bond region for methylacetylene was proposed by Herzberg.[13] Since it does not seem possible to decide which of these two assignments is the most reasonable, both have been given. On the other hand, one might associate the second line with the C^{13} isotope effect, but for methyliodoacetylene and methylbromoacetylene only a shift of 15 cm^{-1} was observed, which is less than the isotope shift for methylacetylene of 25 or 50 cm^{-1} as given by Cleveland and Murray.[14] Hence it does not appear that such an assignment would be reasonable. While the shift for methylchloroacetylene is 32 cm^{-1}, which is near the lower value given by Cleveland and Murray, it seems odd that the isotope shift should be observed for the case where a solution was used and therefore fewer molecules were present, and not in the case where the compounds were used alone in the liquid state. So even for methylchloroacetylene it does not seem reasonable to assign the second

[12] K. W. F. Kohlrausch, *Ramanspektren* (J. W. Edwards, Ann Arbor, Michigan, 1945), p. 239.

[13] Reference 5, p. 267, 338.

[14] F. F. Cleveland and M. J. Murray, J. Chem. Phys. 9, 391 (1941).

line to the C^{13} isotope shift of the C≡C stretching frequency.

In conclusion, it seems worth while to indicate that it is desirable to obtain the Raman spectra of methyldeuteroacetylene, methylfluoroacetylene, and a solution of methylchloroacetylene in a solvent other than ethylbromide. In this way one might see whether the unusual behavior predicted for some of the fundamental frequencies, as a result of the calculations, actually occurs. Also, if the near infra-red absorption spectra of methyldeuteroacetylene and the methylhaloacetylenes could be obtained, they might furnish more information about the value of the C−C stretching frequency for these molecules, since the calculations indicate that this frequency is somewhat greater for the methylhaloacetylenes than for methylacetylene or methyldeuteroacetylene.

ACKNOWLEDGMENTS

The author wishes to express his appreciation to Dr. Forrest F. Cleveland for discussions which have been of help in preparing this paper. He also wishes to thank Mr. Robert Natkin for checking some of the calculations.

THE JOURNAL OF CHEMICAL PHYSICS VOLUME 16, NUMBER 10 OCTOBER, 1948

Low Frequency Dispersion in Ionic Crystals*

R. G. BRECKENRIDGE
Laboratory for Insulation Research, Massachusetts Institute of Technology, Cambridge, Massachusetts

(Received May 10, 1948)

A new region of anomalous electrical response has been observed at low frequencies in ionic crystals that have been treated to introduce relatively large number of lattice defects. The crystals thus far studied include various alkali halides and silver chloride. The effect is attributed to a jumping of the positive ions to vacant lattice sites under the influence of the applied field. This jumping is observed as a relaxation process, producing a change in the dielectric constant which is small and frequently within the limits of error of measurement, and an associated peak in the dielectric loss tangent which is readily measurable. This maximum of tan δ has been studied both as a function of frequency at a fixed temperature and as a function of temperature at fixed frequency. From the magnitude of the peak and position on the frequency or temperature scales it is possible to calculate the number of lattice defects present in the sample and the activation energy for diffusion U of the positive ion in the crystal. A knowledge of U allows a separation of the activation energy for conduction, $(W/2)+U$, into its components, thus determining W, the activation energy for hole formation.

I. INTRODUCTION

FOR many years there has been considerable interest in the problem of calculating the physical properties of simple ionic crystals of the alkali halide types from the properties of the ideal crystal structure revealed by x-ray investigations. The classical work of this type, primarily due to Born,[1] was reasonably successful in predicting the dielectric constants of the alkali halides in terms of two contributions to the polarizability: one electronic α_e arising from the distortion of the electron clouds of the individual ions relative to their nuclei, and the other atomic α_a arising from the displacement of positive and negative ions relative to each other. Since the resonance frequencies of the electronic motions lie in the visible or ultraviolet region, and those for the ionic motions lie in the infra-red, both far removed from the range of ordinary electrical measurements, it is anticipated that a dielectric constant independent of frequency and accompanied by very small losses should be observed.

There are, however, a number of other properties of such crystals that cannot be satis-

* This work was sponsored jointly by the Office of Naval Research and the Army Signal Corps, under Contract N5ori-78, T.O. 1.

[1] M. Born and M. Goeppert-Mayer, *Handbuch der Physik* (1933), second edition, Vol. 24/2, p. 639.

factorily accounted for by the simple picture of a perfectly regular structure of polarizable ions: e.g., the electrical conductivity, self-diffusion, and the various color centers. It has been established by the work of Frenkel[2] and Wagner and Schottky[3] that a real crystal contains a large number of lattice defects either in the form of interstitial ions with accompanying vacant sites (Frenkel defects) as in AgCl, or as equal numbers of vacant positive and negative ion sites (Schottky defects) as in the alkali halides. It has been demonstrated that such defects give a satisfactory explanation of the properties mentioned.

In its simplest form the theory indicates that the conductivity is expressed as[4]

$$\sigma = C[N(ea)^2/kT]\nu_0 \exp\{-[(W/2)+U]/kT\}, \quad (1)$$

where W is the activation energy of formation of a lattice defect and U the activation energy for its diffusion through the crystal, a is the lattice constant, ν_0 is the natural frequency of lattice vibrations, and C is a constant arising from the temperature variation of the exponential terms.

The separation of the exponential term into its component parts is of great theoretical interest since many of the crystal properties depend on one or the other term, but it has been done only in a few special cases. If the number of lattice defects is made practically independent of the temperature by chemical means, e.g., by the addition of $CdCl_2$ to AgCl, thus introducing one vacant site for each Cd^{++} ion, as was done by Koch and Wagner,[5] U may be found from the conductivity. Similarly, U may be found from self-diffusion studies using isotopic or radioactive tracers as has been done for PbI_2 by von Hevesy and Seith[6] and Mapother and Maurer for NaCl[7] since the diffusion constant

$$D = D_0 \exp(-U/kT) \quad (2)$$

contains only U. Finally, theoretical calculations of W have been made for three alkali halide crystals (NaCl, KCl, and KBr) by Mott and Littleton.[8]

While the d.c. conductivity of simple ionic crystals has been studied extensively, it has not been realized that the existence of lattice defects gives a possibility for a new mechanism of dielectric polarization that may be observed in a.c. measurements. Such an effect has now been observed in AgCl and several of the alkali halides. An interpretation of the results is presented which allows a determination of the energy U and the number of defects present.

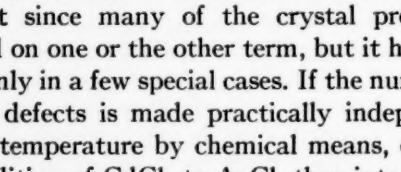

FIG. 1. Dielectric properties of NaCl crystal.

II. PROCEDURE

The measurements were made on crystals from a number of sources. The LiF, NaCl, KBr, and AgCl were commercial crystals from the Harshaw Chemical Company, Cleveland, Ohio. KI, which is not commercially available, was obtained from the same company through the courtesy of Dr. H. C. Kremers. The NaF, RbCl, RbBr, RbI, and KCl were grown by Professor A. von Hippel.

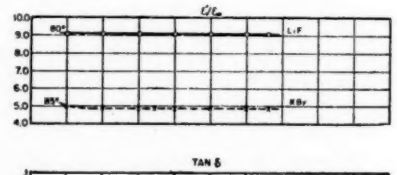

FIG. 2. Dielectric properties of LiF and KBr crystals.

[2] J. Frenkel, Zeits. f. Physik **35**, 652 (1926).
[3] C. Wagner and W. Schottky, Zeits. f. physik. Chemie **B11**, 163 (1930).
[4] W. F. Mott and R. W. Gurney, *Electronic Processes in Ionic Crystals* (Oxford University Press, New York, 1940).
[5] E. Koch and C. Wagner, Zeits. f. physik. Chemie **B38**, 295 (1937).
[6] G. von Hevesy and W. Seith, Zeits. f. Physik **51**, 790 (1929).
[7] D. Mapother and R. Maurer, Bull. Am. Phys. Soc. **23**, 31 (1948).
[8] N. F. Mott and M. J. Littleton, Trans. Faraday Soc. **34**, 485 (1938).

In order to have the a.c. effects readily observable, it was found necessary for the crystal to have a large number of defects present corresponding to an equilibrium temperature near the melting point. With the standard crystals from the Harshaw Chemical Company no further treatment was necessary, but the other crystals were heated to within 25°C of the melting point and cooled rather quickly to room temperature before measuring. The crystals, in general, were about $\frac{1}{2}''$ square and about 0.020″ thick, although the rubidium salt crystals were smaller (*ca.*

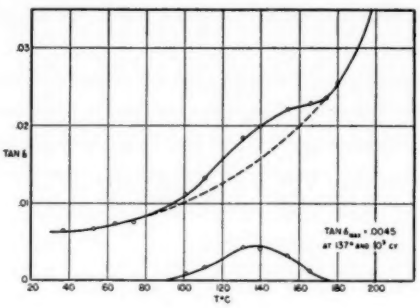

FIG. 3. Loss tangent of NaF crystal.

$\frac{1}{4}''$ square×0.010″ thick). Electrodes were applied by painting the crystal faces with du Pont Silver Paste No. 4351.

A General Radio No. 716-B capacitance bridge for audiofrequencies, a susceptance variation bridge at high frequencies, and standard sample holders were used. The temperatures were determined by a thermocouple placed adjacent to the sample using a Leeds and Northrup potentiometer. In the earlier work, the dielectric constant and loss were measured over a wide frequency range (10^2 to 4×10^7 cy/sec.) at a fixed temperature (*ca.* 85°C). This was done on LiF, NaCl, and KBr. It soon became apparent that it was much more convenient to measure the crystal properties over a wide range of temperature at a fixed frequency (usually 10^3 cy/sec.), and this was done in subsequent work. To verify the agreement between the methods, NaCl was measured by both procedures.

While the loss tangent was the property of greatest interest, and, in fact, the only one studied in most cases, the dielectric constant was also determined on the three crystals that were measured over the wide frequency range. For the

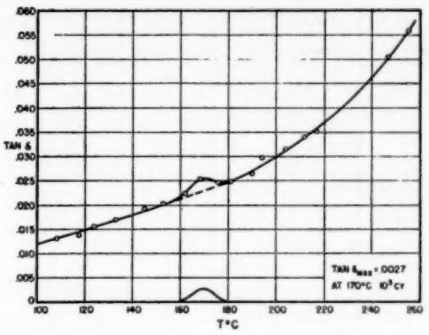

FIG. 4. Loss tangent of KCl crystal.

equipment and samples used, the probable error is about 2 percent in κ' and ±0.0003 in $\tan\delta$ on the larger samples For the Rb salts the accuracy is somewhat less, ±0.0005 in $\tan\delta$. The temperature is accurate to about 1 degree.

III. RESULTS

The results of measurements as a function of frequency are best illustrated by the values found on sodium chloride at 85°C (Fig. 1). The loss tangent shows a peak of 0.024 at 600 cycles/sec. and the dielectric constant an accompanying decrease. For LiF and KBr (Fig. 2) the height of the peak is much smaller and no effect is observed in κ'. A clearly defined maximum is seen in KBr at 2×10^4 cycles/sec. and 85°C with the value 0.0011. In LiF the maximum, also 0.0011, is at 10^4 cycles/sec., but it is superimposed on a true conduction loss which masks the dispersion loss on the low frequency side of the curve.

The measurements as a function of temperature as the independent variable are best illustrated by the results on sodium fluoride (Fig. 3). The contribution to the loss tangent from the dispersion effect of the ions is always superimposed on a loss due to conductivity, but it is possible to subtract this loss from the total, leaving only the dispersion peak. Since we are in the "structure sensitive" conduction region, the conductivity does not increase with temperature according to a simple exponential law, hence this subtraction is done graphically rather than analytically. The resultant loss peak is also shown in Fig. 3. In the case of the NaF it will be observed that the maximum value of the loss tangent, 0.0045, occurs at 137°C at a frequency of 10^3 cycles/sec.

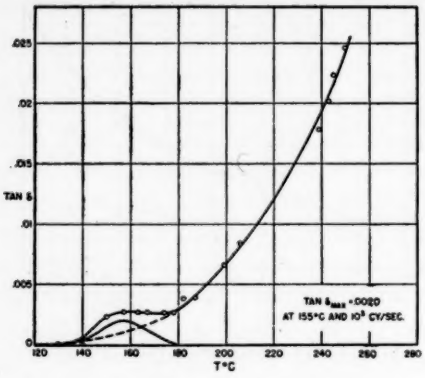

FIG. 5. Loss tangent of RbCl crystal.

Similar measurements at 10^3 cycles/sec. (Fig. 4) on KCl indicate a $\tan\delta_{max}$. of 0.0027 at 170°C, on RbCl (Fig. 5) 0.0020 at 155°C, and on RbBr (Fig. 6) 0.0017 at 57°C.

The measurements given thus far indicate that, as in the usual dipole rotation investigations, the peak may be shifted to higher frequencies by a rise in temperature or conversely. Since the bridge measurements are most easily carried out at 10^3 cycles/sec., this frequency is usually chosen. In some cases of readily mobile ions, it was found that the loss maxima occurred so far below room temperature that it was necessary to measure at higher frequencies to make the temperature range accessible. This was true for RbI and KI (Fig. 7). The measurements are somewhat less satisfactory on the iodide samples at low temperatures than on other crystals, as indicated by the scattering of the points and the less characteristic shape of the curves, but again the peak is clearly presented. The value for RbI is $\tan\delta_{max}=0.018$ at -130°C and 10^4 cycles/sec. For KI the peak was estimated to be $\tan\delta_{max}=0.03$ at -200°C and 10^4 cycles/sec., since the peak could not be completely traversed even at 10^4 cycles/sec. The results on AgCl are of particular interest (Fig. 8), since in contrast to the previous cases, it will be noted that two peaks are found for this crystal. The values are $\tan\delta_{max}=0.0003$ at -153°C and 0.0008 at -124°C and 10^3 cycles/sec.

Although the data presented here are on single samples, it should be stated that in a number of cases several crystals were studied. The magnitude of the loss peaks was found to vary, but the location of the peaks was constant within a few degrees. This was true for samples of different dimensions as well, which would eliminate the possibility of interfacial polarization effects.

IV. MECHANISM OF POLARIZATION

As a first step in the interpretation of the experimental results, it will be observed that the behavior of $\tan\delta$ and κ' is that of a typical dielectric relaxation process. Since the effect is small, in most cases the change in the real part of the dielectric constant is within the limits of error of this measurement, but it was found in NaCl. The more sensitive measurements of $\tan\delta$, however, clearly show the behavior expected in such a process.

A discussion of dielectric effects of this type has been given[9] in terms of rate processes in which it was shown that the real and imaginary parts of the specific dielectric constant are given as in the Debye calculation,

$$\kappa' = \kappa_\infty' + \frac{\kappa_s' - \kappa_\infty'}{1+(\omega\tau^*)^2},$$
$$\kappa'' = \frac{(\kappa_s' - \kappa_\infty')\omega^*}{1+(\omega\tau^*)^2}, \qquad (3)$$

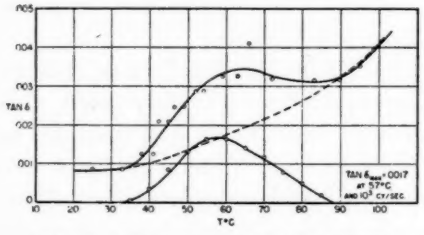

FIG. 6. Loss tangent of RbBr crystal.

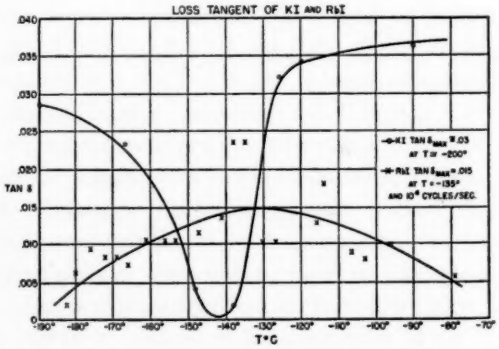

FIG. 7. Loss tangent of KI and RbI crystals.

[9] (a) S. Glasstone, K. J. Laidler, and H. Eyring, *The Theory of Rate Processes* (McGraw-Hill Book Company, Inc., New York, 1941); (b) R. Kauzmann, Rev. Mod. Phys. **14**, 12 (1942).

where $\tau^*=(\kappa_s'+2)\tau/(\kappa_\infty'+2)$ and κ_s' and κ_∞' are defined as the values of κ' for $\omega=0$ and $\omega\gg\tau$, respectively. τ is defined as the time constant for the orientation process. τ may be expressed as

$$\tau=\tau_0\exp(+U/kT), \tag{4}$$

where U is the height of the potential barrier and τ_0 is the time constant of free vibration.

These equations may be modified suitably for application to the present case. It is observed that $\kappa'\simeq\kappa_\infty'$ and $\kappa_s'+2\simeq\kappa_\infty'+2$, so that

$$\tan\delta=\frac{\kappa''}{\kappa_\infty'}=\frac{(\kappa_s'-\kappa_\infty')\omega\tau}{\kappa_\infty'[1+(\omega\tau)^2]}. \tag{5}$$

The maximum value for $\tan\delta$ is found when $\omega\tau=1$; thus from a measure of the frequency at a given temperature or vice versa for which $\tan\delta_{max}$ is found, U may be determined if we assume that τ_0 is the time constant for the natural frequency of lattice vibrations, that is,

$$2\pi\nu_m\tau_0=\exp(-U/kT_j). \tag{6}$$

Then, if this information is combined with values for the activation energy for conduction, $(W/2+U)$, values for the activation energy for hole formation, W, may be found.

The calculated values of the activation energies are given in Table I. The values of τ_0 are calculated from the natural frequencies given by Barnes[10] for the alkali halides. That for AgCl is computed from the data of Rubens,[11] using Försterling's formula[12] to find the natural frequency from the observed reststrahl frequency. The same value of τ_0 is used for both peaks. The activation energies for conduction are those given by Lehfeldt[13] for the alkali halides, RbI being estimated (Fig. 9); for AgCl, however, the data are those of Koch and Wagner,[5] so that a direct comparison may be made with their results. The τ_0 used in the calculations of U corresponds to room temperature rather than the measurement temperature. The little information available indicates a shift to lower frequencies of only a few percent between room temperature and 100°C; thus this factor can probably be neglected. A more serious difficulty is the fact that the natural frequency of an ion adjacent to a vacant site may be quite different from that of an ion in the regular structure, possibly even a factor of two lower. This would make U about 5 percent larger.

The data on the activation energies in the alkali halides are illustrated in Fig. 9 in which U, W, and $(W/2)+U$ from Table I are plotted as a function of the anion radius.

Thus far the interpretation of the results has not involved the properties of the substances being measured beyond the assignment of τ_0 as the natural frequency of lattice vibrations, since the polarization must be due to a motion of the ions of the crystal. Further progress may be made if the mechanism of polarization is detailed in terms of the nature of the lattice defects.

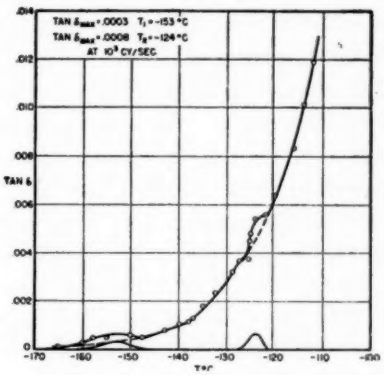

FIG. 8. Loss tangent of AgCl crystal.

In the alkali halides, the defects are of the Schottky type, so that there are equal numbers of vacant positive and negative ion sites. At temperatures below *ca.* 500°C only the positive ions are mobile, however, as has been shown by transference studies;[14] thus in this case the polarization must be attributed solely to a motion of the positive ion vacancies. It is evident that the relaxation effects observed cannot be due to an unrestricted motion of holes or interstitial ions since this process gives rise to the normal conductivity found in all cases. Instead, the polarization probably depends on the redistribution of the positive ion vacancies relative to the negative ion vacancies, or the interstitial

[10] R. B. Barnes, Zeits. f. Physik **75**, 723 (1932).
[11] H. Rubens, Sitz. Ber. Preuss. Akad. Wiss., 513 (1913).
[12] K. Försterling, Ann. d. Physik **61**, 577 (1920).
[13] W. Lehfeldt, Zeits. f. Physik **85**, 717 (1933).
[14] W. Jost, *Diffusion und Chemische Reaktion in Festen Stoffen* (T. Steinkopff, Dresden, 1937).

TABLE I.

Salt	T_j °C	ν_m cy/sec.	τ_0 sec. $\times 10^{12}$	U ev	$\frac{W}{2}+U$[13] ev	W ev	U ev
LiF	80	10^4	0.109	0.58	2.20	3.24	
NaF	137	10^3	0.135	0.74	2.25	3.02	
NaCl	85	6×10^2	0.204	0.65	1.90	2.50	0.97[8]
	114	10^3	0.204	0.68	1.90	2.44	0.77[7]
KCl	170	10^3	0.236	0.78	2.06	2.56	1.02[8]
KBr	85	2×10^4	0.294	0.53	1.97	2.88	1.01[8]
KI	(−200)	10^4	0.340	(0.11)	1.77	(3.32)	
RbCl	155	10^3	0.281	0.75	2.12	2.74	
RbBr	57	10^3	0.380	0.58	2.03	2.90	
RbI	−135	10^4	0.430	0.21	(1.84)	(3.26)	
AgCl	−153	10^3	0.31	0.21	0.80	1.20	0.26[5]
	−124	10^3	0.31	0.26	0.80	1.08	

ions relative to the vacant sites as found in the case of Frenkel defects. It seems likely that the polarizing units correspond to a pair of associated lattice defects on adjacent sites. This redistribution of charge under the influence of the external field may be described in terms of jumps of the holes over a potential barrier to the adjacent sites in the field direction, thus producing a net moment in this direction. Under a.c. excitation the moment has two possible orientations in opposite directions. The total moment may be calculated from the relative population of sites opposed to or in the field direction relative to the equilibrium distribution. This calculation is analogous to that given by Debye [15] of the moment of an assembly of permanent dipoles with two possible orientations; it was described in terms of a rate process by Kauzmann.[9b] As a simple picture of this process, we may represent the occupied site and an adjacent vacant site at a distance, a, which is of the order of the normal lattice constant as a double potential well, the heights of the two wells being altered by the applied field as in Fig. 10.

If the moment of a moving charge Ze in one potential well is

$$\mu_0 = Zea, \tag{7}$$

the total moment M will be

$$M = \mu_0(n_1 - n_2), \tag{8}$$

where n_1 is the number of ions in the direction opposed to the field and n_2 is the number in the field direction.

The values of n_1 and n_2 may be found from the equations for change of these quantities with time, assuming a Boltzmann distribution between the wells:

$$\begin{aligned} 2\tau(dn_1/dt) &= -n_1 \exp(-ZeaF/2kT) \\ &\quad + n_2 \exp(+ZeaF/2kT), \\ 2\tau(dn_2/dt) &= n_1 \exp(-ZeaF/2kT) \\ &\quad - n_2 \exp(+ZeaF/2kT). \end{aligned} \tag{9}$$

F is the locally acting field which varies sinusoidally as $F = F_0 \exp(j\omega t)$. τ is the same time constant previously considered. Following the method of solution given by Debye, it is found that the average moment $\bar{\mu}$ per potential well is

$$\bar{\mu} = (1/1+j\omega\tau)[(Zea)^2F/kT]; \tag{10}$$

hence its polarizability is

$$\alpha_j = (1/1+j\omega\tau)[(Zea)^2/kT]. \tag{11}$$

A completely satisfactory relation between dielectric constant and polarizability in a crystal is not available, hence the Clausius-Mossotti equation is generally used, so that

$$\frac{\kappa^*-1}{\kappa^*+2} = \frac{N}{3\epsilon_0}\left(\alpha_e+\alpha_a+\frac{n}{N}\alpha_j\right), \tag{12}$$

where n is the number of polarizing units. Since we are dealing with materials of relatively low κ', the choice of the relation is not critical. The use of the Drude equation as a limiting case would introduce a factor of about 7 in the result while some intermediate value is probably the correct one. From Eq. (12) the values of $\kappa_s'-\kappa_\infty'$ needed in Eq. (3) may be readily found in terms of the jump polarizability.

$$\frac{\kappa_s'-1}{\kappa_s'+2} = \frac{\kappa_\infty'-1}{\kappa_\infty'+2} + \frac{n(Zea)^2}{3\epsilon_0 kT}, \tag{13}$$

so

$$\kappa_s'-\kappa_\infty' \equiv \frac{n(Zea)^2}{9\epsilon_0 kT}(\kappa_s'+2)(\kappa_\infty'+2), \tag{14}$$

which is given as

$$\kappa_s'-\kappa_\infty' \simeq \frac{n(Zea)^2(\kappa_\infty'+2)^2}{9\epsilon_0 kT} \tag{15}$$

to the same approximation as used for Eq. (5). The maximum value of $\tan\delta$ is then given by

$$\tan\delta_{\max} = \frac{n(Zea)^2(\kappa_\infty'+2)^2}{18\epsilon_0 kT\kappa_\infty'}. \tag{16}$$

[15] P. Debye, *Polar Molecules* (Chemical Catalog Company, New York, 1929).

In these equations rationalized m.K.S. units have been used so that n is the number of lattice defects per cubic meter; the lattice constant a is in meters; the dielectric constant of free space ϵ_0 is 8.865×10^{-12} farad per meter; the electronic charge e is 1.59×10^{-19} coulomb; and Boltzmann's constant k is 1.38×10^{-23} joules per degree.

The values of n calculated for the various salts using Eq. (16) are given in Table II. The values of κ_∞' used for LiF, NaCl and KBr were those measured in these experiments. The others are those given by Højendahl.[16]

In the case of Frenkel defects, either the interstitial ion or the hole or both may be mobile. As pointed out by Mott and Gurney,[4] there seems no easy way of deciding which would be more mobile, although it would seem likely to be the hole. This would, of course, be identical with the behavior of the Schottky defect. If the interstitial ion is actually the more mobile, the ionic jump would be one lattice distance to the next stable interstitial position in the field direction so that the effect would again be describable by the previous model.

It is formally possible to calculate the mobility of the polarizing units with the information at hand. In view of the differences expected in the energy and constant terms for the mobility in the conduction or reorientation process, however, it seems that the calculation would be fruitful only in terms of a more detailed model. It is planned to investigate this further at a later date.

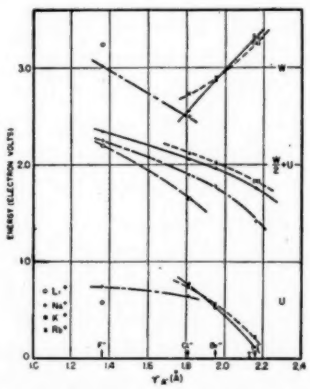

FIG. 9. Activation energies of the alkali halides.

[16] K. Højendahl, Kgl. Danske Vid. Sels. Math.-fys. Medd **16**, No. 2 (1938).

V. DISCUSSION

A. The Activation Energies in the Alkali Halides

It will be noted that the values of U are of reasonable magnitude, although not in complete agreement with the calculated values obtained by Mott and Littleton.[8] These authors estimate an accuracy of 10 percent in the computed W, with somewhat less accuracy in U, while the experimental values found for U are about 30 percent higher. While the previously mentioned corrections are in the direction of improved agreement, it does not seem that this much difference can be accounted for. It is likely that the U values found by this method ought to differ from those of Mott and Littleton. Their calculation assumed that the lattice defects are widely separated while the relaxation effect depends on a coupling between holes of opposite sign which would modify the energy. The agreement with the experimental results of Mapother and Maurer[7] is reasonably good, which indicates that the results of Mott and Littleton are somewhat too high.

The systematic variation of U from salt to salt is illustrated in Fig. 9. As pointed out by Lehfeldt,[13] there are two important factors contributed to U. First, there is a purely steric effect so that U diminishes as the ratio of the cation to anion radius decreases, which is clearly in evidence. Secondly, the polarizability of the cation increases with increasing cation radius. The larger ions then may be more readily distorted, thus requiring less energy to pass between the neighbors to the vacant site than if it were a hard sphere. Thus the rubidium salts have values

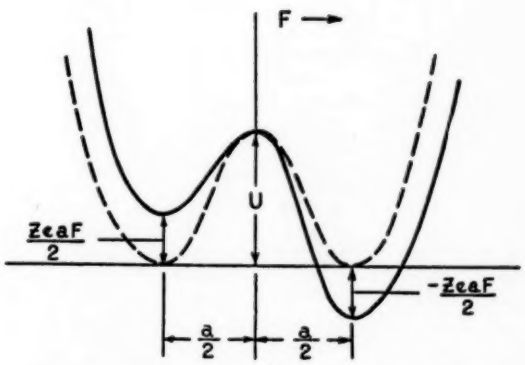

FIG. 10. Schematic potential for ionic motion in an electrical field.

of U which are almost the same as for the potassium salts in all the measured crystals, even though the normal ion radius is larger.

This type of measurement may be easily extended to more complicated cases. Although the interpretation becomes more difficult, it seems from experiments in progress that activation energies for the motion of foreign ions in crystals or for mixed crystals with a diffusing ion in common may be measured equally readily. These experiments will be described in a subsequent paper.

B. Lattice Defects and Activation Energies of Hole Formation in the Alkali Halides

The figures for the number of polarizing units present in the samples, while they are not characteristic but depend on the prehistory of the crystal, are, none the less, of interest. The data show that a crystal may have somewhat more defects than previously had been thought likely. Seitz[17] had estimated that, at the melting point, NaCl might have about 10^{22} holes per cubic meter. This value was based on d.c. conductivity data alone. More recent studies on F centers[18] have suggested that this estimate was too low and that 10^{24} defects per cubic meter could be produced easily in evaporated layers. This being the case, the value of 2.1×10^{23} is not unreasonable. A crystal containing this number of lattice defects is obviously not in thermodynamic equilibrium; the value instead corresponds to a temperature close to the melting point. It may seem remarkable that such an unstable condition could be frozen in, but when it is realized that the crystals, particularly those from Harshaw, are obtained from the melt in a rather large block and that the only mechanism for the disappearance of Schottky defects is the diffusion of the holes to the crystal surface, which would be a very slow process at room temperature in a large sample, the large number of defects becomes reasonable. Heating the small samples used for dielectric measurements for a short time at 500°C is sufficient to destroy the effect since the equilibrium concentration of defects is quickly reached and is too small to be readily observable. Because the disappearance of the defects also depends on the diffusion mechanism, it seems that a study of the time decay of the loss should also give a measure of the activation energy of diffusion. It is planned to investigate this further.

TABLE II.

Salt	κ'	$\tan\delta_{max}$	$n\times10^{-23}$ No./m^3	$N\times10^{-28}$ No./m^3	$\frac{n}{N}\times10^6$
LiF	9.11	0.0011	0.15	6.07	0.25
NaF	6.00	0.0045	0.70	4.00	1.7
NaCl	5.90	0.024	2.1	2.26	9.4
	5.90	0.0014	0.15	2.26	0.67
KCL	4.68	0.0027	0.27	1.61	1.7
KBr	4.90	0.0011	0.081	1.40	0.58
KI	4.94	(0.03)	(0.4)	1.14	(4.)
RbCl	5.0	0.0020	0.17	1.36	1.3
RbBr	5.0	0.0017	0.10	1.12	0.93
RbI	5.0	0.018	0.40	1.01	4.0
AgCl	12.3	0.0003	0.006	2.36	0.03
	12.3	0.0008	0.03	2.36	0.1

The importance of measurements of the number of defects to related fields, e.g., the color centers or electron trapping in crystal counters, is evident. Unfortunately, the interpretation of the measured n is made difficult by the fact that the mechanism of polarization is not completely described by the simple model. A more general treatment of the polarizability of a lattice containing defects is in progress and it is hoped that this study will give a clearer insight into the true situation in such crystals.

When a comparison is made of the calculated values of Mott and Littleton for W with the results in Table I, a difference is found that parallels that found for the U values. The experimental figures are about 25 percent higher for the chlorides and 50 percent higher for the bromides. This difference is accentuated by the fact that the observed values seem to pass through a minimum for the chlorides and so larger differences are expected for the other salts.

This minimum is not entirely unexpected, as can be seen from a simple calculation of the activation energies of hole formation given by Jost.[19] This author pointed out that the energy of hole formation could be computed from the difference of the lattice energy W_L, which is known, and the polarization energy of the crystal

[17] F. Seitz, *Modern Theory of Solids* (McGraw-Hill Book Company, Inc., New York, 1941).
[18] F. Seitz, Rev. Mod. Phys. **18**, 384 (1946).
[19] W. Jost, J. Chem. Phys. **1**, 466 (1933).

when the defect is formed. If the defect is represented as a hole of radius R in a continuous homogeneous medium of dielectric constant κ_∞',

$$W = W_L - (e^2/2R)[1-(1/\kappa_\infty')]. \quad (17)$$

The radius of the cavity, R, must be considered as an arbitrary parameter, but, if it is of the order of a lattice distance a, appropriate values of W are obtained. Both the lattice energy and the polarization energy decrease as the anion size increases, but not necessarily at the same rate.

We may, of course, calculate the values of R appropriate for our results. They are found to be of reasonable magnitude ranging from *ca.* 0.36a for AgCl to *ca.* 2.0a in RbBr.

The values of W found in this way are of interest in the same type of studies as the values of n previously mentioned. In addition, the depth of the electron traps is dependent on W so that we may expect to obtain further information about the color centers from the measurements.

C. Activation Energies and Lattice Defects in Silver Chloride

The results with silver chloride give the most striking evidence in favor of the general interpretation of the dispersion in terms of moving lattice imperfections. In particular, the discovery of two peaks for silver chloride, whereas only one was found for the alkali halides, is immediately explained by the nature of the Frenkel defects present in this crystal, since one peak may be assigned to the effect of the moving holes and the other to interstitial ions. The identification of the peaks with the proper process is also of interest, but, with the information at hand, seems to be uncertain. It is likely, however, that the lower peak corresponds to the migration of the holes since Mott and Littleton[8] had found that this process should require a somewhat lower energy. There is a further experiment that should identify the peaks unequivocally. Measurements on mixed crystals such as those of Koch and Wagner,[5] that contain far more vacant sites than interstitial ions, should show one peak much higher than the other, thus indicating the peak due to the holes. It is planned to carry out this experiment shortly.

In both cases there is a slight ambiguity in the experimental value of U, since there is some uncertainty in the value of τ_0 needed. As was mentioned, the same value of τ_0 was used for both processes. While, in general, the assumption that the natural lattice frequency may be used for the frequency of the defect is justified, it is true that the frequency of an interstitial ion is probably greater than the natural lattice frequency rather than less as is the case for the neighbors to a hole, so that U would tend to be decreased. If the tentative assignment on the basis of Mott and Littleton's calculation is true, these corrections would tend to make the values of U more nearly the same, so that the true values of mobilities may be very similar for holes or interstitial ions. In any case, the agreement between the experimental results of Koch and Wagner ($U=0.26$ ev)[5] and that found by this method ($U_1=0.21$ ev and $U_2=0.26$ ev) is excellent.

While the particular sample of AgCl used in Table I has relatively few lattice defects, the very low value of $W(\simeq 1.1$ ev) allows a great number of imperfections in the normal crystal. Another sample, for example, measured without preheating, was found to have 1.3×10^{23} polarizing units per cubic meter and in no case was heat treatment needed to make the effect measurable.

ACKNOWLEDGMENT

The author wishes to thank the Measurements Group, directed by W. B. Westphal, of the Laboratory for Insulation Research, which carried out the dielectric measurements reported in this paper.

THE JOURNAL OF CHEMICAL PHYSICS VOLUME 16, NUMBER 10 OCTOBER, 1948

The Transport Properties for Non-Polar Gases*

JOSEPH O. HIRSCHFELDER, R. BYRON BIRD, AND ELLEN L. SPOTZ
Department of Chemistry and Naval Research Laboratory, University of Wisconsin, Madison, Wisconsin

(Received May 5, 1948)

Chapman and Cowling have related the coefficients of viscosity, diffusion, thermal diffusion, and heat conductivity to a set of integrals, $\Omega_n^{(l)}(T)$ involving the law of force between pairs of molecules. We have evaluated these integrals for $l=1$, $n=1, 2, 3$; $l=2$, $n=2, 3, 4, 5, 6$; $l=4$, $n=4$, assuming that the energy of attraction is inversely proportional to the sixth power of the separation and the energy of repulsion is inversely proportional to the twelfth power. This assumption is excellent for spherical non-polar molecules and a big improvement on the Sutherland assumption. The mathematical analysis was very difficult but the results are simple. The transport integrals are evaluated for all temperatures in terms of the maximum energy of interaction and the collision diameters. This gives a "corresponding states" relationship which should apply to extremely hot and extremely cold temperatures where good experimental data are not available. The molecular constants can be obtained very accurately from experimental viscosity data, and they agree with values previously obtained from equation of state data.

I. INTRODUCTION

THE general relationship between the transport properties of gases and the intermolecular forces has been known for a long time, the basic theory having been developed by Chapman, Enskog, and others. Chapman and Cowling[1] have expressed the transport coefficients in terms of a set of integrals which they call $\Omega^{(l)}(n)$. Up to this time the actual evaluation of these integrals and the calculation of the transport properties as functions of temperature have been accomplished only for a certain few simple molecular models, in which the laws of interaction are quite artificial and unrealistic. The role of the interaction law in determining the coefficient of viscosity is not too important; however, other properties, such as thermal diffusion, are exceedingly sensitive to the form of the potential.

In this report, the transport coefficients are evaluated, making use of a more realistic law of interaction. The form selected for the potential is the one which has proven very satisfactory in explaining the equation of state data for simple non-polar gases:

$$E(r)=4\epsilon[-(r_o/r)^6+(r_o/r)^{12}], \qquad (1)$$

in which r = the separation between the molecules, r_o = the separation for which the energy of interaction is zero (i.e., collision diameter for low velocity head-on collisions), ϵ = energy difference between the separated molecules and the molecules in the configuration for which they have the maximum energy of attraction. The inverse sixth-power form for the energy of attraction represents faithfully the induced dipole-induced dipole interaction between two non-polar molecules. The inverse twelfth-power form for the repulsive component is a rough approximation to the exponential form required from quantum-mechanical considerations. The values of ϵ and r_o are obtainable from equation of state data and second virial coefficients.

Using the potential function in Eq. (1), it is possible to derive an expression for the angle of deflection, χ, of two colliding molecules; the development of a formula for χ is straightforward and follows from standard dynamical considerations. But the integration of the particularly awkward hyper-elliptic integrals which result is a major problem. Each collision, and hence each value of χ, is characterized by two parameters: K = the relative kinetic energy at large separations of the colliding molecules along the line of centers in units of ϵ [see Eq. (22)]. β = distance of closest approach in units of r_o if there were no interaction between molecules [see Eq. (23)].

The reduced collision cross sections, $S^{(l)}(K)$,

* This work was carried out under Contract NORD-9938 between the Navy Bureau of Ordnance and the University of Wisconsin.

[1] S. Chapman and T. G. Cowling, *Mathematical Theory of Non-Uniform Gases* (Cambridge University Press, Teddington, 1939).

are then determined by[2]

$$S^{(l)}(K)=4\Big/\left[2-\frac{1+(-1)^l}{1+l}\right]\times\int_0^\infty[1-\cos^{(l)}\chi]\beta d\beta. \quad (2)$$

The functions, $S^{(l)}(K)$, are variously defined collision cross sections divided by πr_o^2, the latter being the cross section for rigid molecules of collision diameter r_c. Hence, for rigid spheres the values of the $S^{(l)}(K)$ are unity. The usual transport cross section corresponds to $l=2$; other kinetic theory properties require $l=1$, 4, etc.

Next the functions $W^{(l)}(n;x)$ are obtained from

$$W^{(l)}(n;x)=\frac{1}{8}\left[2-\frac{1+(-1)^l}{1+l}\right]x^{n+2}\times\int_0^\infty e^{-xK}K^{n+1}S^{(l)}(K)dK, \quad (3)$$

in which

$$x=\epsilon/kT, \quad (4)$$

where k is Boltzmann's constant. The $W^{(l)}(n;x)$ are related to the $\Omega^{(l)}(n)$ of Chapman and Cowling by

$$\Omega^{(l)}(n)=r_o^2\left(\frac{2\pi kT}{\mu}\right)^{\frac{1}{2}}W^{(l)}(n;x). \quad (5)$$

The values of $W^{(l)}(n)$ for various values of kT/ϵ are presented in Table I. In Eq. (5), μ is the reduced mass of the colliding molecules,

$$\mu=m_1m_2/(m_1+m_2). \quad (6)$$

Here the m_1 and the m_2 are the molecular weights of the colliding molecules divided by Avogadro's number.

The mechanical accuracy of the $W^{(l)}(n;x)$ is of the order of one part in three hundred, but there are certain physical limitations to their validity. First of all, the calculations were made on the basis of classical mechanics, and therefore it is to be expected that quantum corrections must be added at the lowest temperatures. Secondly, the form for the energy of interaction is substantially correct but not precisely accurate —for example, the energy of repulsion between helium atoms should increase less rapidly than the inverse twelfth power of the separation. And finally, all of the collisions are supposed to be elastic—an assumption which is valid for the noble gases but not altogether true for polyatomic molecules where the transfer of energy from translation to rotations and vibrations sometimes takes place. This latter effect is of considerable importance with respect to heat conductivity but does not seem to affect viscosity.

The coefficient of viscosity, η, of a pure component can be written in the form:

$$\eta=(5/(8r_o^2))(\mu kT/(2\pi))^{\frac{1}{2}}[V/W^{(2)}(2)]. \quad (7)$$

Here V is a slowly varying function of kT/ϵ given in Table II. It can be expressed in terms of the Chapman and Cowling "b_{ij}" by the relation:

$$V=\left[1+[b_{12}^2/(b_{11}b_{22}-b_{12}^2)]+\frac{b_{11}(b_{12}b_{23}-b_{22}b_{13})^2}{(b_{11}b_{22}-b_{12})^2(b_{11}b_{22}b_{33}+2b_{12}b_{13}b_{23}-b_{12}^2b_{33}-b_{23}^2b_{11}-b_{13}^2b_{22})}\right]. \quad (8)$$

The values of the individual "b_{ij}" are also given in Table II. They are simply related to the $W^{(l)}(n;x)$ in the following manner:

$$\begin{aligned}
b_{11}/Q&=4W^{(2)}(2),\\
b_{12}/Q&=7W^{(2)}(2)-2W^{(2)}(3),\\
b_{22}/Q&=(301/12)W^{(2)}(2)-7W^{(2)}(3)+W^{(2)}(4),\\
b_{13}/Q&=(63/8)W^{(2)}(2)-(9/2)W^{(2)}(3)+\tfrac{1}{2}W^{(2)}(4),\\
b_{23}/Q&=(1365/32)W^{(2)}(2)-(321/16)W^{(2)}(3)+(25/8)W^{(2)}(4)-\tfrac{1}{4}W^{(2)}(5),\\
b_{33}/Q&=[(25137/256)W^{(2)}(2)-(1755/32)W^{(2)}(3)+(381/32)W^{(2)}(4)-(9/8)W^{(2)}(5)\\
&\quad+(1/16)W^{(2)}(6)+\tfrac{1}{2}W^{(4)}(4)],
\end{aligned} \quad (9)$$

in which

$$Q=r_o^2(2\pi kT/\mu)^{\frac{1}{2}}.$$

In a similar way, the coefficient of thermal conductivity, λ, may be written:

$$\lambda=[c_v+(9/4)(k/m_1)](5/8r_o^2)\times(\mu kT/2\pi)^{\frac{1}{2}}(H/W^{(2)}(2)). \quad (10)$$

Here c_v is the specific heat per gram of the gas.

[2] The $S^{(l)}(K)$ are simply related to the Chapman and Cowling functions, $\phi^{(l)}$, by the equation

$$S^{(l)}(K)=4\phi^{(l)}/gr_o^2[2-\{1+(-1)^l\}/(l+1)].$$

Here g is the initial velocity along the line of centers.

TABLE I. Collision integrals.

kT/ϵ	$\Omega^{(l)}(n)=r_0^2[2\pi kT/\mu]^{\frac{1}{2}}W^{(l)}(n)$ $W^1(1)$	$W^1(2)$	$W^1(3)$	$kT/\epsilon=1/x$ $W^2(2)$	$W^2(3)$	$W^2(4)$	$W^2(5)$	$W^2(6)$	$W^4(4)$
0.3	1.331	3.384	11.77	2.785	10.14	46.66	258.3	1672.0	61.36
0.35	1.238	3.117	10.77	2.628	9.498	43.26	237.4	1528.0	57.06
0.4	1.159	2.896	9.976	2.492	8.927	40.32	220.0	1413.0	53.36
0.45	1.092	2.712	9.333	2.368	8.419	37.78	205.6	1322.0	50.17
0.5	1.033	2.557	8.809	2.257	7.968	35.62	193.7	1248.0	47.41
0.55	0.9829	2.427	8.377	2.156	7.570	33.77	183.9	1189.0	45.01
0.6	0.9383	2.315	8.016	2.065	7.222	32.19	175.6	1139.0	42.92
0.65	0.8991	2.218	7.711	1.982	6.915	30.84	168.7	1098.0	41.09
0.7	0.8644	2.135	7.452	1.908	6.645	29.67	162.9	1064.0	39.49
0.75	0.8335	2.062	7.228	1.841	6.407	28.67	157.8	1034.0	38.09
0.8	0.8058	1.998	7.033	1.780	6.195	27.78	153.4	1009.0	36.83
0.85	0.7809	1.942	6.862	1.725	6.006	27.00	149.6	986.9	35.72
0.9	0.7585	1.892	6.711	1.675	5.838	26.32	146.3	967.5	34.73
0.95	0.7382	1.847	6.577	1.629	5.686	25.71	143.3	950.3	33.84
1.0	0.7197	1.806	6.456	1.587	5.550	25.16	140.7	935.0	33.04
1.05	0.7028	1.769	6.347	1.549	5.426	24.67	138.3	921.1	32.32
1.1	0.6873	1.736	6.248	1.514	5.315	24.23	136.2	908.8	31.66
1.15	0.6731	1.706	6.159	1.482	5.214	23.84	134.3	897.5	31.06
1.2	0.6601	1.678	6.077	1.452	5.121	23.47	132.5	887.2	30.52
1.25	0.6479	1.653	6.001	1.424	5.036	23.14	130.9	877.8	30.02
1.3	0.6367	1.629	5.932	1.399	4.957	22.84	129.4	869.1	29.57
1.35	0.6263	1.608	5.868	1.375	4.885	22.56	128.1	861.1	29.15
1.4	0.6166	1.588	5.808	1.353	4.819	22.30	126.8	853.6	28.76
1.45	0.6075	1.569	5.753	1.333	4.757	22.06	125.6	846.7	28.40
1.5	0.5991	1.551	5.701	1.314	4.699	21.83	124.5	840.1	28.06
1.55	0.5912	1.535	5.652	1.296	4.646	21.62	123.5	834.0	27.75
1.6	0.5837	1.520	5.607	1.279	4.596	21.43	122.6	828.2	27.46
1.65	0.5767	1.506	5.563	1.264	4.549	21.25	121.7	822.8	27.19
1.7	0.5701	1.492	5.523	1.248	4.505	21.08	120.8	817.7	26.93
1.75	0.5639	1.479	5.485	1.234	4.464	20.92	120.0	812.9	26.69
1.8	0.5580	1.467	5.449	1.221	4.425	20.76	119.3	808.3	26.47
1.85	0.5523	1.456	5.414	1.209	4.388	20.62	118.5	803.8	26.25
1.9	0.5471	1.445	5.381	1.197	4.353	20.48	117.9	799.7	26.05
1.95	0.5421	1.435	5.350	1.186	4.321	20.35	117.2	795.7	25.86
2.0	0.5373	1.425	5.320	1.175	4.290	20.23	116.6	791.9	25.68
2.1	0.5284	1.407	5.265	1.156	4.218	20.00	115.4	784.8	25.35
2.2	0.5203	1.390	5.213	1.138	4.179	19.79	114.3	777.9	25.04
2.3	0.5129	1.375	5.167	1.122	4.131	19.60	113.4	772.0	24.77
2.4	0.5061	1.361	5.123	1.107	4.087	19.42	112.5	766.1	24.51
2.5	0.4998	1.348	5.082	1.093	4.047	19.26	111.6	760.9	24.28
2.6	0.4939	1.336	5.044	1.081	4.009	19.11	110.8	755.7	24.06

The factor in the first parenthesis is the "Eucken correction" for the heat conductivity of molecules with internal degrees of freedom.[3] The rigorous kinetic theory is only intended to apply to the noble gases for which $c_v=3k/2m_1$. The factor, H, is a slowly varying function of kT/ϵ, given in Table III. It can be expressed in terms of the Chapman and Cowling "a_{ij}":

$$H=\left[1+[a_{12}^2/(a_{11}a_{22}-a_{12}^2)]+\frac{a_{11}(a_{12}a_{23}-a_{22}a_{13})^2}{(a_{11}a_{22}-a_{12}^2)(a_{11}a_{22}a_{33}+2a_{12}a_{13}a_{23}-a_{11}a_{23}^2-a_{22}a_{13}^2-a_{33}a_{12}^2)}\right]. \quad (11)$$

The values of the individual "a_{ij}" are also given in Table III. They are simply related to the $W^{(l)}(n,x)$ in the following manner:

$$a_{11}=b_{11},\quad a_{12}=b_{12},\quad a_{13}=b_{13},$$
$$a_{22}/Q=(77/4)W^{(2)}(2)-7W^{(2)}(3)+W^{(2)}(4), \quad (12)$$
$$a_{23}/Q=(945/32)W^{(2)}(2)-(261/16)W^{(2)}(3)+(25/8)W^{(2)}(4)-\tfrac{1}{4}W^{(2)}(5), \quad (13)$$
$$a_{33}/Q=[(14553/256)W^{(2)}(2)-(1215/32)W^{(2)}(3)+(313/32)W^{(2)}(4)-(9/8)W^{(2)}(5)+(1/16)W^{(2)}(6)+\tfrac{1}{6}W^{(4)}(4)]. \quad (14)$$

The equations for the viscosity and thermal conductivity of a pure component can be written in the convenient forms:

[3] C. F. Curtiss and J. O. Hirschfelder, *The Kinetic Theory of Multicomponent Systems of Gases* (University of Wisconsin, Madison, July 1947), CF-727. Here an attempt is made to derive this factor but its validity is somewhat questionable.

TABLE I.—*Continued.*

kT/ϵ	$W^{1}(1)$	$\Omega^{(l)}(n)=r_o^2[2\pi kT/\mu]^{\frac{1}{2}}W^{(l)}(n)$ $W^{1}(2)$	$W^{1}(3)$	$W^{2}(2)$	$W^{2}(3)$	$W^{2}(4)$	$kT/\epsilon=1/x$ $W^{2}(5)$	$W^{2}(6)$	$W^{4}(4)$
2.7	0.4885	1.325	5.008	1.069	3.974	18.97	110.1	751.0	23.86
2.8	0.4836	1.315	4.974	1.058	3.942	18.83	109.4	746.5	23.67
2.9	0.4788	1.305	4.942	1.048	3.912	18.71	108.7	742.2	23.50
3.0	0.4745	1.296	4.912	1.039	3.883	18.59	108.1	738.2	23.33
3.1	0.4703	1.287	4.883	1.030	3.857	18.48	107.5	734.3	23.18
3.2	0.4664	1.278	4.856	1.022	3.831	18.37	106.9	730.6	23.03
3.3	0.4628	1.271	4.829	1.014	3.807	18.27	106.4	727.1	22.89
3.4	0.4593	1.263	4.804	1.007	3.785	18.17	105.9	723.8	22.76
3.5	0.4560	1.256	4.780	0.9999	3.763	18.08	105.4	720.5	22.64
3.6	0.4529	1.249	4.757	0.9932	3.743	17.99	104.9	717.3	22.52
3.7	0.4499	1.243	4.735	0.9870	3.723	17.91	104.4	714.3	22.40
3.8	0.4471	1.236	4.714	0.9811	3.705	17.83	104.0	711.4	22.29
3.9	0.4444	1.230	4.693	0.9755	3.687	17.75	103.6	708.6	22.19
4.0	0.4418	1.225	4.674	0.9700	3.670	17.68	103.1	705.9	22.09
4.1	0.4394	1.219	4.655	0.9649	3.653	17.61	102.7	703.2	22.00
4.2	0.4370	1.214	4.636	0.9600	3.637	17.54	102.4	700.7	21.90
4.3	0.4347	1.209	4.618	0.9553	3.622	17.47	102.0	698.2	21.81
4.4	0.4326	1.204	4.601	0.9507	3.607	17.41	101.6	695.8	21.73
4.5	0.4305	1.199	4.584	0.9464	3.594	17.34	101.3	693.5	21.65
4.6	0.4284	1.194	4.568	0.9422	3.580	17.28	100.9	691.2	21.57
4.7	0.4265	1.190	4.551	0.9382	3.567	17.22	100.6	689.0	21.49
4.8	0.4246	1.186	4.536	0.9343	3.554	17.17	100.3	686.8	21.42
4.9	0.4228	1.181	4.521	0.9305	3.542	17.11	99.99	684.8	21.34
5.0	0.4211	1.177	4.506	0.9269	3.529	17.06	99.68	682.7	21.27
6	0.4062	1.141	4.377	0.8963	3.426	16.59	97.00	664.6	20.67
7	0.3948	1.113	4.272	0.8727	3.344	16.21	94.82	649.8	20.19
8	0.3856	1.089	4.184	0.8538	3.277	15.89	92.99	637.3	19.79
9	0.3778	1.069	4.108	0.8379	3.219	15.62	91.40	626.5	19.46
10	0.3712	1.052	4.041	0.8242	3.169	15.38	90.01	617.0	19.17
20	0.3320	0.9439	3.629	0.7432	2.864	13.90	81.40	558.0	17.38
30	0.3116	0.8863	3.408	0.7005	2.700	13.11	76.75	526.2	16.42
40	0.2980	0.8477	3.259	0.6718	2.590	12.57	73.62	504.6	15.77
50	0.2878	0.8188	3.149	0.6504	2.507	12.17	71.28	488.6	15.28
60	0.2798	0.7960	3.060	0.6335	2.442	11.86	69.41	475.8	14.90
70	0.2732	0.7772	2.988	0.6194	2.388	11.59	67.88	465.3	14.58
80	0.2676	0.7613	2.927	0.6076	2.342	11.37	66.58	456.4	14.31
90	0.2628	0.7476	2.874	0.5973	2.302	11.18	65.45	448.7	14.08
100	0.2585	0.7354	2.828	0.5882	2.268	11.01	64.45	441.9	13.87
200	0.2322	0.6605	2.540	0.5320	2.051	9.956	58.29	399.6	12.59
300	0.2180	0.6203	2.385	0.5016	1.934	9.388	54.96	376.8	11.89
400	0.2085	0.5932	2.281	0.4811	1.855	9.004	52.72	361.4	11.42

$$\eta = 2.6693\times10^{-5}(MT)^{\frac{1}{2}}(r_o(\mathrm{A}))^{-2} \times(V/W^{(2)}(2))\ (\mathrm{g/cm\text{-}sec.}), \quad (7')$$

$$\lambda = 2.6693\times10^{-5}(T/M)^{\frac{1}{2}}(r_o(\mathrm{A}))^{-2} \times(H/W^{(2)}(2))(C_v+(9/4)R) \ (\mathrm{cal./cm\text{-}sec.\text{-}deg.}). \quad (10')$$

In Eqs. (7′) and (10′) M is the molecular weight; r_o(A) is the low velocity collision diameter in angstroms; C_v is the specific heat in cal./mole deg., and R is the gas constant expressed in the same units.

The transport properties for gaseous mixtures can also be expressed in terms of the same collision integrals. The three parameters most useful in this connection are (using Chapman and Cowling notation):

$$A = W^{(2)}(2)/[5W^{(1)}(1)], \quad (15)$$

$$B = [5W^{(1)}(2) - W^{(1)}(3)]/[5W^{(1)}(1)], \quad (16)$$

$$C = 2W^{(1)}(2)/[5W^{(1)}(1)]. \quad (17)$$

The values of A, B, and C are given in Table IV. The viscosity, heat conductivity, diffusion, and thermal diffusion in mixtures can be determined for any particular case, but the formulas are not suited to any simple tabulations.

In order to use the collision integrals for any practical purposes, it is necessary to know the values of ϵ/k and r_o. Up to now they have been determined from experimental measurements of the second virial coefficient at two different temperatures. In a few cases they have been determined from the specific volume and compressibility of crystals. As a result of Eq. (7′), these constants can also be determined from measure-

TABLE II. Viscosity.

$\eta = 2.6693 \times 10^{-5}(MT)^{\frac{1}{2}}(r_o(\text{A}))^{-2}[V/W^{(2)}(2)]$ (g/cm-sec.)

kT/ϵ	b_{11}/Q	b_{12}/Q	b_{22}/Q	b_{13}/Q	b_{23}/Q	b_{33}/Q	V	$V/W^{(2)}(2)$
0.30	11.14	−0.79	45.54	−0.37	−3.4	117.5	1.0014	0.3596
0.50	9.028	−0.14	36.46	−0.27	−0.7	92.5	1.0002	0.4432
0.75	7.364	+0.07	30.00	0.00	+0.1	76.9	1.0000	0.5432
1.00	6.348	+0.01	26.12	0.10	−0.2	67.7	1.0000	0.6301
1.25	5.696	−0.10	23.61	0.12	−0.7	61.8	1.0001	0.7023
1.5	5.256	−0.200	21.90	0.12	−1.13	57.7	1.0004	0.7613
2.0	4.700	−0.355	19.67	0.06	−1.88	52.1	1.0014	0.8523
2.5	4.372	−0.443	18.35	0.03	−2.28	48.8	1.0025	0.9172
3.0	4.156	−0.493	17.47	0.00	−2.51	46.6	1.0034	0.9657
4.0	3.880	−0.550	16.32	−0.04	−2.78	43.6	1.0049	1.036
5.0	3.708	−0.570	15.61	−0.05	−2.87	41.8	1.0058	1.085
10.0	3.297	−0.569	13.87	−0.08	−2.86	37.1	1.0075	1.222
50.0	2.602	−0.461	10.94	−0.07	−2.34	29.3	1.0079	1.550
100.0	2.353	−0.419	9.89	−0.07	−2.12	26.5	1.0080	1.714
400.0	1.924	−0.342	8.09	−0.057	−1.74	21.7	1.0080	2.095

ments of viscosity as a function of temperature. The experimental technique for measuring viscosity of gases has been perfected to such a degree that the experimental errors are less than our intrinsic computational errors of one part in three hundred. This accuracy is considerably better than can be obtained for second virial coefficients. This means that the experimental measurements of viscosity provide a superior means for determining the intermolecular force constants.

The experimental viscosity measurements of Herrick Johnston and his colleagues for twelve common gases at various temperatures are shown in Table V. By adjusting the constants, ϵ/k and r_o, and using Eq. (7′) we obtained the calculated values given in this same table. These constants can be compared with those previously obtained from an analysis of second virial coefficient data; this comparison is made in Table VI. Some of the discrepancies are shockingly large, but in each of these cases the disagreement is less than the uncertainty of the constants determined from second virial data. The agreement between the calculated and the experimental viscosities in Table V is excellent for the following gases:

air, H_2, N_2, CO_2, N_2O, NO, and CH_4.

The agreement is only fair for

O_2, CO, and A.

The agreement is unsatisfactory in the cases of

Ne and He.

The poor agreement for helium should be expected, because theoretical considerations have shown that helium atoms are considerably less rigid than the inverse twelfth-power energy of repulsion would indicate; also, quantum corrections may be important at the lower temperatures.

The coefficient of diffusion, to the first approximation, depends only on collisions between unlike molecules. The temperature variation of the experimental coefficients of diffusion can therefore be used to determine the minimum energy of interaction, ϵ_{12}, and the collision diameter, $(r_o)_{12}$, between unlike molecules with considerable accuracy. The determination of these constants will be considered in a subsequent report.

TABLE III. Thermal conductivity.

$\lambda = 2.6693 \times 10^{-5}(T/M)^{\frac{1}{2}}(r_o(\text{A}))^{-2} \times [H/W^{(2)}(2)]\{C_v + (9/4)R\}$ (cal./cm-sec.-deg.)

kT/ϵ	a_{22}/Q	a_{23}/Q	a_{33}/Q	H	$H/W^{(2)}(2)$	H/V
0.30	29.29	−1.9	53.8	1.0022	0.3599	1.0008
0.50	23.29	−0.4	42.2	1.0003	0.4432	1.0001
0.75	19.26	0.0	35.3	1.0000	0.5432	1.0000
1.00	16.86	−0.2	31.2	1.0001	0.6302	1.0001
1.25	15.30	−0.5	28.7	1.0002	0.7024	1.0001
1.5	14.23	−0.75	26.9	1.0006	0.7615	1.0002
2.0	12.82	−1.21	24.4	1.0021	0.8529	1.0007
2.5	11.97	−1.45	22.9	1.0038	0.9184	1.0013
3.0	11.41	−1.59	21.9	1.0052	0.9675	1.0018
4.0	10.66	−1.75	20.5	1.0076	1.039	1.0027
5.0	10.20	−1.80	19.6	1.0090	1.089	1.0032
10.0	9.06	−1.80	17.5	1.0116	1.227	1.0041
50.0	7.14	−1.48	13.7	1.0124	1.557	1.0045
100.0	6.46	−1.34	12.4	1.0125	1.721	1.0045
400.0	5.28	−1.10	10.2	1.0125	2.105	1.0045

II. DETAILED DISCUSSION OF DERIVATIONS AND CALCULATIONS

A. The Dynamics of a Collision

The energy of interaction between colliding molecules, $E(r)$, is assumed to have the form

given in Eq. (1) with an energy of attraction varying as the inverse sixth power and the energy of repulsion varying as the inverse twelfth power of the separation. Since this corresponds to a radial law of force, it is possible to express the trajectories in the form of well-known quadratures. These quadratures cannot be expressed in analytical form and must be evaluated by numerical procedures.

Kirkwood[4] has considered the effect of collisions in which the relative kinetic energy is not sufficient to permit the molecules to separate completely. The trajectories of these "bound molecules" are periodic with orbits large compared to molecular dimensions. Kirkwood showed that such collisions do not contribute to the transport properties. In an ionic gas in which the energy of interaction varies as the inverse first power of the separation, there are a large number of "bound molecules." Since the number of molecules in a spherical shell of thickness dr at a distance r varies as r^2, if $E(r)$ decreases more rapidly than r^{-2} the fraction of "bound molecules" is small. In our case, at large distances $E(r)$ varies as r^{-6}, and the number of "bound molecules" is negligible. However, for very low energy encounters we sometimes obtain trajectories in which the molecules circle about each other for a few times at a distance of a few angstroms and separate of their own accord. In this respect they differ from Kirkwood's "bound molecules," which require the influence of a third molecule to effect the separation. Our examples of close orbiting correspond to well

TABLE IV. Constants for determination of transport properties of gaseous mixtures.

kT/ϵ	A	B	C
0.3	0.4185	0.7739	1.017
0.35	0.4246	0.7779	1.007
0.4	0.4300	0.7772	0.9995
0.45	0.4337	0.7742	0.9934
0.5	0.4370	0.7698	0.9901
0.55	0.4387	0.765	0.9877
0.6	0.4402	0.759	0.9869
0.65	0.4409	0.752	0.9868
0.7	0.4415	0.746	0.9880
0.75	0.4418	0.740	0.9896
0.8	0.4418	0.734	0.9918
0.85	0.4418	0.729	0.9947
0.9	0.4417	0.725	0.9978
0.95	0.4413	0.720	1.001
1.00	0.4410	0.715	1.004
1.05	0.4408	0.711	1.007
1.10	0.4406	0.707	1.010
1.15	0.4404	0.705	1.014
1.20	0.4399	0.701	1.017
1.25	0.4396	0.696	1.021
1.30	0.4395	0.695	1.023
1.35	0.4391	0.694	1.027
1.40	0.4389	0.692	1.030
1.45	0.4388	.689	1.033
1.50	0.4387	0.687	1.036
1.55	0.4384	0.684	1.039
1.60	0.4382	0.683	1.042
1.65	0.4384	0.682	1.045
1.70	0.4378	0.679	1.047
1.75	0.4377	0.677	1.049
1.80	0.4376	0.676	1.052
1.85	0.4377	0.676	1.054
1.90	0.4376	0.674	1.056
1.95	0.4376	0.673	1.059
2.00	0.4374	0.671	1.061
2.1	0.4375	0.670	1.065
2.2	0.4374	0.670	1.069
2.3	0.4375	0.666	1.072
2.4	0.4375	0.665	1.076
2.5	0.4374	0.664	1.079
2.6	0.4377	0.663	1.082
2.7	0.4377	0.662	1.085
2.8	0.4376	0.662	1.088
2.9	0.4378	0.661	1.090
3.0	0.4379	0.661	1.093
3.1	0.4380	0.660	1.095
3.2	0.4383	0.658	1.096
3.3	0.4382	0.659	1.099
3.4	0.4385	0.658	1.100
3.5	0.4386	0.658	1.102
3.6	0.4386	0.657	1.103
3.7	0.4388	0.658	1.105
3.8	0.4389	0.656	1.106
3.9	0.4389	0.656	1.107
4.0	0.4391	0.657	1.109
4.1	0.4392	0.655	1.110
4.2	0.4393	0.656	1.111
4.3	0.4395	0.656	1.112
4.4	0.4395	0.656	1.113
4.5	0.4396	0.656	1.114
4.6	0.4398	0.655	1.115
4.7	0.4399	0.656	1.116
4.8	0.4400	0.656	1.117
4.9	0.4402	0.655	1.117
5.0	0.4402	0.655	1.118
6	0.4413	0.656	1.125
7	0.4421	0.655	1.128
8	0.4428	0.657	1.131
9	0.4435	0.655	1.132
10	0.4441	0.657	1.134
20	0.4477	0.6569	1.137
30	0.4496	0.6569	1.138
40	0.4508	0.6574	1.138
50	0.4520	0.6567	1.138
60	0.4528	0.6569	1.138
70	0.4535	0.6574	1.138
80	0.4540	0.6573	1.138
90	0.4546	0.6575	1.138
100	0.4551	0.6569	1.138
200	0.4582	0.6568	1.138
300	0.4602	0.6573	1.138
400	0.4615	0.6571	1.138

TABLE IV.—*Continued.*

[4] John G. Kirkwood, J. Chem. Phys. **15**, 72 (1947).

TABLE V. Viscosity, η (in units 10^{-7} grams/cm-sec.).

T(°K)	Air $\epsilon/k=97.0$ $r_0=3.617$ η_{exp}[a]	η_{calc}	H_2 $\epsilon/k=33.3$ $r_0=2.968$ η_{exp}[a]	η_{calc}	N_2 $\epsilon/k=91.46$ $r_0=3.681$ η_{exp}[a]	η_{calc}	CO_2 $\epsilon/k=190$ $r_0=3.996$ η_{exp}[a]	η_{calc}	N_2O $\epsilon/k=220$ $r_0=3.879$ η_{exp}[a]	η_{calc}	NO $\epsilon/k=119$ $r_0=3.470$ η_{exp}[a]	η_{calc}
80												
100	713	702	421	416	698	687						
120	846	840	481	477	826	820					844	841
140	975	972	535	533	948	947					981	980
160	1101	1099	585	586	1068	1070					1115	1116
180	1221	1221	634	635	1183	1186			898	898	1245	1246
200	1336	1337	681	683	1295	1296	1015	1014	999	998	1371	1371
220	1448	1447	727	728	1403	1402	1112	1114	1099	1100	1493	1492
240	1556	1554	771	773	1505	1503	1209	1212	1198	1199	1610	1608
260	1659	1657	814	815	1603	1600	1303	1308	1296	1297	1711	1719
280	1756	1756	856	856	1696	1693	1400	1402	1393	1394	1838	1828
293.16	1819[b]	1819										
300	1851	1851	896	896	1786	1785	1495	1495	1489	1489	1934	1935
400	2294[d] 2342[f]	2290	1127[f]	1073	2270[f]	2202	2015[f]	1923				
500	2680[d] 2740[f]	2678	1305[f]	1237	2657[f]	2570	2450[f]	2309				
800	3613[d] 3763[f]	3680	1744[f]	1689	3493[d] 3610[f]	3528	3391[d] 3567[f]	3285				
1000	4165[d] 4349[f]	4257	1987[f]	1958	4011[d] 4066[f]	4068	3935[d] 4198[f]	3839				
1200	4631[d] 4869[f]	4761	2205[f]	2199	4452[d] 4613[f]	4554	4453[d] 4766[f]	4348				
1500	5262[d] 5524[f]	5494	2496[f]	2542	5050[d] 5247[f]	5268	5139[d] 5529[f]	5052				
5,000		12080										
10,000		18870										

T(°K)	CH_4 $\epsilon/k=136.5$ $r_0=3.822$ η_{exp}[a]	η_{calc}	O_2 $\epsilon/k=113.2$ $r_0=3.433$ η_{exp}[a]	η_{calc}	CO $\epsilon/k=110.3$ $r_0=3.590$ η_{exp}[c]	η_{calc}	Argon $\epsilon/k=124.0$ $r_0=3.418$ η_{exp}[c]	η_{calc}	Neon $\epsilon/k=35.7$ $r_0=2.80$ η_{exp}[c]	η_{calc}	Helium $\epsilon/k=6.03$ $r_0=2.70$ η_{exp}[c]	η_{calc}
80					533	523	688	649	1198	1212	821	827
100	403	393	768	757	669	657	839	814	1435	1451	947	957
120	478	472	917	910	796	788	993	979	1646	1665	1068	1086
140	560	553	1061	1059	919	916	1146	1142	1841	1867	1182	1197
160	629	630	1202	1203	1038	1040	1298	1300	2026	2054	1290	1305
180	703	707	1341	1342	1154	1160	1447	1454	2204	2231	1395	1413
200	778	780	1476	1474	1268	1274	1594	1601	2376	2396	1496	1509
220	850	852	1604	1602	1379	1384	1739	1744	2544	2558	1595	1605
240	919	921	1728	1726	1486	1489	1878	1882	2708	2713	1692	1700
260	986	987	1845	1845	1589	1591	2014	2014	2867	2862	1789	1789
280	1053	1052	1958	1959	1688	1689	2145	2143	3021	3008	1888	1877
300	1116	1116	2071	2070	1785	1784	2270	2269	3173	3149	1987	1964
400	1453[f]	1405	2644[f]	2578	2235[f]	2219						
500	1729[f]	1661	3112[f]	3031	2608[f]	2607						
800	2421[f]	2312	4115[e] 4273[f]	4183	3529[f]	3595	4621[d]	4641	5918[e]	5945	3840[e]	3665
1000	2806[f]	2687	4720[e] 4917[f]	4853	4040[f]	4168	5302[d]	5391	6800[e]	6872	4455[e]	4237
1200	3151[f]	3034	5492[f]	5457	4496[f]	4681	5947[d]	6083				
1500	3612[f]	3498	6264[f]	6264	5109[f]	5380	6778[d]	6983				

[a] H. L. Johnston and K. E. McCloskey, J. Phys. Chem. **44**, 1038 (1939).
[b] J. A. Bearden, Phys. Rev. **56**, 1023 (1939).
[c] H. L. Johnston and E. R. Grilly, J. Phys. Chem. **46**, 948 (1942).
[d] V. Vasilesco, Ann. Phys. (Paris), Sér. 11, **20**, 292 (1945).
[e] M. Trautz and R. Zink, Ann. der Physik **7**, 427 (1930).
[f] E. Rammler and K. Breitling, Die Wärme (Z. für Dampfkessel u. Maschinenbetrieb) **60**, 620 (1937).

defined collisions and contribute to the transport properties.

Let the Cartesian coordinates of two colliding molecules, A and B (of mass m_A and m_B), be expressed in terms of the Cartesian coordinates of the center of mass, C, and the variables r and θ (see Fig. 1), thus:

$$\begin{aligned} x_A &= x_C + [m_B/(m_A+m_B)]r\cos\theta, \\ y_A &= y_C + [m_B/(m_A+m_B)]r\sin\theta, \\ z_A &= z_C, \\ x_B &= x_C - [m_A/(m_A+m_B)]r\cos\theta, \\ y_B &= y_C - [m_A/(m_A+m_B)]r\sin\theta, \\ z_B &= z_C. \end{aligned} \tag{18}$$

The kinetic energy is then given by the sum of two terms, one referring to the motion of the center of mass and the other to the motion relative to the center of mass:

$$T = T_C + \tfrac{1}{2}\mu[\dot{r}^2 + r^2\dot{\theta}^2]. \tag{19}$$

From Eqs. (1) and (19), the Lagrangian for the motion may then be obtained, and from it the equations of motion:

$$r^2\dot{\theta} = bg. \tag{20}$$

$$\tfrac{1}{2}\mu\dot{r}^2 + \tfrac{1}{2}\mu\left[\frac{b^2g^2}{r^2}\right] + E(r) = \tfrac{1}{2}\mu g^2, \tag{21}$$

in which b = the distance of closest approach if $E(r)$ were zero so that the molecules would not be deflected, and g = initial velocity with which the molecules approach one another, while they are still far apart. At this point it is convenient to introduce the following reduced variables:

$$R = r/r_o, \tag{22}$$

$$\beta = b/r_o, \tag{23}$$

$$K = \tfrac{1}{2}\mu g^2/\epsilon, \tag{24}$$

$$V = (K\beta^2/R^2) - (4/R^6) + (4/R^{12}). \tag{25}$$

Then Eq. (21) becomes:

$$K = \tfrac{1}{2}[\mu r_o^2/\epsilon]\dot{R}^2 + V. \tag{26}$$

This represents the one-dimensional motion (with respect to R) of a particle of mass $[\mu r_o^2/\epsilon]$ and total energy K moving in a potential field, V; the latter potential field is defined in Eq. (25).

Figure 2 shows the shape of the V-curves for several values of $K\beta^2$; the hump in the effective potential is due to the term $K\beta^2/R^2$, which is called the centrifugal potential. It is not difficult to show that there exists a critical value of $K\beta^2$:

$$[K\beta^2]_C = (36/25)(5)^{\frac{1}{3}} = 2.4624, \tag{27}$$

above which there are no humps in the effective potential curves; from this, it may be shown that when K is greater than $\frac{4}{5}$ the system can pass over the hump for all values of β.

For values of K less than $\frac{4}{5}$, there is a critical value of beta, β_o; when β is larger than β_o, the system does not have enough energy to get over the hump, and consequently the molecules are not able to get very close together; when β is less than β_o, on the other hand, the system passes over the hump and the molecules are permitted to come close together. In the latter case, if K is just slightly larger than the value of V at the hump, the two molecules will spend a considerable time at a separation, R, corresponding to the hump; meanwhile they are rotating with an angular velocity given by Eq. (20). Hence, for such collisions the molecules "orbit" for an indefinite number of revolutions before flying apart.

B. Development of Formula for Angle of Deflection

The only feature of a collision which affects the transport properties is the angle of deflection of the trajectory

$$\chi = \pi - 2\theta_m. \tag{28}$$

Here θ_m, as may be seen from Fig. 1, is the value of θ at the point of closest approach. To determine the trajectory, it is necessary to obtain an expression for θ_m which is independent of time. If we let

$$y = 1/R = r_o/r, \tag{29}$$

then

$$dy/d\theta = -\dot{R}/R^2\dot{\theta}. \tag{30}$$

On substituting for $\dot{R}$ and $\partial^2\theta/\partial t^2$ from Eqs. (26) and (20), and for $b = \beta r_o$

$$dy/d\theta = -(1/\beta)[1 - (V/K)]^{\frac{1}{2}}, \tag{31}$$

TABLE VI. Tabulation and comparison of force constants from viscosity data and 2nd virial coefficients.

Gas	Constants determined from viscosity data (See Table V) ϵ/k	r_0	Ref.	Constants determined from 2nd virial coefficient ϵ/k	r_0	Ref.
Air	97.0	3.617	a			
H_2	33.3	2.968	a	37.02	2.92	c,d
N_2	91.46	3.681	a	95.9	3.72	e
CO_2	190	3.996	a	185	4.57	f
N_2O	220	3.879	a	189	4.59	f
NO	119	3.470	a	131	3.17	f
CH_4	136.5	3.822	a	142.7	3.81	f
O_2	113.2	3.433	a	117.5	3.58	e
CO	110.3	3.590	a	95.33	3.65	d
A	124.0	3.418	b	119.5	3.41	g
Ne	35.7	2.80	b	35.7	2.74	g
He	6.03	2.70	b	6.03	2.63	g

[a] H. L. Johnston, and K. E. McCloskey, J. Phys. Chem. **44**, 1038 (1939).
[b] H. L. Johnston and E. R. Grilly, J. Phys. Chem. **46**, 948 (1942).
[c] J. DeBoer and A. Michels, Physica **5**, 945 (1938); **6**, 97 (1939).
[d] J. Corner, Proc. Roy. Soc. **58**, 737 (1946).
[e] J. O. Hirschfelder and W. E. Roseveare, J. Phys. Chem. **43**, 15 (1939).
[f] J. O. Hirschfelder, F. T. McClure, C. F. Curtiss, and D. W. Osborne, NDRC-A 116.
[g] R. A. Buckingham, Proc. Roy. Soc. **A168**, 264 (1938).

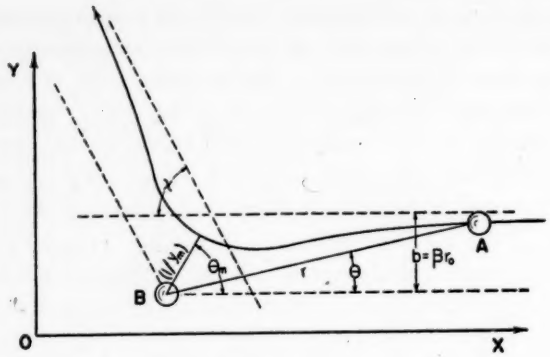

FIG. 1a. Pictorial representation of a normal molecular encounter.

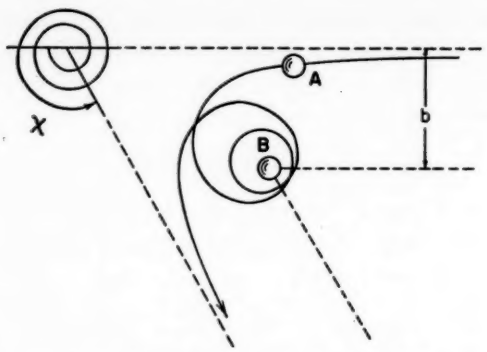

FIG. 1b. The molecular encounter typical of certain low energy collisions in which orbiting takes place at distances of a few angstroms and the molecules separate of their own accord. Such collisions occur when K is less than 0.8 and β is in the vicinity of β_0.

and integrating,

$$\chi=\pi-2\beta \times\int_0^{y_m} dy/[1-\beta^2y^2+(4/K)(y^6-y^{12})]^{\frac{1}{2}}, \quad (32)$$

where y_m is the lowest root for which the denominator of the integrand vanishes.

To facilitate the numerical integration, y was replaced by uy_m and the integral rearranged into the form

$$\chi=\pi-\frac{2\beta y_m}{a}\int_0^1 du/t[1+(4/Ka^2)f(t^2)]^{\frac{1}{2}}, \quad (33)$$

where

$$t=(1-u^2)^{\frac{1}{2}}, \quad (34)$$

$$a^2=1-(8/K){y_m}^6+(20/K){y_m}^{12}, \quad (35)$$

$$\beta^2{y_m}^2=1+(4/K){y_m}^6-(4/K){y_m}^{12}, \quad (36)$$

$$f(t^2)={y_m}^6[3t^2-t^4] +{y_m}^{12}[1-6t^2-(1-t^2)^6](1/t^2). \quad (37)$$

When $t=0$, $f(t^2)$ and $df(t^2)/d(t^2)$ are both zero. The value of $[1+(4/Ka^2)f(t^2)]$ varies smoothly as t^2 goes from one, when $u=0$, to zero, when $u=1$.

We can approximate the function

$$F(t^2)=1/[1-(4/Ka^2)f(t^2)]^{\frac{1}{2}} \quad (38)$$

by the polynomial:

$$F(t^2)=1+At^2+Bt^4+Ct^6+Dt^8, \quad (39)$$

evaluating $F(t^2)$ at $t^2=0$, $\frac{1}{4}$, $\frac{1}{2}$, $\frac{3}{4}$, and 1 to determine the constants. With this transformation of the integrand, it is now easy to evaluate χ.

$$\chi=\pi-(2\beta y_m/a)\int_0^1 [F(t^2)/t]du, \quad (40)$$

$$\chi=\pi-2\beta y_m/a[k_{-1}+Ak_1+Bk_3+Ck_5+Dk_7], \quad (41)$$

in which

$$k_n=\int_0^1 t^n du=(\pi/2)\left[\frac{(n+1)!}{2^{n+1}\left[\left(\frac{n+1}{2}\right)!\right]^2}\right]. \quad (42)$$

To consolidate this formula for computing, we introduce the new parameters c and z defined by the relations:

$$c=(2/K)[1+(1+K)^{\frac{1}{2}}], \quad (43)$$

$$cz=(4/K){y_m}^6, \quad \text{or} \quad (c+1)z^2=(4/K){y_m}^{12}. \quad (44)$$

Then

$$\chi=\pi-(\pi/6)[1+cz-(c+1)z^2]^{\frac{1}{2}} \times\{1+1/[1-2cz+5(c+1)z^2]^{\frac{1}{2}} +2/[1-(21/16)cz +(2343/1024)(c+1)z^2]^{\frac{1}{2}} +2/[1-(5/16)cz +(341/1024)(c+1)z^2]^{\frac{1}{2}}\}. \quad (45)$$

Equation (45) is not sufficiently accurate for $0.1\leq K\leq 0.8$. However, a closer approximation may be had for χ in the vicinity of orbiting by requiring that the curve fit include $F(t_1^2)$, where t_1^2 is defined as the value of t^2 for which

$$[1+(4/Ka^2)f(t^2)]^{\frac{1}{2}}=0 \quad (46)$$

or

$$t_1^2=1-[z/z_o]^{\frac{1}{2}}=1-u_1^2. \quad (47)$$

The result of this integration is an elaboration of the previous equation:

$$\chi=\pi-Y_1[Z_1+Y_2Z_2+Y_3(Z_3+Z_3')+Y_4Z_4+Y_5Z_5+Y_6Z_6],$$

in which

$$\begin{aligned}
Y_1&=2[1+cz-(c+1)z^2]^{-\frac{1}{2}},\\
Y_2&=[t_1^2-\tfrac{3}{4}]^{-1}[1-(5/16)cz+(341/1024)(c+1)z^2]^{-\frac{1}{2}},\\
Y_3&=\{1+[3t_1^2-2-t_1^4]cz+[5+(1/t_1^2)(1-6t_1^2-(1-t_1^2)^6)](c+1)z^2\}^{-\frac{1}{2}},\\
Y_4&=[\tfrac{1}{2}-t_1^2]^{-1}[1-\tfrac{3}{4}cz+(31/32)(c+1)z^2]^{-\frac{1}{2}},\\
Y_5&=[t_1^2-\tfrac{1}{4}]^{-1}[1-(21/16)cz+(2343/1024)(c+1)z^2]^{-\frac{1}{2}},\\
Y_6&=t_1^{-2}[1-2cz+5(c+1)z^2]^{-\frac{1}{2}},\\
Z_1&=4[1-t_1^2]^{-1}[h_3-(\tfrac{3}{4}+t_1^2)h_1+\tfrac{3}{4}t_1^2h_{-1}],\qquad (48)\\
Z_2&=4[h_3-(1+t_1^2)h_1+t_1^2h_{-1}],\\
Z_3&=[(t_1^2-1)(t_1^2-\tfrac{3}{4})]^{-1}[h_3-(7/4)h_1+\tfrac{3}{4}h_{-1}],\\
Z_3'&=[t_1^2(t_1^2-\tfrac{1}{4})(t_1^2-\tfrac{1}{2})]^{-1}[(5\pi/32)-h_5-\tfrac{3}{4}((3\pi/16)-h_3)+\tfrac{1}{8}((\pi/4)-h_1)],\\
Z_4&=8[((5\pi/32)-h_5)-(\tfrac{1}{4}+t_1^2)((3\pi/16)-h_3)+\tfrac{1}{4}t_1^2((\pi/4)-h_1)],\\
Z_5&=16[((5\pi/32)-h_5)-(\tfrac{1}{2}+t_1^2)((3\pi/16)-h_3)+\tfrac{1}{2}t_1^2((\pi/4)-h_1)],\\
Z_6&=8[(\tfrac{3}{4}+t_1^2)((3\pi/16)-h_3)-((5\pi/32)-h_5)-(\tfrac{1}{8}+\tfrac{3}{4}t_1^2)((\pi/4)-h_1)+\tfrac{1}{8}t_1^2((\pi/2)-h_{-1})],
\end{aligned}$$

and where

$$h_n(u_1)=\int_0^{u_1}(1-u^2)^{n/2}du.$$

For values of K greater than 0.8 there is no physical basis for using t_1, and the function is satisfactorily represented by either equation, as was shown by the fact that both formulas gave the same results for $K=1$ and $K=100$, letting $t_1^2=0.6$ in the modified form.

For small values of z, it is convenient to express χ in the series:

$$\chi=-0.9375\pi cz-0.5713\pi c^2z^2+1.3535(c+1)z^2. \qquad (49)$$

This was obtained by expanding

$$[1+(4/Ka^2)f(t^2)]^{-\frac{1}{2}}$$

into powers of z and integrating directly the resulting polynomial in t^n.

Values of the angle of deviation χ have been tabulated,** along with the values of K, z, and β. The value of β corresponding to each value of z can be determined from the relation

$$\beta=[2/[1+(1+K)^{\frac{1}{2}}]]^{1/6}\times z^{-1/6}[1+cz-(c+1)z^2]^{\frac{1}{2}}, \qquad (50)$$

from which it is clear that z goes from zero (corresponding to β infinite) to unity (corresponding to β zero). As long as K is equal to, or greater than 0.8, there is a one-to-one correspondence between values of z and values of β. When K is equal to or less than 0.8, there are additional complications corresponding to orbiting for critical values of β. The orbiting occurs

TABLE VII. Conditions for orbiting.

K	β_0	z_0	z_1
0.1	2.5367	0.01261	0.8299
0.2	2.2549	0.02557	0.7260
0.4	1.9988	0.05366	0.5566
0.6	1.8567	0.08830	0.4030
0.8	1.7544	0.17082	0.17082

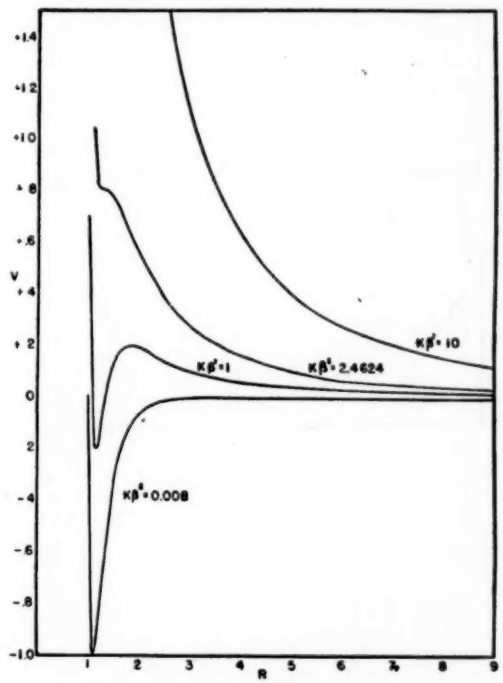

FIG. 2. Effective potential curves for several values of $K\beta^2$. The combination of the original potential and the centrifugal energy leads to effective potential energy curves exhibiting humps when $K\beta^2$ is less than the critical value, 2.4624. No orbiting is possible for collisions in which K is greater than 0.8.

** Tabulations of the numerical values of the angle deviation χ have been mimeographed and may be obtained from the authors on request. Approximately 600 values of χ were computed for different values of the collision parameters. This table would be directly usable for various types of molecular collision properties, such as those encountered in molecular beam experiments. Unfortunately, the length of this table prevented its publication in the present paper.

when

$$[d^2\theta/dy^2]_{ym}=0. \tag{51}$$

This can be expressed by the requirement that $a=0$ [note Eq. (22)], or, letting the subscript "o" indicate orbiting:

$$z_o=\frac{2}{5}\left[\frac{1-(1-(5/4)K)^{\frac{1}{2}}}{1+(1+K)^{\frac{1}{2}}}\right]. \tag{52}$$

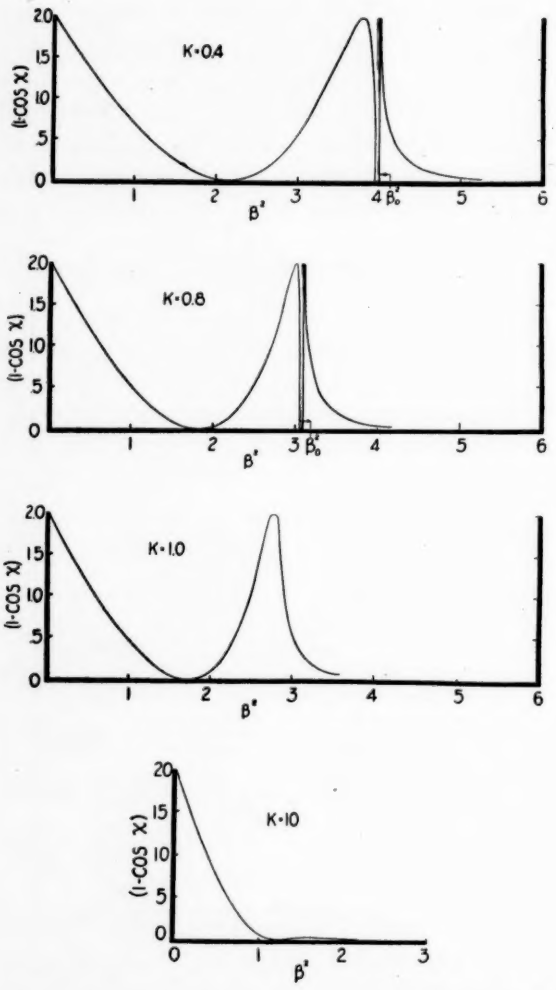

FIG. 3. $(1-\cos\chi)$ *versus* β^2 for several values of K. For small values of K, corresponding to low energy collisions, the molecules "orbit" around each other when β^2 is close to the critical value, β_0^2. In this region, $1-\cos\chi$ oscillates rapidly between the values zero and two. This orbiting no longer takes place when K is greater than 0.8. The collision cross section, $S^{(1)}(K)$, is the integral of $(1-\cos\chi)$ with respect to β^2. The contribution to this integral from collisions in which β^2 is less than 2 is due to the repulsive component of the intermolecular potential. The contribution due to collisions in which β^2 is greater than 2 is due to the energy of attraction; this area disappears for high energy collisions as, for example, in the case $K=10$.

TABLE VIII. Collision cross sections.

K	$S^1(K)$	$S^2(K)$†	$S^4(K)$
0.1	5.445	6.107	6.57
0.2	4.476	4.800	5.16
0.4	3.368	3.846	4.17
0.6	2.909	3.347	3.601
0.8	2.523	3.082	3.312
0.9	2.505	2.933	3.183
0.95	2.467	2.840	3.055
1.0	2.401	2.798	2.988
1.2	2.1007	2.7392	2.9186
1.4	1.8714	2.6399	2.7741
1.6	1.6974	2.4722	2.6244
1.8	1.5656	2.2958	2.4858
2.0	1.4801	2.1513	2.3582
2.5	1.2938	1.8240	2.0644
3.0	1.1890	1.6173	1.8382
4.0	1.0673	1.3755	1.5415
5.0	0.9981	1.2439	1.3697
10.0	0.8558	1.0113	1.0664
15.0	0.7974	0.9345	0.9749
20.0	0.7612	0.8910	0.9263
50.0	0.6610	0.7784	0.8085
100.0	0.5936	0.7036	0.7326

For each value of z_o there is a critical value of beta, β_o; these are given for the various values of K in Table VII. As z approaches z_o, χ becomes infinite. This behavior is correctly represented by the approximate expression for χ, [Eq. (45)]. Here the term $[1-2cz+5(c+1)z^2]^{-\frac{1}{2}}$ approaches infinity. When $K=0.8$, there is a critical value of β for which orbiting occurs, but there is still a one-to-one correspondence between z and β. For collisions where the energy K is less than 0.8 between $z=z_o$ and $z=z_1$, there are two values which when substituted into Eq. (50) give the same value of β. It is convenient to define z_1 as the second value of z for which $\beta=\beta_o$, and its numerical value is also given in Table VII.

Physically there is no significance to values of z lying between z_o and z_1. If β is just barely larger than β_o, the molecules after orbiting at a separation corresponding to z must separate because they do not have quite enough energy to get over the energy hump. The value of χ at z_1 should be infinite. Although it becomes very large according to the approximate formula, Eq. (45), it does not actually become infinite unless one of the values of $t^2=\frac{1}{4}$, $\frac{1}{2}$, or $\frac{3}{4}$, should accidentally correspond to the separation of the energy hump. However, this does not lead to any serious error in the next integration to obtain the reduced cross section, $S^{(1)}(K)$.

TABLE IX. Tabulation of the constants for the equations of $S^{(l)}(K)$.

$$S(K)^{(l)}=\sum_i A_i^{(l)} K^{n_i^{(l)}} e^{-a_i^{(l)}K}$$

i	$A_i^{(1)}$	$n_i^{(1)}$	$a_i^{(1)}$
1	+1.2120	−0.155	0
2	+1.0782	−0.5	0.439
3	+19.49	+2.126	3.675
4	-4.255×10^{81}	+154	194
5	-1.677×10^{16}	+23.4	45
6	$+1.705\times10^{5}$	+4.425	29.1
i	$A_i^{(2)}$	$n_i^{(2)}$	$a_i^{(2)}$
1	+1.3719	−0.145	0
2	+1.1812	−0.789	0.190
3	+2.724	−0.697	0.67742
4	-8.9976×10^{2}	+3.01	6.7461
5	$+3.162\times10^{56}$	+118.6	132.2
6	$+9.3325\times10^{188}$	+363.5	443.25
7	$+8.4723\times10^{54}$	+82.51	140.42
8	-5.0315×10^{6}	+3.958	35.989
i	$A_i^{(4)}$	$n_i^{(4)}$	$a_i^{(4)}$
1	+1.3959	−0.140	0
2	+0.5722	−0.5	0.1350
3	+2.9001	−0.41085	0.49593
4	-7.1895×10^{2}	+7.300	7.5377
5	-3.19×10^{29}	+66.103	69.1675
6	-7.9433×10^{366}	+771.9	851.73
7	-1.3975×10^{3}	+1.809	16.282
8	-1.1067×10^{31}	+37.162	92.906
9	-8.6147×10^{47}	+73.074	121.79
10	-4.3055×10^{362}	+683.53	854.41

C. Evaluation of the Reduced Collision Cross-Section Integrals

Once the angles of deflection, χ, have been determined for individual collisions, the task of evaluating the reduced collision cross sections presents itself. The integrals $S^{(l)}(K)$ were defined in Eq. (2).

When K is greater than 0.8 the integral is easily evaluated by changing the integration variable from β to z and writing $S^{(l)}(K)$ in the form:

$$S^{(l)}(K)=\frac{[\frac{2}{3}(4/cK)^{\frac{1}{4}}]}{\left[2-\frac{[1+(-1)^l]}{[l+1]}\right]}\times\int_0^1(1-\cos^l\chi)\frac{[1-2cz+(c+1)z^2]}{\dot{z}^{4/3}}dz. \quad (53)$$

This can be integrated numerically by using the χ values described in the previous section. The curves of $(1-\cos\chi)$ *versus* β^2 are shown in Fig. 3.

On the other hand, when K is less than 0.8, the curve of χ *versus* β is discontinuous at β_o, as is shown in Fig. 4. Accordingly, it is convenient to break up the integral in Eq. (2) into five

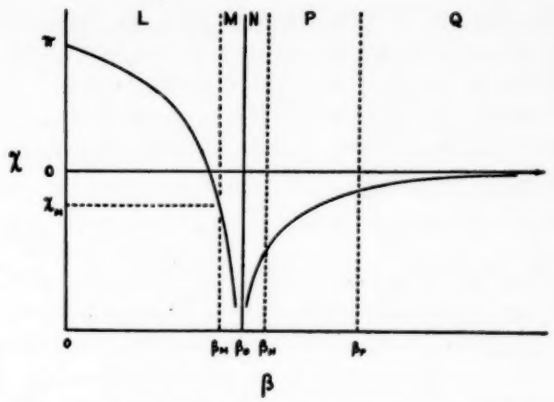

FIG. 4. Schematic diagram of χ *versus* β, showing the zones used in the evaluation of the collision cross sections for low energy collisions.

integrals, as is indicated in the figure, thus:

$$S^{(l)}(K)=L^{(l)}(K)+M^{(l)}(K)+N^{(l)}(K)+P^{(l)}(K)+Q^{(l)}(K). \quad (54)$$

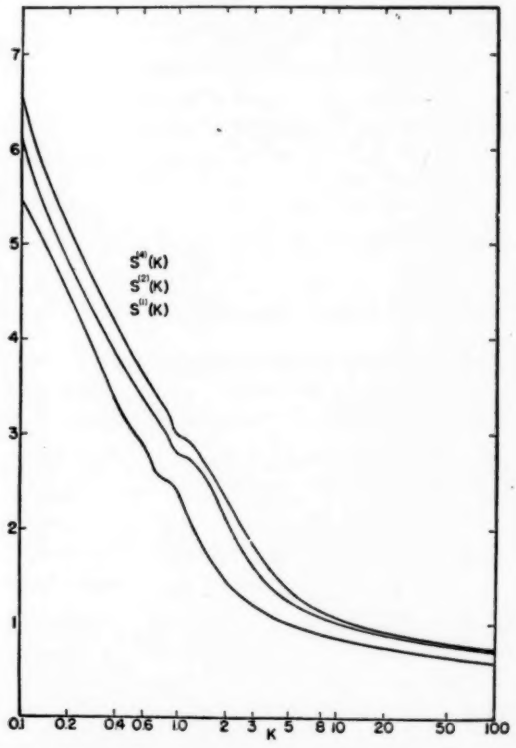

FIG. 5. The reduced collision cross sections, $S^{(l)}(K)$. The function $S^{(1)}(K)$ is used to determine diffusion coefficients. It is considerably smaller than the cross section $S^{(2)}(K)$, used for heat conductivity and viscosity. $S^{(4)}(K)$ is used for third-order corrections. The indentation for K between 0.8 and 1.0 is due to the orbiting. The irregular wavy pattern of the cross sections for small values of K is real and not due to computational errors. The cross sections for very low velocity collisions should be corrected for quantum-mechanical effects.

The integrals $L^{(l)}(K)$ and $P^{(l)}(K)$ are obtained by using numerical integration in the form given in Eq. (53) with the appropriate limits. The integrals $M^{(l)}(K)$ and $N^{(l)}(K)$ are evaluated by curve-fitting χ *versus* β with an equation of the form

$$\chi^2 = a'/(\beta^2-\beta_o^2), \quad \text{where} \quad a' = \text{a constant}, \tag{55}$$

and integrating Eq. (2) analytically between the proper limits. The integrals $Q^{(l)}(K)$, which extend from $\beta=\beta_P$ to $\beta=\infty$ (or $z=z_P$ to $z=0$), are calculated by making use of Eq. (49), which gives χ for small values of z; the latter is substituted into Eq. (53) and $(1-\cos^l\chi)$ is expanded, the integration then being executed analytically.

The equations obtained for the $Q^{(l)}(K)$ and the $M^{(l)}(K)$ are:

$$\begin{aligned}
Q^{(1)}(K) &= \tfrac{1}{3}[4/cz_PK]^{\frac{1}{2}}[2.6024(cz_P)^2 \\
&\quad -1.2707(cz_P)^3-3.2991(cz_P)^4 \\
&\quad +0.65345(cz_P)^5], \\
Q^{(2)}(K) &= \tfrac{1}{2}[4/cz_PK]^{\frac{1}{2}}[5.2047(cz_P)^2 \\
&\quad -2.5414(cz_P)^3-11.7286(cz_P)^4 \\
&\quad +20.1185(cz_P)^5], \\
Q^{(4)}(K) &= (5/12)[4/cz_PK]^{\frac{1}{2}}[10.4094(cz_P)^2 \\
&\quad -13.0117(cz_P)^3],
\end{aligned} \tag{56}$$

$$\begin{aligned}
M^{(1)}(K) &= (\beta_o^2-\beta_M^2)[1-\cos\chi_M \\
&\quad +\chi_M\sin\chi_M+\chi_M^2Ci(-\chi_M)], \\
M^{(2)}(K) &= \tfrac{3}{4}(\beta_o^2-\beta_M^2)[1-\cos2\chi_M \\
&\quad +2\chi_M\sin2\chi_M-4\chi_M^2Ci(-2\chi_M)], \\
M^{(4)}(K) &= (5/32)(\beta_o^2-\beta_M^2)[5-4\cos2\chi_M \\
&\quad -\cos4\chi_M+8\chi_M\sin2\chi_M \\
&\quad +4\chi_M\sin4\chi_M \\
&\quad -16\chi_M^2Ci(-2\chi_M) \\
&\quad -16\chi_M^2Ci(-4\chi_M)].
\end{aligned} \tag{57}$$

The $N^{(l)}(K)$ have the same form as the $M^{(l)}(K)$.

The values of the $S^{(l)}(K)$ obtained by the two procedures outlined above are shown graphically in Fig. 5 and the values are tabulated in Table VIII. These three curves were then fitted with equations of the form

$$S^{(l)}(K) = \sum_i A_i^{(l)} K^{n_i(l)} e^{-a_i(l)K}, \tag{58}$$

the constants for the equations appearing in Table IX.

D. Evaluation of $W^{(l)}(n;x)$

To obtain the $W^{(l)}(n;x)$, the expressions for the $S^{(l)}(K)$ of Eq. (58) are substituted into Eq. (3),

TABLE X. Expressions for $W^{(l)}(n;x)$.

$x=\epsilon/kT$

$$\begin{aligned}
W^{(1)}(1;x) &= \tfrac{1}{4}x^3[2.11114x^{-2.845}+1.43329(x+0.439)^{-2.5}+566.494(x+3.675)^{-5.126}-0.02077\exp(-0.8093x) \\
&\quad -0.2159\exp(-0.5867x)+0.003726\exp(-0.2552x)] \\
W^{(1)}(2;x) &= \tfrac{1}{4}x^4[6.00619x^{-3.845}+3.58323(x+0.439)^{-3.5}+2903.85(x+3.675)^{-6.126}-0.01681\exp(-0.8144x) \\
&\quad -0.01267\exp(-0.6089x)+0.0009506\exp(-0.2895x)] \\
W^{(1)}(3;x) &= \tfrac{1}{4}x^5[23.0938x^{-4.845}+12.5413(x+0.439)^{-4.5}+17789(x+3.675)^{-7.126}-0.01369\exp(-0.8196x) \\
&\quad +0.0002752\exp(-0.3239x)-0.007714\exp(-0.6311x)] \\
W^{(2)}(2;x) &= \tfrac{1}{8}x^4[6.88155x^{-3.855}+2.89488(x+.190)^{-3.211}+7.33242(x+.67742)^{-3.303}-660079(x+6.7461)^{-7.01} \\
&\quad +0.03950\exp(-0.9274x)+0.03732\exp(-0.8291x) \\
&\quad +0.03888\exp(-0.6161x)-0.009625\exp(-0.2211x) \\
W^{(2)}(3;x) &= \tfrac{1}{8}x^5[26.5284x^{-4.855}+9.29546(x+0.190)^{-4.211}+24.2190(x+.67742)^{-4.303}-4627150(x+6.7461)^{-8.01} \\
&\quad +0.03663\exp(-0.9349x)+0.03094\exp(-0.8314x) \\
&\quad +0.02395\exp(-0.6232x)-0.002128\exp(-0.2489x)] \\
W^{(2)}(4;x) &= \tfrac{1}{8}x^6[128.795x^{-5.855}+39.1432(x+0.190)^{-5.211}+104.214(x+0.67742)^{-5.303}-37063500(x+6.7461)^{-9.01} \\
&\quad +0.03425\exp(-0.9425x)+0.02573\exp(-0.8336x) \\
&\quad +0.01493\exp(-0.6303x)-0.0005298\exp(-0.2767x)] \\
W^{(2)}(5;x) &= \tfrac{1}{8}x^7[754.095x^{-6.855}+203.975(x+0.190)^{-6.211}+552.647(x+0.67742)^{-6.303}-33942000(x+6.7461)^{-10.01} \\
&\quad +0.03228\exp(-0.9501x)+0.02145\exp(-0.8359x) \\
&\quad +0.009408\exp(-0.6374x)-0.0001466\exp(-0.3045x)] \\
W^{(2)}(6;x) &= \tfrac{1}{8}x^8[5169.32x^{-7.855}+1266.89(x+0.190)^{-7.211}+3483.33(x+0.67742)^{-7.303}-3342750000(x+6.7461)^{-11.01} \\
&\quad +0.03067\exp(-0.9576x)+0.01793\exp(-0.8381x) \\
&\quad +0.005997\exp(-0.6446x)-0.00004463\exp(-0.3323x)] \\
W^{(4)}(4;x) &= \tfrac{1}{8}x^6[132.154x^{-5.86}+29.9505(x+0.1350)^{-5.5}+175.386(x+0.49593)^{-5.58915}-737383000000(x+7.5377)^{-13.3} \\
&\quad -0.09163\exp(-1.0424x)-0.002420\exp(-0.9133x)-0.001657\exp(-0.4796x) \\
&\quad -0.003243\exp(-0.4646x)-0.01629\exp(-0.6493x)-0.008924\exp(-0.8070x)]
\end{aligned}$$

which integrates to complete gamma-functions:

$$W^{(l)}(n;x)=\tfrac{1}{8}[2-[(1+(-1)^l)/(l+1)]]x^{n+2} \times\sum_i A_i^{(l)}\frac{\Gamma[n+n_i^{(l)}+2]}{[x+a_i^{(l)}]^{(n+n_i^{(l)}+2)}}. \quad (59)$$

Equations for the most important $W^{(l)}(n;x)$ are stated explicitly in Table X. The exponential terms are obtained by letting terms of the form

$$C/(x+p)^q=Cp^{-q}e^{-q/p}, \quad C=\text{a constant}. \quad (60)$$

The work presented in this report could not have been carried out without the help of a very efficient computing group under the direction of Jean Patterson. These calculations were made by Ruth Shoemaker, Doris Jayne, Mary Sullivan, Theodore Mesmer, Freda Coen, and Florence Cappon.

The authors wish to thank the Navy Bureau of Ordnance for their financial support under Contract NOrd 9938.

One of the authors, R. Byron Bird, wishes to acknowledge the financial help he has received from the Wisconsin Alumni Research Foundation.

THE JOURNAL OF CHEMICAL PHYSICS VOLUME 16, NUMBER 10 OCTOBER, 1948

The Energy of the C−H Bond in the Three Picolines (Methyl Pyridines)

J. S. Roberts and M. Szwarc
Department of Chemistry, The University, Manchester, England

(Received May 5, 1948)

The pyrolysis of the three picolines was investigated and the rates of the decomposition were compared with the rate of the decomposition of toluene. It was found that the process of the decomposition of the picolines is analogous to that of toluene, i.e., the rate determining step is the splitting of the picoline molecule into H atom and a picolyl radical. Comparison of the decomposition rates of the picolines and of toluene made it possible to calculate the C−H bond energy for these compounds. These were estimated at 75.5 kcal./mole for α-picoline, 76.5 kcal./mole for β-picoline, and 77.5 kcal./mole for γ-picoline. It was concluded therefore that the resonance energy of the picolyl radical approximates within a few kcal. the resonance energy of the benzyl radical.

THE aim of the present work was to investigate how the resonance energy of an aromatic system is changed when one of the CH groups in the ring is replaced by a N atom. Comparison of the energies of the C−H bond (the bond energy is defined here as the dissociation energy of the bond) in the methyl group of the picolines with that of toluene ought to reveal whether there are any significant variations in the resonance energies of the radicals produced by breaking this bond. Such variations would be shown by parallel differences between the rate of pyrolysis of toluene on the one hand and the picolines on the other.

EXPERIMENTAL

The rates of pyrolysis of the three picolines were measured by the method and technique previously used for toluene, the xylenes,[1] and the fluorotoluenes.[2]

[1] M. Szwarc, J. Chem. Phys. **16**, 128 (1948).
[2] M. Szwarc and J. S. Roberts, J. Chem. Phys. **16**, 609 (1948).

MATERIAL USED

The commercial picolines were purified by several distillations using an efficient column. As in previous work,[1,2] the criterion of purity was that the product recovered from any pyrolysis should give the same rate of decomposition on being pyrolysed once more. By this standard, the distilled β-picoline was sufficiently pure. The α- and γ-picolines gave a constant rate of decomposition after the first pyrolysis, and thus all results reported for these compounds refer to material previously pyrolysed at least once.

RESULTS

The results summarized in Tables IA and B and II indicate that the essential features of the mechanism of the decomposition of the picolines were the same as in the previous cases,[1,2] i.e., the rate determining step is the splitting of the picoline molecule into H and a $C_5H_5N\cdot CH_2\cdot$ radical. The gases produced in the pyrolysis of γ-picoline consist of 70 percent of H_2 and 30

percent of CH_4, whereas the α- and β-picolines gave 60 percent H_2 and 40 percent of CH_4; the last are the same as were found with toluene. In addition there was always a small percentage of decomposition into what was measured as "C_2 hydrocarbons" (i.e., products volatile at -78°C but not at -180°C), amounting in the case of α- and β-picolines to about 5 percent of the total gases and to about 10 percent in the case of γ-picoline. The accuracy of the results is rather lower than in the previous cases, partly because of the low vapor pressure of the picolines.

TABLE IA. T about 780°C.

Compound	Run	T°K	% decomp.	$k_T \cdot 10^3$ sec.$^{-1}$	$k_{780} \cdot 10^3$ sec.$^{-1}$	$\frac{k_{780}}{k_{\text{average of toluene}}}$	Remarks
toluene	110	1054	0.28	1.7	1.7	0.81	
	111	1054	0.30	1.9	1.8	0.86	
	112	1055	0.33	2.0	1.9	0.90	
	114	1055	0.42	2.5	2.4	1.14	
	115	1055	0.45	2.7	2.5	1.19	
	124	1058	0.33	2.4	2.0	0.95	
	125	1058	0.34	2.5	2.1	1.00	
	126	1058	0.35	2.8	2.4	1.14	
	127	1055	0.31	2.4	2.3	1.10	
	128	1054	0.28	2.1	2.0	0.95	
				average	2.11		
γ-picoline	116	1058		2.8	2.3	1.09	once pyrolysed
	117	1056		2.7	2.3	1.09	once pyrolysed
	118	1057		3.0	2.6	1.24	once pyrolysed
	119	1056		2.6	2.3	1.09	twice pyrolysed
	120	1057		2.8	2.4	1.14	twice pyrolysed
					average	1.13	
β-picoline	102	1051		2.9	3.2	1.52	once pyrolysed
	103	1054		3.1	3.0	1.43	once pyrolysed
	105	1051	0.12	2.6	2.8	1.33	twice pyrolysed
	106	1054	0.19	3.7	3.6	1.70	twice pyrolysed
	107	1054	0.18	3.0	2.9	1.37	twice pyrolysed
	108	1051	0.12	2.6	2.8	1.33	twice pyrolysed
	109	1053	0.20	3.5	3.5	1.66	twice pyrolysed
					average	1.48	
α-picoline	96	1053	0.19	5.5	5.5	2.60	once pyrolysed
	97	1054	0.18	5.6	5.4	2.56	once pyrolysed
	98	1051	0.15	4.7	5.0	2.37	once hyrolysed
	99	1051	0.16	4.2	4.5	2.13	twice pyrolysed
	100	1053	0.17	4.7	4.7	2.22	twice pyrolysed
	101	1053	0.17	5.0	5.0	2.37	twice pyrolysed
	121	1058	0.18	6.1	5.1	2.42	once pyrolysed
	122	1056	0.16	5.6	5.0	2.37	once pyrolysed
	123	1056	0.16	5.6	5.0	2.37	once pyrolysed
					average	2.38	

TABLE IB. T about 823°C.

Compound	Run	T°K	% decomp.	$k_T \cdot 10^3$ sec.$^{-1}$	$k_{823} \cdot 10^3$ sec.$^{-1}$	$\frac{k_{823}}{k_{\text{averages of toluene}}}$	Remarks
toluene	70	1090	0.18	8.0	7.8	0.99	
	71	1091	0.19	8.6	8.0	1.02	
	72	1091	0.18	8.3	7.7	0.98	
				average	7.84		
γ-picoline	82	1091	0.27	6.7	6.5	0.83	once pyrolysed
	84	1092	0.30	8.0	7.4	0.95	twice pyrolysed
	87	1092	0.24	7.5	7.0	0.90	thrice pyrolysed
	88	1094	0.21	7.6	6.6	0.84	once pyrolysed
	89	1090	0.19	6.6	6.6	0.84	once pyrolysed
	90	1092	0.20	7.1	6.5	0.83	once pyrolysed
	91	1092	0.16	6.8	6.3	0.81	twice pyrolysed
	92	1094	0.22	9.0	7.8	1.00	twice pyrolysed
					average	0.88	
β-picoline	65	1092		12.5	11.7	1.50	not pyrolysed
	66	1091	0.32	12.5	12.5	1.54	not pyrolysed
	68	1091	0.44	12.9	12.5	1.60	once pyrolysed
	69	1092	0.37	13.4	12.5	1.60	once pyrolysed
					average	1.56	
α-picoline	60	1085	0.50	16.2	19.0	2.42	once pyrolysed
	61	1089	0.60	20.6	20.9	2.66	once pyrolysed
	62	1094	0.72	26.0	22.6	2.88	once pyrolysed
	63	1088	0.62	20.9	22.0	2.80	twice pyrolysed
					average	2.69	

As with toluene and the fluorotoluenes, slightly volatile products were obtained in the trap cooled to 0°C.* These were dark violet liquids in the case of α- and β-picoline and a dark violet solid in the case of γ-picoline. The molecular weight of the last compound (which was not isolated in a pure state) is approximately twice that of picoline. This is to be expected, if the picolyl radicals dimerise. The picoline recovered in the trap cooled at -78°C* was colorless, when under vacuum, but after admitting air developed a pink coloration which gradually deepened on standing, finally becoming almost black. This change did not affect the rate of the subsequent pyrolysis of this sample, and therefore the dark liquid could be used for further work. The color is probably due to some secondary reactions of the picolyl radicals. However, the matter was not pursued further.

With γ-picoline at 1090°K it was found that the first run of every series gave a k_u smaller (by about 30 percent) than the subsequent runs. This tendency was traced to the wall activity of the reaction vessel which disappears if the reaction vessel is kept continuously under vacuum. Probably the clean silica surface causes some back reaction.

For comparison the decomposition of toluene was repeated at the same temperature. It was found that the rates of decomposition for toluene, γ-picoline, β-picoline, and α-picoline were:

$$1:1:1.5:2.5.$$

DISCUSSION

Assuming that the temperature independent factor is the same for the picolines as for toluene, comparison of the values of k_u indicates a decrease in the magnitude of the activation energy of the decomposition. For the γ-picoline the activation energy is the same as for toluene (within the experimental error of ± 0.4 kcal.), whereas

* See diagram of apparatus given in reference 1.

for the β-picoline and α-picoline we observed a decrease amounting to 0.9 kcal. and 2.0 kcal., respectively. These variations in the magnitude of the energy of activation must be taken to represent the changes in the C−H bond energies.** Assuming for the C−H bond energy in toluene the value 77.5 kcal./mole reported by Szwarc,[1] we obtain the following values (smoothed to the nearest 0.5 kcal.):

Compound	The energy of the C−H bond
α-picoline	75.5 kcal./mole
β-picoline	76.5 kcal./mole
γ-picoline	77.5 kcal./mole

We emphsize that these values are based on the assumption of the constancy of the temperature independent factor for all the pyrolytic processes mentioned. This assumption is favored by the finding that substitution in the para or meta position does not change the temperature independent factor in a series of similar reactions,[3] and it is made particularly plausible by the fact that the rates of decomposition of toluene, the three fluorotoluenes, meta-xylene (taking into account the probability factor 2), and γ-picoline are equal within 20 percent.

It seems, therefore, that the resonance energies of the benzyl radical and the picolyl radicals are equal within a few kcal. It would appear that the introduction of a N atom into the benzene ring does not cause any great changes in the energy of the system. This is in agreement with the calculations of Pauling,[4] who found the resonance energy of pyridine to be only by 4 kcal. greater than that of benzene.

The unexpected gradation in the C−H bond energies of the three picolines, α, β, γ, can be explained tentatively as a result of the contribution of the ionic structures such as (I) to the ground state of the radical

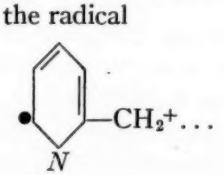

(I)

** We assume that the recombination of H atoms and picolyl radicals does not involve any energy of activation.

[3] E. G. Williams and C. N. Hinshelwood, J. Chem. Soc. 1079 (1934); C. K. Ingold and W. S. Nathan, *ibid* 222 (1936).

[4] L. C. Pauling, *The Nature of the Chemical Bond* (Cornell University Press, Ithaca, New York, 1940), p. 137.

TABLE II. Picolines. Gas analyses.

Run	$\%H_2$	$\%CH_4$
	α-picoline	
59	63	37
61	63	37
98	60	40
	β-picoline	
66	61	39
109	55	45
	γ-picoline	
79	71	29
82	69	31
90	70	30

TABLE III.

Radical	α-aryl-pyridine	β-aryl-pyridine	γ-aryl-pyridine
Phenyl	12 g	5 g	5 g
p-nitro-phenyl	54 g	20 g	10 g
o-nitro-phenyl	20 g	23 g	<1.5 g

The importance of these ionic structures will decrease in the order α, β, γ because of the increasing charge separation. We should note in this connection that the usual pairing of the α- and γ-picolines in contrast to β-picoline is justified for reactions in which the reagent is electrophilic or nucleophilic. However, the pyrolysis should be compared to radical reactions. There is not much information on this subject; the only case in the literature is reported by Haworth, Heilbron, and Hey,[5] who investigated the reaction of phenyl and nitro-phenyl radicals with pyridine. They found that the reaction produces the α-, β-, and γ-aryl-pyridines, and the yields are given in Table III. Even if we take into account the factor 2 for the α- and β-portions, the results seem to offer some support to the gradation α, β, γ.***

ACKNOWLEDGMENTS

We wish to thank Professor M. Polanyi for his interest and encouragement. One of us (J. S. Roberts) is indebted to the Department of Scientific and Industrial Research for a grant.

[5] Haworth, Heilbron, and Hey, J. Chem. Soc. 349 (1940).

*** For a theoretical consideration of this subject see G. W. Wheland, J. Am. Chem. Soc. **64**, 900 (1942). This calculation favors the usual pairing α and γ.

THE JOURNAL OF CHEMICAL PHYSICS VOLUME 16, NUMBER 10 OCTOBER, 1948

Carbon-Hydrogen Bond Strengths in Methane

H. H. VOGE
Shell Development Company, Emeryville, California
(Received June 7, 1948)

Earlier formulas for the electron-pair bonding energies of methane, and radicals derivable from methane, are combined with recent data on the energy levels of the carbon atom, the heat of sublimation of carbon, the energy for removal of the first hydrogen, and the dissociation energy of CH to obtain the energies of CH_3 and CH_2. A consistent set of values is found which is in agreement with a heat of sublimation of carbon of 120–140 kcal. and gives for the energies of successive removals of hydrogen atoms from methane 101, 90, 80, and 80 kcal., respectively.

IN an earlier paper[1] an extended Heitler-London-Pauling-Slater valence calculation was made for methane, following methods developed by J. H. Van Vleck,[1] and the relative energies of CH_4, CH_3, CH_2, and CH were computed, using certain experimental data to fix the values of the integrals occurring in the formulas for electron pair bonds. Subsequent new and more accurate experimental values are used in the present note to correct the computed energies and to obtain some information about the heat of sublimation of carbon. The new data now taken into account include a careful theoretical calculation of the term values of the carbon atom by Ufford,[2] the experimental location of the $sp^3\ ^5S$ state of carbon by Shenstone,[3] a more accurate value of the dissociation energy of CH given by Herzberg,[4] and the energy for the reaction $CH_4=CH_3+H$ from some recent experiments that are in good agreement.[5]

The procedure for utilizing this information is essentially the same as that followed before.[1] No changes have been made in the formulas for the energies according to the electron pair theory. The formulas are presumed to give the energies at the potential minima in the energy *versus* distance curves, and all energy values cited are for molecules at the potential minimum unless marked W_0 or otherwise noted. To obtain dissociation energies from the lowest vibrational levels, the zero point energies of Smith[6] are used. These are: CH, 0.18; CH_2, 0.46; CH_3, 0.82; and CH_4, 1.17 ev.

CARBON ATOM INTEGRALS

Of the integrals describing the carbon atom according to the Slater theory and for which numerical values are necessary in computing the valence energy, a minimum number are taken from the paper of Ufford[2] and the remainder are chosen to fit the known levels of the carbon atom. Since the Slater $F-G$ relationships (see ref. 1, Table II) cannot perfectly fit all the carbon levels, a selection is made which fits most closely those levels important in the quadrivalent state of carbon. The values employed are as follows, those from Ufford being averages for the excited and normal states.

Integral	Value, ev	Source
$F_0(2s, 2s)$	14.87	Ufford
$F_0(2s, 2p)$	14.00	Ufford
$F_0(2p, 2p)$	13.26	Ufford
G_1	2.24	To fit carbon levels
F_2	0.21	To fit carbon levels
$I(2p)-I(2s)$	10.85	To fit carbon levels

The carbon levels computed from these values are compared with the accurately known observed levels in Table I. Other selections for the carbon atom integrals were tried and were not found to give important differences in results for bond energies. The set listed above yields, for the valence state of carbon in methane, $W_v(C)=6.97$ ev (see Eq. (21) of ref. 1). For plane CH_3 the

[1] H. H. Voge, J. Chem. Phys. **4**, 581 (1936). Also papers of J. H. Van Vleck referred to there.
[2] C. W. Ufford, Phys. Rev. **53**, 569 (1938).
[3] A. G. Shenstone, Phys. Rev. **72**, 411 (1947).
[4] G. Herzberg, *Molecular Spectra and Molecular Structure, I, Diatomic Molecules* (Prentice-Hall, Inc., New York, 1939). The CH values were recomputed by Herzberg from observations of Shidei.
[5] D. P. Stevenson, J. Chem. Phys. **10**, 291 (1942); G. B. Kistiakowsky and E. R. van Artsdalen, J. Chem. Phys. **12**, 469 (1944); H. C. Andersen and G. B. Kistiakowsky, J. Chem. Phys. **11**, 6 (1943); E. T. Butler and M. Polanyi, Trans. Farad. Soc. **39**, 19 (1943).
[6] L. G. Smith, Phys. Rev. **51**, 263 (1937).

valence state is

$$W_v'(\mathrm{C}) = I(2p) - I(2s) - (1/6)[5F_0(2s, 2s) + 8F_0(2s, 2p) - 13F_0(2p, 2p) + G_1 + 29F_2]. \quad (1)$$

The above values lead to $W_v'(\mathrm{C}) = 7.13$ ev.

RELATIVE ENERGIES OF CH_2 AND CH

The heat of dissociation, D_0, of CH is 3.47 ev,[4] and the zero point energy is 0.18, so that the energy of dissociation from the potential minimum is 3.65 ev. In the previous formula,

$$W(\mathrm{CH}) - W(\mathrm{C}) - W(\mathrm{H}) = (3/2)F_2 + K(\mathrm{CH}) + N_{ss} - N_{s\sigma} + (1/2)N_{\pi\pi}, \quad (2)$$

substitution of -3.65 on the left, together with the values $N_{ss} = 2.0$, $N_{s\sigma} = 2.3$, and $N_{\pi\pi} = -0.6$ ev, used throughout, leads to -3.36 for the quantity $K(\mathrm{CH})$. Then, from the formula for right-angled CH_2,

$$W(\mathrm{CH_2}) - W(\mathrm{C}) - 2W(\mathrm{H}) = (3/2)F_2 + 2K(\mathrm{CH}) + K(\mathrm{H_2}) - (1/2)\beta + 2N_{ss} - 2N_{s\sigma} + N_{\pi\pi} - 0.4, \quad (3)$$

where the -0.4 ev term is the correction necessary for an accurate solution of the secular equation in this case, and $K(\mathrm{H_2}) - (1/2)\beta = 0.63$,[1] it is found that the energy necessary to dissociate CH_2 into atoms is 7.38 ev from the potential minimum, or 6.92 ev from the ground state.

RELATIVE ENERGIES OF CH_4 AND CH_3

Four alternative cases are considered: (a) that in which the heat of sublimation of carbon to $s^2p^2\,{}^3P$ is considered to be 135.7 kcal. according to Hagstrum;[7] (b) the heat of sublimation is 125 kcal. according to Herzberg as quoted by Hagstrum;[7] (c) the heat for the reaction $CH_4 = CH_3 + H$ is 101 kcal. from close values recently published;[5] and (d) the heat of sublimation is 170.4 kcal.[8] In cases (a), (b), and (d) the energy of formation of methane is calculated from experimental data and is used to evaluate the unknown integral $N_{s\sigma}$ in the theoretical formula for the energy, which then permits the energy of formation of CH_3 to be calculated. In case (c), $N_{s\sigma}$ is evaluated from the energy difference between methane and CH_3, and from it the energy of formation of methane and a value of the heat of sublimation of carbon, $L(\mathrm{C})$, is obtained. The formulas employed are

$$W(\mathrm{CH_4}) - W(\mathrm{C}) - 4W(\mathrm{H}) = W_v(\mathrm{C}) + 4K(\mathrm{CH_4}) + 6K(\mathrm{H_2}) - 3\beta + (1/2)N_{ss} - (5/2)N_{s\sigma} - 3\sqrt{3}N_{s\sigma} + 4N_{\pi\pi}, \quad (4)$$

$$W(\mathrm{CH_3}) - W(\mathrm{C}) - 3W(\mathrm{H}) = W_v'(\mathrm{C}) + 3K(\mathrm{CH_4}) + 3K(\mathrm{H_2}) - (3/2)\beta - (3/2)N_{s\sigma} - 3\sqrt{2}N_{s\sigma} + 3N_{\pi\pi}. \quad (5)$$

Here $K(\mathrm{CH_4}) = -2.64$, and $K(\mathrm{H_2}) - (1/2)\beta = 0.41$ for CH_4 and 0.34 for CH_3, from the Morse function for H_2.[1]

The method of computing the energy of formation of methane is as follows:

$\mathrm{C(gr.)} + 2\mathrm{H_2} = \mathrm{CH_4}$	$W_0(\mathrm{CH_4}) - 2W_0(\mathrm{H_2}) - W(\mathrm{C_{gr.}})$	$= -0.69$ ev[9]
$\mathrm{C(g)} = \mathrm{C(gr.)}$	$W(\mathrm{C_{gr.}}) - W(\mathrm{C})$	$= -L(\mathrm{C})$
$4\mathrm{H} = 2\mathrm{H_2}$	$2W_0(\mathrm{H_2}) - 4W(\mathrm{H})$	$= -8.95$[4]
$\mathrm{CH_4} = \mathrm{CH_4}$ (pot. min.)	$W(\mathrm{CH_4}) - W_0(\mathrm{CH_4})$	$= -1.17$[6]
$\mathrm{C(g)} + 4\mathrm{H} = \mathrm{CH_4}$ (pot. min.)	$W(\mathrm{CH_4}) - W(\mathrm{C}) - 4W(\mathrm{H})$	$= -10.81 - L(\mathrm{C})$

Results obtained are summarized below.

Case	a	b	c	d
$L(\mathrm{C})$, kcal.	(135.7)	(125)	126.5	(170.4)
$N_{s\sigma}$, ev	1.62	1.53	1.54	1.91
$W(\mathrm{CH_4}) - 4W(\mathrm{H}) - W(\mathrm{C})$, ev	−16.70	−16.23	−16.29	−18.20
$W(\mathrm{CH_3}) - 3W(\mathrm{H}) - W(\mathrm{C})$, ev	−11.88	−11.51	−11.56	−13.12

[7] H. D. Hagstrum, Phys. Rev. **72**, 947 (1947).
[8] L. Brewer, P. W. Gilles, and F. A. Jenkins, paper presented before American Chemical Society meeting, Chicago, April, 1948.
[9] $\Delta H^0_0 = -15.99$ kcal., D. D. Wagman *et al.*, J. Res. Nat. Bur. Stand. **34**, 143 (1945).

TABLE I. Energy levels of the carbon atom, above $s^2p^2\ ^3P$, in electron volts.

State	Observed	Computed
$sp^3\ ^3S$	13.10[b]	13.12
^3P	9.32[b]	9.55
^3D	7.95[b]	8.29
^5S	4.16[a]	4.16
$s^2p^2\ ^1S$	2.68[a]	3.15
^1D	1.26[b]	1.26
^3P	0.00	0.00

[a] (See reference 3.)
[b] Edlen, quoted by Ufford (see reference 2).

The result in case (c) indicates a value of L(C) in the neighborhood of 120 to 140 kcal. but cannot with certainty exclude L(C) = 170.4. A similar line of reasoning was set forth by Long and Norrish[10] as an argument in favor of L(C) = 125 kcal.

HEATS OF REMOVAL OF HYDROGEN ATOMS

Heats necessary for the removal of successive hydrogen atoms from methane, according to the cases outlined above, are summarized in Table II. These heats are, of course, computed from the lowest vibrational states and not from potential minima. The average bond energies—namely, one-fourth the heat required to remove all four hydrogen atoms—are: (a) 89.6, (b) 86.8, (c) 87.2, and (d) 98.2 kcal. The individual bond strengths differ considerably from the averages. Within the accuracy of this method of calculation, in the first three cases the heats of removal of successive hydrogens from methane are 101, 90, 80, and 80 kcal., respectively. This is the most significant result of calculations such as the present. There is no evidence that CH_3 will part with a hydrogen atom more readily than the other radicals, although this has often been suggested because the carbon atom drops down into the divalent s^2p^2 state in this step. The explanation for the absence of such an effect is, of course, that intrinsically stronger bonds are formed by sp^3 carbon and that these more than compensate for

[10] L. H. Long and R. G. W. Norrish, Proc. Roy. Soc. **A187**, 337 (1946).

TABLE II. Heats of removal of hydrogen atoms from methane and radicals, in kcal.

Process	(a) L(C) = 135.7	(b) L(C) = 125	(c) $W_0(CH_3)-W_0(CH_4)+W(H)=101$	(d) L(C) = 170.4
$CH_4=CH_3+H$	103.1	100.8	(101.0)	109.1
$CH_3=CH_2+H$	95.5	86.9	88.1	124.0
$CH_2=CH+H$	79.6	79.6	79.6	79.6
$CH=C+H$	(80.0)	(80.0)	(80.0)	(80.0)

the necessary promotional energy of the carbon atom. It may be noted, however, that no effort is made here to evaluate the intrinsic bond strengths corresponding to a process in which hydrogens are removed while the state of the carbon remains unchanged, because these are not at present measurable or useful quantities. The attempt of Long and Norrish[10] to express bond energies in terms of the heat of sublimation of carbon to the $sp^3\ ^5S$ state does not appear to be helpful since the ^5S state is not observed as a metastable product; their attempt also disagrees with calculations of the present type which show that the ^5S level does not properly measure the energy of the carbon atom in the quadrivalent state.

It is pointed out by Stevenson[11] that the present values for the relative energies of CH_4 and CH_2 in cases (a), (b), and (c) are in good agreement with the following estimates from electron impact data.

Process	Energy, ev	Reference
$CH_4=CH_2^++H_2$	15.7 ±0.5	Smith[6]
$H_2=2H$	4.48	Herzberg[4]
$CH_2^+=CH_2$	−11.9 ±0.2	Langer and Hipple[12]
$CH_4=CH_2+2H$	8.28	

For the same process in cases (a), (b), and (c) the computed energies are 8.61, 8.14, and 8.20 ev, respectively. For case (d) the computed value is 10.11 ev, and the disagreement of this with 8.28 ev may also be taken as evidence against L(C) = 170.4 kcal.

[11] D. P. Stevenson, these laboratories, private communication.
[12] A. Langer and J. A. Hipple, Phys. Rev. 69, 691 (1946).

THE JOURNAL OF CHEMICAL PHYSICS VOLUME 16, NUMBER 10 OCTOBER, 1948

The Mercury Photosensitized Reaction of Dimethyl Ether

R. A. MARCUS, B. DEB. DARWENT, AND E. W. R. STEACIE
Division of Chemistry, National Research Council, Ottawa, Canada

(Received June 1, 1948)

The mercury photosensitized reaction of dimethyl ether has been investigated at pressures between 28 and 500 mm and at temperatures between 25°C and 292°C. At 25°C the products consist almost entirely of hydrogen and 1,2-dimethoxyethane, and the initial step has been shown to be the abstraction of a hydrogen atom.

At higher temperatures CH_2O, CH_4, C_2H_6 and probably $CH_3OC_2H_5$ become important products. They are derived from the decomposition of the methoxy methyl radical followed by subsequent radical recombination reactions. Carbon monoxide is produced in the later stages from the decomposition of formaldehyde.

By varying the light intensity and pressure it has been shown that ethane and dimethoxyethane are produced by second order recombination of methyl and methoxy methyl radicals respectively. The activation energies of the following reactions have been estimated:

$$CH_3+CH_3OCH_3\rightarrow CH_4+CH_3OCH_2 \quad E=9.0 \text{ kcal.}$$
$$CH_3OCH_2\rightarrow CH_3+CH_2O \quad E=19 \text{ kcal.}$$

the only assumption being that methyl and methoxy methyl radicals recombine with zero activation energy.

INTRODUCTION

AN investigation[1] of the mercury photosensitized reactions of diethyl ether showed that the initial step probably consists of the abstraction of a hydrogen atom resulting in the formation of the radical $C_2H_5O\cdot C_2H_4$; however, the products were complex and the possibility that the reaction proceeded through the formation of an active ether molecule could not be excluded. The mercury photosensitized reactions of dimethyl ether, being simpler, should give more definite information about the nature of the primary act in these reactions of the simple ethers.

The only previous investigation of the photodecomposition of dimethyl ether is that of Berthelot and Gaudechon,[2] who used the full light from a mercury lamp. This was most likely a photosensitized reaction since no precautions were taken to ensure the absence of mercury and since dimethyl ether is transparent to about 2000A. They reported methane, carbon monoxide, hydrogen and an unidentified liquid as the products, but their results were not sufficiently detailed to give information about the primary act.

This investigation has established the occurrence of a C−H split and the formation of the radical CH_3OCH_2 as the initial step. The chain-carrying steps in the thermal decomposition of dimethyl ether, as postulated by Rice and Herzfeld[3] were:

$$CH_3OCH_2\rightarrow CH_3+CH_2O,$$
$$CH_3+CH_3OCH_3\rightarrow CH_4+CH_3OCH_2.$$

The present investigation has enabled an estimate to be made of the activation energies of these reactions.

EXPERIMENTAL

Dimethyl ether was obtained in cylinders from the Ohio Chemical and Manufacturing Company, Cleveland, Ohio. It was stated to be 99.97 percent pure and was used without further purification except for a simple bulb to bulb distillation and degassing by repeated freezing and melting in vacuum. It was stored as a liquid in a cooled vessel isolated by a mercury cut-off.

The reaction system was of conventional design in which the gases were circulated by a pump of the type described by Puddington[4] through a mercury saturator, desaturator and a

TABLE I. Analysis of liquid product.

	b.p.	n_D^{20}	$n_\beta^{20}-n_\alpha^{20}$	% C	% H	% O
Product	82.5	1.3796	0.00652	53.3	11.1	35.6
1,2-dimethoxy ethane	84.8	1.37965	0.00654	52.6	11.1	36.3

[1] B. deB. Darwent, E. W. R. Steacie, and A. F. Van Winckel, J. Chem. Phys. **14**, 551 (1946).
[2] D. Berthelot and H. Gaudechon, Comptes rendus **153**, 383 (1911).
[3] F. O. Rice and K. F. Herzfeld, J. Am. Chem. Soc. **56**, 284 (1934).
[4] I. E. Puddington, Ind. Eng. Chem. (Anal. Ed.) **17**, 592 (1945).

TABLE II. Mercury photosensitized decomposition of dimethyl ether.*

No.	Pressure (mm)	Time (hr.)	Products, cc at N.T.P. H_2	CO	CH_4	RCHO
I. Runs at 25°C						
1	28	2.0	1.00	0.00	0.00	
2	28	4.0	1.96	0.01	0.01	*ca.* 0.02
3	28	6.0	2.80	0.01	0.01	
4	49	1.0	0.58			
5	83	1.0	0.61			
6	127	1.0	0.63			
7	127	2.0	1.23	0.00	0.00	
8	127	5.0	3.16	0.01	0.01	
9	489	2.0	1.28	0.00	0.00	
10	489	5.25	3.36	0.00	0.00	

No.	Pressure (mm)	Time (hr.)	Products, cc at N.T.P. H_2	CO	CH_4	C_2H_6	CH_2O	RCHO	CO_2
Runs at 265°C									
26	28	0.5	0.27	0.03	0.26	0.11	0.50	0.49	—
24	28	1.5	0.83	0.14	0.64				
23	28	3.0	1.71	0.43	1.32	0.39	2.36	2.26	0.07
25	28	6.0	3.91	1.40	2.94	0.83	4.26	4.18	0.11

* Volume of system—3790 cc. Volume of reaction vessel—240 cc. Circulation rate—300 cc $min.^{-1}$ at prevailing pressure. λ2537 absorbed —*ca.* 3.5×10^{-5} einstein $hr.^{-1}$ Hg pressure—1.5×10^{-3} mm.

cylindrical quartz reaction cell enclosed in a concentric tubular furnace. A large dead space was included in the system to lower the partial pressures of the products. This allowed appreciable amounts of products to be obtained even though the reaction was restricted to small conversions. Mercury cut-offs were used to separate the reaction system from the rest of the apparatus because of the high solubility of ether in stopcock grease. The total volume of the system was 3790 cc and of the quartz reaction cell 240 cc.

The furnace temperature, controlled manually to ±1°C, was measured by a copper-constantan thermocouple affixed to the rear face of the quartz cell. This in turn was calibrated against a similar couple placed inside the cell close to the incident face. The correction varied from +3°C at 170°C to +6°C at 265°C, and was independent of the pressure of the circulating gas.

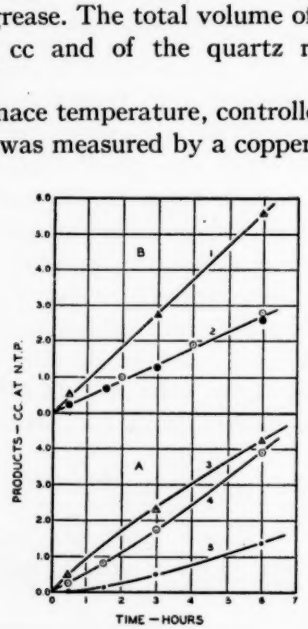

FIG. 1. The products of the reaction.

Curve 1—$CH_2O + CO$ at 265°C. Curve 2—Open circles: H_2 at 25°C; filled circles: $H_2 - CO$ at 265°C. Curve 3—CH_2O at 265°C. Curve 4—H_2 at 265°C. Curve 5—CO at 265°C.

Unreversed λ2537 was obtained from a low pressure mercury lamp with neon (3 mm) as carrier gas. It is reasonably certain that little λ1849 entered the cell since the light path from the lamp, through a quartz furnace window, to the incident face of the reaction cell, was about 20 cm in air. The intensity of λ2537 was estimated from the rate of hydrolysis of monochloracetic acid (0.5N), by assuming a value of 0.315 for the quantum yield of the hydrolysis[5] and applying a small correction for the dark reaction.

The products were largely hydrogen and 1,2-dimethoxyethane ("dimer") at room temperature; at higher temperatures methane, ethane, formaldehyde, carbon monoxide and traces of carbon dioxide were also detected. Spot tests[6] for alcohols and peroxides proved to be negative. A positive test[7] for acetaldehyde was obtained, but determinations of the formaldehyde[8] and total aldehydes[9] showed that the acetaldehyde was present in negligible quantities. To eliminate errors inherent in the use of two different methods the former procedure, a colorimetric method, was calibrated against the latter. Negligible blanks were obtained when pure dimethyl ether was submitted to tests for the various products.

After given reaction times, the condensible products were immediately frozen out. The products were separated by pumping from a trap kept successively at −183°C, −135°C and −100°C. The products volatile at −183°C (CH_4, CO, H_2) were analyzed by conventional methods. Some methane was retained by the substantial amount of solid dimethyl ether pres-

[5] R. N. Smith, P. A. Leighton, and W. G. Leighton, J. Am. Chem. Soc. **61**, 2299 (1939).
[6] F. Feigl, *Qualitative Analysis by Spot Tests* (Elsevier Publishing Company, New York, 1946).
[7] A. Ley, J. Pharm. chim. (6) **22**, 107 (1897).
[8] D. Matuakawa, J. Biochem. (Tokyo) **30**, 386 (1939).
[9] I. M. Kolthoff and N. H. Furman, *Volumetric Analysis* (John Wiley and Sons, Inc., New York, 1929), Vol. II, p. 450.

ent, but this was removed by repeated melting, freezing and pumping.

The gas volatile at −135°C, a mixture of ethane and methyl ether with traces of CO_2 and CH_2O, was analyzed in a modification[10] of the Ward[11] fractionation system. In the early runs, the ethane was identified by combustion over a hot platinum wire. No ethylene was detected. A small "C_3" fraction, analyzed by combustion, proved to be a mixture of CO_2 and dimethyl ether. The presence of CO_2 was further established with the limewater test.

The fraction volatile at −100°C consisted of CH_2O and the bulk of the ether. The residue remaining in the trap, liquid at room temperature, was frozen out in a small pycknometer $(3.35\pm0.05)\times10^{-3}$ cc cm^{-1} attached to the trap by a mercury cut-off. The dead space above the pycknometer, 0.15 cc, ensured only a small correction for the amount of material in the vapor phase. The amount of liquid was estimated after standing for several hours at room temperature. Prior to this, the liquid at no time came into contact with stopcock grease.

This fraction was identified by its boiling point, refractive index, and carbon, hydrogen and oxygen analysis.* The properties of the liquid product, given in Table I, are compared with those of 1,2-dimethoxy ethane. In reporting the "dimer" in subsequent tables, its quantity has been expressed as cc of gas at N.T.P. on the assumption that its molecular weight corresponds to that of 1,2-dimethoxy ethane.

The latter two fractions, volatile at −100°C, and residue, were combined, and frozen out in a tube containing ice which was sealed off and the formaldehyde content determined by the bisulphite method.[9] This value was corrected for the amount (av. 2 percent) present in the second fraction.

Finally, blank experiments in the dark showed that the thermal decomposition of dimethyl ether and products was negligible at all temperatures employed in this investigation.

[10] J. J. Savelli, W. D. Seyfried and B. M. Filbert, Ind. Eng. Chem. (Anal. Ed.) **13**, 868 (1941).
[11] E. C. Ward, Ind. Eng. Chem. (Anal. Ed.) **10**, 169 (1938).
* We are indebted to Dr. L. Marion of this Laboratory for the C:H analyses.

TABLE III. Mercury photosensitized decomposition of dimethyl ether.*

No.	Pressure (mm)	Time (hr.)	Products, cc at N.T.P. H_2−CO	CO	CH_4	CH_2O +CO	C_2H_6	Dimer (found)	Dimer (calc.)
I. Runs at 25°C									
99	4.9	8.75	1.77	0.15	0.09				
84	28	1.5	0.62	(0.00)	—				
87	28	1.0	0.42	(0.00)	—				
85	110	1.0	0.49	(0.00)	—				
86	110	1.0	0.49	(0.00)	—				
II. Runs at 165°C									
82	110	22.0	11.0	0.27	0.51	1.24		10.7	10.5
III. Runs at 199°C									
62	28	9.5	4.65	0.39	0.40	1.46	0.081	3.5	3.7
72	28	9.5	4.41	0.33	0.39	1.37	0.082	3.3	3.5
61	110	10.0	6.10	0.26	1.03	2.08	0.079	5.4	5.1
75	110	7.5	4.10	0.15	0.72				
IV. Runs at 237°C									
50	28	4	2.10	0.35	0.87	2.20	0.27		1.04
77	28	4	1.83	0.31	0.81	2.08	0.24	0.7	0.80
81	28	4	1.64	0.27	0.79	1.91	0.20		0.71
76	28	4.25	1.81	0.30	0.80	2.04	0.26		0.83
51	110	2.5	1.59	0.18	1.65	2.65	0.18		0.77
63	110	3	1.70	0.21	2.11	3.16	0.31		0.96
64	110	3.1	1.76	0.24	2.18				
V. Runs at 265°C									
47	28	1.3	0.72	0.11	0.67	1.43			0.15
68	28	2	1.02	0.22	0.99	1.98	0.29		0.33
59	28	2.5	1.36	0.36	1.36	2.72	0.41		0.38
44	28	3	1.20	0.38	1.49	2.64	0.45		0.50
42	110	1	0.55	0.09	1.75	2.13	0.19		0.36
58	110	1	0.63	0.09	1.60	2.25	0.13		0.13
65	110	1.2	0.73	(0.12)**	1.80				
46	110	1.5	0.94	0.21	2.45	3.27	0.21		0.34
43	110	2.5	1.33	0.44	4.09	5.26	0.37		0.53
45	500	0.67	0.42	0.08	3.10	3.37	0.08		0.24
48	500	1.5	0.99	0.30	7.63	8.03	0.09		0.68
60	500	1.5	0.96	0.28	7.37				
VI. Runs at 292°C									
52	28	1.5	0.75	0.31	1.50	2.36	0.41		(0.3)
53	110	1.3	0.84	0.48	4.48	5.37	0.39		(0.3)

* Conditions as in Table II, but light input—2.7×10^{-5} einstein $hr.^{-1}$
** Interpolated.

RESULTS

The results of preliminary experiments to investigate the effects of time and ether pressure on the nature of the products of the mercury photosensitized reactions of dimethyl ether at 25°C and 265°C are given in Table II of which column 7, headed RCHO, denotes total aldehydes. Inspection of these data shows that, at 25°C and between 28 and 489 mm, hydrogen (and presumably 1,2-dimethoxy ethane) are the only important products, and that the rate of production of hydrogen is independent of time

TABLE IV.*

No.	Time (hr.)	Products, cc at N.T.P. H_2−CO	CO	CH_4	CH_2O +CO	C_2H_6	Dimer (found)	Dimer (calc.)
78	22	0.96	0.39	1.82	2.63	0.25	0.2	0.40
79	48.5	1.72	1.17	3.17	4.58	0.37	0.5	0.68
80	48.5	1.76	1.20	3.40	4.75	0.35	0.5	0.76

* Conditions as in Table II, but light input=2.2×10^{-6} einstein $hr.^{-1}$ Temp.—237°C; Pressure—28 mm.

TABLE V. Effect of light intensity on methane and ethane formation at 237°C.

No.	Light input (einstein hr.$^{-1}$×10^6)	$k_{CH_4}/k_{C_2H_6}^{\frac{1}{2}}$	$k_{CH_4}/k_{C_2H_6}$
50	27	0.84	3.2
76	27	0.78	2.8
77	27	0.84	3.1
81	27	0.89	4.0
		Av. 0.81	Av. 3.3
78	2.2	0.78	7.4
79	2.2	0.76	8.7
80	2.2	0.82	9.7
		Av. 0.79	Av. 8.6

TABLE VI. Effect of light intensity on CH_2O and dimer.

No.	Light input (einstein hr.$^{-1}$×10^6)	$[CH_2O+CO]/[dimer]^{\frac{1}{2}}$	$[CH_2O+CO]/[dimer]$
50	27	1.06	2.1
76	27	1.04	2.5
77	27	1.16	2.6
81	27	1.13	2.7
		Av. 1.10	Av. 2.5
78	2.2	0.90	6.7
79	2.2	0.81	6.8
80	2.2	0.79	6.3
		Av. 0.83	Av. 6.6

(Fig. 1), but increases with ether pressure up to about 100 mm, probably as a result of incomplete quenching, above which pressure the rate is pressure independent and quenching is essentially complete. At 265°C, CO, CH_4, C_2H_6 and CH_2O become important products. The data in Table II show that at 265°C rates of formation of CH_4 and C_2H_6 are independent of time but that the rate of formation of H_2 increases with time and is paralleled by a corresponding increase in the rate of formation of CO and by a decrease in the rate of formation of CH_2O; this is illustrated in Fig. 1(a). If it be assumed that this deviation from linearity is due to decomposition of the formaldehyde:

$$CH_2O \rightarrow CO + H_2$$

then the rates of formation of (H_2-CO) and of (CH_2O+CO) should be independent of time; Fig. 1(b) shows clearly that those rates are in fact independent of time and that the rate of formation of (H_2-CO) at 265°C is the same as the rate of production of hydrogen at 25°C,

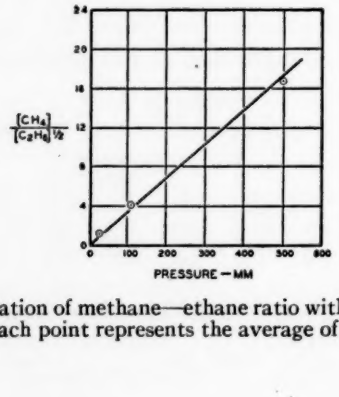

FIG. 2. Variation of methane—ethane ratio with pressure at 237°C. Each point represents the average of all runs.

indicating that the production of hydrogen in the initial stage is temperature independent.

The results of experiments to determine the effect of temperature on the products of the reaction are given in Table III. Here the production of hydrogen and formaldehyde are corrected for the decomposition of formaldehyde and are quoted as (H_2-CO) and (CH_2O+CO) respectively, and, since the amount of CO produced is listed the uncorrected figures for H_2 and CH_2O may be obtained. The amount of "dimer" $(CH_3OCH_2)_2$ calculated from a material balance may be compared in some experiments with the amounts actually found; the agreement is shown to be satisfactory. Material balance calculations show that the C:O ratio of the products is less than the value of 2:1 in dimethyl ether. If ethane and dimer are formed by radical recombination then a logical additional product would be methyl ethyl ether with a C:O ratio of 3:1. The presence of this product has been assumed and its amount can be calculated from the stoichiometric equations:

$$2(CH_3)_2O \rightarrow H_2 + (CH_3OCH_2)_2$$
$$2(CH_3)_2O \rightarrow C_2H_6 + 2CH_2O + H_2$$
$$(CH_3)_2O \rightarrow CH_4 + CH_2O$$
$$2(CH_3)_2O \rightarrow CH_3OC_2H_5 + CH_2O + H_2$$
$$CH_2O \rightarrow CO + H_2$$

from which

$$CH_3OC_2H_5 = (CH_2O+CO) - CH_4 - C_2H_6$$
$$(CH_3OCH_2)_2 = (H_2-CO) + CH_4 + C_2H_6 - (CH_2O+CO).$$

On this basis, the calculated pressure increase for experiment 25 is 1.50±0.05 mm, while the

observed value was 1.55±0.05 mm. The calculated and experimentally determined values of dimer are compared in the final column of Tables III and IV. The agreement is excellent when the amount of dimer is not so small that experimental losses become important.

Quantum Yield

At room temperature the quantum yield for ether reacted was determined to be 1.60 under conditions of complete quenching. The lamp emits some light other than λ2537 which is active in the hydrolysis of monochloroacetic acid. The amount, however, is small, and the error in the quantum yield is not over 10 percent.

At 292°C and with an ether pressure of 110 mm, the calculated amount of ether reacted is 2.1×10^{-4} mole hr.$^{-1}$, so that under these conditions, a quantum yield of 8 is found.

In some experiments the light intensity was reduced by altering the current to the lamp. The effect on the products of a twelvefold change of intensity is given in Table IV.

DISCUSSION

(a) The Photosensitized Reaction

The great preponderance of hydrogen and 1,2-dimethoxy ethane in the products at 25°C is explained adequately by the reactions:

$CH_3OCH_3+Hg(^3P_1)\rightarrow$

$$CH_3OCH_2+H+Hg(^1S_0) \quad (1)$$

$$H+CH_3OCH_3\rightarrow CH_3OCH_2+H_2 \quad (2)$$

$$2CH_3OCH_2\rightarrow(CH_3OCH_2)_2. \quad (3)$$

The reaction rate does not decrease with increasing pressure above 100 mm and there is no evidence for collisional deactivation, or for the formation of an excited molecule in the primary step. Reaction (2) has been shown[12] to proceed rapidly at room temperature and probably represents the sole means of formation of hydrogen in those experiments since the experimental quantum yield of 1.6, a minimum value, compares favorably with the predicted value of 2.0. The fact that reaction (3), and not a first-order recombination of methoxy methyl radicals on the wall, represents the mode of formation of 1,2-dimethoxy ethane will be discussed later. The very small amounts of aldehydes and other products found indicate that reactions of the "atomic cracking" type do not occur significantly.

[12] W. R. Trost, B. deB. Darwent and E. W. R. Steacie, J. Chem. Phys. **16**, 353 (1948).

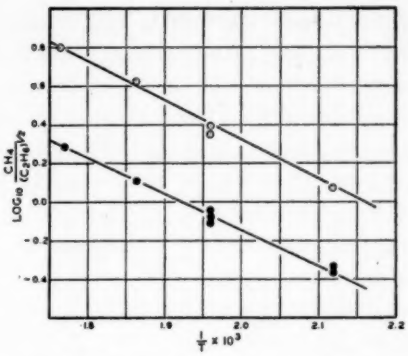

FIG. 3. Effect of temperature on CH_4 and C_2H_6 production. Open circles: runs at 110 mm; filled circles: runs at 28 mm.

These results indicate the probability that diethyl ether[1] also reacted with $Hg(^3P_1)$ atoms by a C−H split. Re-examination of the results of that investigation shows that, at the higher pressures, no CH_4 or CO are produced initially, and that any differences between the types of products obtained previously with diethyl ether and those now reported at room temperature, probably are due to the higher intensity used with diethyl ether, resulting in higher radical concentrations, leading to an increase in the "atomic cracking" type of reaction.

At higher temperatures additional products CH_4, C_2H_6, CO and CH_2O are formed in increasing amounts. These undoubtedly arise from the decomposition of the methoxy methyl radical;

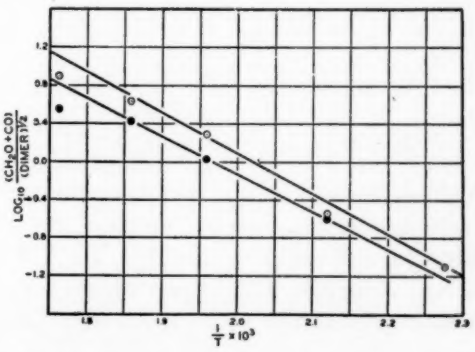

FIG. 4. The effect of temperature on the production of formaldehyde and dimer. Open circles: runs at 110 mm; filled circles: runs at 28 mm.

they are not due to increased "atomic cracking" since the rate of production of methane at 265°C increases markedly with increasing ether pressure (Table III). It is also significant that the corrected value (H_2-CO) for the rate of production of hydrogen is unaltered by an increase of temperature from 25° to 265°C (Fig. 1), indicating that reaction (1) is, as expected, temperature independent and that, even at 25°C, all H atoms produced eventually react with ether, as indicated by reaction (2).

(b) The decomposition of CH_3OCH_2 and the reaction between CH_3 and CH_3OCH_3

The results show that the quantum yield of ether disappearance increases from 1.6 at 25°C to 8 at 295°C; a chain reaction is therefore involved. Also at elevated temperatures CH_4, C_2H_6 and CH_2O are formed in increasing amounts. The chain carrying steps proposed by Rice and Herzfeld[3] for the thermal decomposition of dimethyl ether:

$$CH_3OCH_2 \rightarrow CH_3+CH_2O \qquad (4)$$

$$CH_3+CH_3OCH_3 \rightarrow CH_3OCH_2+CH_4 \qquad (5)$$

together with the usual recombination steps:

$$2CH_3 \rightarrow C_2H_6 \qquad (6)$$

$$CH_3+CH_2OCH_3 \rightarrow C_2H_5OCH_3 \qquad (7)$$

and reaction (3) account for the nature of the products and the increased quantum yield at elevated temperatures. As mentioned previously CO is produced by secondary decomposition of formaldehyde and enters the kinetics only as a correction term in the production of hydrogen and formaldehyde. On the basis of reactions (4) and (5) we get

$$d/dt[CH_2O]=k_4[CH_3OCH_2]$$

and

$$d/dt[CH_4]=k_5[CH_3][CH_3OCH_3]$$

To evaluate E_4 and E_5, the corresponding activation energies, it is necessary to know the effect of temperature on $[CH_3OCH_2]$ and $[CH_3]$, which are reflected in the rates of formation of 1,2-dimethoxy ethane and ethane respectively. However, these compounds may have been formed either by the second order processes (3) and (6) or by first order recombination on the wall:

$$CH_3OCH_2 \xrightarrow{\text{wall}} \tfrac{1}{2}(CH_3OCH_2)_2, \qquad (3')$$

$$CH_3 \xrightarrow{\text{wall}} \tfrac{1}{2}C_2H_6. \qquad (6')$$

The rate of ethane formation is given by the equation

$$\{d/dt[C_2H_6]=k_6[CH_3]^2.$$

Thus at a given time we have,

$$\frac{d/dt[CH_4]}{(d/dt[C_2H_6])^{\frac{1}{2}}}=\frac{k_5}{k_6^{\frac{1}{2}}}[CH_3OCH_3].$$

This relation demands that ($k_{CH_4}/k_{C_2H_6}^{\frac{1}{2}}$) (1) be independent of radical concentration, i.e. of light intensity and (2) increase linearly with dimethyl ether pressure. The approximate validity of these assumptions are shown in Table V and in Fig. 2. In Table V changing light intensity by a factor of twelve is seen to have no effect on the ratio ($k_{CH_4}/k_{C_2H_6}^{\frac{1}{2}}$). The units of CH_4 and C_2H_6 are cc hr.$^{-1}$.

First-order recombination of methyl radicals would necessitate that $k_{CH_4}/k_{C_2H_6}$ be independent of light intensity, a conclusion in strong disagreement with the data given in Table V.

Other processes for methane formation, such as

$$2CH_3 \rightarrow CH_4+CH_2 \qquad (12)$$

$$CH_3+H \rightarrow CH_4, \qquad (13)$$

or three-body recombination in the gas phase are excluded, either on the basis of the effect of pressure and light intensity on the $k_{CH_4}/k_{C_2H_6}^{\frac{1}{2}}$ ratio, or on the basis of the temperature-independent rate of production of (H_2-CO).

The rates of formation of formaldehyde and dimer are given by

$$d/dt[CH_2O+CO]=k_4[CH_3OCH_2] \qquad (14)$$

$$d/dt[\text{dimer}]=k_3[CH_3OCH_2]^2. \qquad (15)$$

Thus at any given reaction time,

$$[CH_2O+CO]/[\text{dimer}]^{\frac{1}{2}}=k_4/k_3^{\frac{1}{2}}. \qquad (16)$$

The effect of light intensity on the ratio of these products is given in Table VI.

The ratio $[CH_2O+CO]/[\text{dimer}]^{\frac{1}{2}}$ is approximately independent of intensity as demanded by the second order recombination process, whereas the ratio $[CH_2O+CO]/[\text{dimer}]$ is quite strongly

dependent on intensity. Hence it is evident that the formation of "dimer" is a second-order process. The apparent slight dependence of the ratio $[CH_2O+CO]/[\text{dimer}]^{\frac{1}{2}}$ on intensity is probably due to increased polymerization of the formaldehyde in the long runs at low intensity.

Activation Energies

The slopes of the plot $\log(k_{CH_4}/k_{C_2H_6}^{\frac{1}{2}})$ *vs.* $1/T$, given in Fig. 3, correspond to activation energies of 8.8 at 28 mm, and 9.2 at 110 mm. On the basis of the previous discussion this is equal to $E_5-\frac{1}{2}E_6$. Assuming E_6, the activation energy for recombination of two methyls, to be zero, the activation energy for the reaction of methyl radicals with dimethyl ether (E_5) is equal to 9.0 kcal. Similarly, from a plot of $\log[CH_2O+CO]/[\text{dimer}]^{\frac{1}{2}}$ *vs.* $1/T$, given in Fig. 4, the activation energy for the unimolecular decomposition of the CH_3OCH_2 radical is equal to 18.5 and 20.0 kcal. at 28 mm and 110 mm respectively, and if the activation energy for the recombination of two methoxy-methyl radicals is assumed to be zero, then E_4 may be taken as 19 kcal. In plotting the curves in Fig. 4, the runs at the highest temperature have been given little weight, since experimental errors are much larger at the highest temperatures.

THE JOURNAL OF CHEMICAL PHYSICS VOLUME 16, NUMBER 10 OCTOBER, 1948

Isotope Effect in the Thermal Cracking of Propane-1-C^{13}

D. P. Stevenson, C. D. Wagner, O. Beeck, and J. W. Otvos
Shell Development Company, Emeryville, California

(Received June 21, 1948)

It was recently found that the dissociation probabilities of the $C^{12}-C^{12}$ and the $C^{12}-C^{13}$ bonds of the molecule-ions formed from propane-$1-C^{13}$ by electron impact differ by *ca.* 20 percent.[1] This observation led us to look for a similar difference in ordinary chemical reactions of propane-$1-C^{13}$. The pyrolysis of propane was selected for study, since this reaction is one whose mechanism is presumably well understood.[2] Significant differences were found in the reactivities of bonds to terminal C^{13} and C^{12} atoms. The magnitude of the effect, 8 percent more frequent rupture of $C^{12}-C^{12}$ bonds than of $C^{12}-C^{13}$ bonds, is such that the effect should not be neglected in quantitative tracer experiments with carbon isotopes where reaction rates are involved.

Propane-$1-C^{13}$ (53 percent), prepared as previously described and with the isotopic species distribution shown in Table I, was cracked to a depth of approximately 10 percent (three separate experiments) at temperatures between 500 and 550°C. The product was separated into three fractions, hydrogen and methane, ethane, and ethylene, and propylene and propane, by one plate, isothermal distillation at very low pressure (low temperature). The relative concentrations of the isotopic methanes, ethylenes, and ethanes, as well as the total concentrations of hydrogen, methane, ethylene, ethane, propylene, and pro-

Table I. Composition of feed propane-1-C^{13} (53%).

Species	Mole fraction
$C^{12}H_3C^{12}H_2C^{12}H_3$	$0.457_5 \pm .0015$
$C^{12}H_3C^{12}H_2C^{13}H_3$	$.526_5 \pm .0017$
$C^{12}H_3C^{13}H_2C^{12}H_3$	$.0048 \pm .0001$
$C^{12}H_3C^{13}H_2C^{13}H_3$	$.0056 \pm .0001$
$C^{13}H_3C^{12}H_2C^{13}H_3$	$.0056 \pm .0001$
$C^{13}H_3C^{13}H_2C^{13}H_3$	—

Table II. Mole fractions of "heavy" products.

	Found‡	Calculated, assuming no isotope effect
$C^{13}H_4$ in methane	$0.263 \pm .002$	0.272
$C^{12}C^{13}H_4$ in ethylene	$.288 \pm .004$	.277
$C^{12}C^{13}H_6$ in ethane	$.252 \pm .010$	.277

‡ The original data were empirically corrected for mass dependent, ion source discrimination effects. The indicated uncertainties are the mean deviations of analyses in three separate cracking experiments.

[1] Beeck, Otvos, Stevenson, and Wagner, J. Chem. Phys. 16, 255 (1948).

[2] E. W. R. Steacie, *Atomic and Free Radical Reactions* (Reinhold Publishing Corporation, New York, 1946). Particularly pages 103–105.

TABLE III. Material balance in the cracking of propane-1-C^{13}.

Starting material C_3H_8	Mole percent of total 100	Millimoles 0.445	Milligram-atoms of carbon 1.34
Product			
H_2	2.79	0.0133	—
CH_4	3.50	.0167	0.0167
C_2H_4	3.41	.0163	.0326
C_2H_6	0.27	.0013	.0026
C_3H_6	2.94	.0141	.0423
C_3H_8	87.1	.415	1.245
Total	100.0	0.476	1.34

pane, were determined mass spectrometrically. The mole fractions of "heavy" methane, ethylene, and ethane in the product methane, ethylene, and ethane, computed from the analytical data, are shown in Table II, where these mole fractions are compared with those computed from the isotopic composition of the original propane-1 – C^{13} on the assumption of no isotope effects.

The concentration of total ethane relative to that of total ethylene plus propylene in the reaction product indicates an effective chain length of about 20. Thus to the extent that the Rice-Herzfeld mechanism applies to the pyrolysis of propane, the methane is primarily a product of the chain carrying reaction,

$$n\text{-}C_3H_7 \rightarrow C_2H_4 + CH_3, \qquad (1)$$

as is all of the ethylene. Thus it would be expected that any isotope effects observed in ethylene formation would be complementary in methane formation, as is observed (Table II). Interpreting the "low" methane-C^{13} and the "high" ethylene-C^{13} in terms of the Rice-Herzfeld mechanism, one concludes hydrogen atoms to be preferentially removed from the C^{13} methyl group in the chain carrying step,

$$C_3H_8 + R \rightarrow n\text{-}C_3H_7 + RH. \qquad (2)$$

Such greater reactivity of C^{13} – H bonds is contrary to expectations based on the known effect of mass on zero point energy, which should affect the difference in activation energies and thus the relative reactivities of C^{12} – H and C^{13} – H bonds. Whatever the origin of the effect may be, the data indicate for the over-all reaction an 8 percent greater frequency of rupture of C^{12} – C^{12} than of C^{12} – C^{13} bonds.

The ethane presumably arises primarily from the chain initiating reaction,

$$C_3H_8 \rightarrow C_2H_5 + CH_3; \qquad (3)$$

thus the "low" concentration of ethane-C^{13} in the product indicates a preferential breaking of the C^{12} – C^{13} bond of propane-1 – C^{13} in the chain initiating reaction. The relatively poorer reproducibility of the mole fraction of heavy ethane indicates a need for further study of the chain initiating step, with particular reference to possible wall effects.

A material balance for one of the cracking experiments, as shown in Table III, is in complete agreement with earlier studies of the reaction.[2]

Neglecting chain terminating reactions between radicals, the following relationships should hold among quantities of products formed: $CH_4 = C_2H_6 + C_2H_4$; $H_2 = C_3H_6$. To the extent that methyl radicals and hydrogen atoms participate in chain breaking steps, the quantities on the left of the above equations should be smaller than those on the right. This was found to be the case by 5 and 6 percent, respectively. The ratio $(C_2H_4 + C_3H_6)/C_2H_6$ is a measure of chain length, which in this experiment was about 23. The ratio $6 \times C_3H_6/2 \times C_2H_4$ gives the relative reactivity of a secondary hydrogen to that of a primary in the reaction $R + C_3H_8 \rightarrow RH + C_3H_7$. This value is 2.6, which may be compared with the value 3.5 corresponding to a 2.0 kcal./mole difference in the activation energies for removal of secondary and primary hydrogen atoms at 525°C.[3]

[3] Reference 2, pages 318–319.

Letters to the Editor

THIS section will accept reports of new work, provided these are terse and contain few figures, and especially few halftone cuts. The Editorial Board will not hold itself responsible for opinions expressed by the correspondents. Contributions to this section should not exceed 600 words in length and must reach the office of the Managing Editor not later than the first of the month preceding that of the issue in which the letter is to appear. No proof will be sent to the authors. The usual publication charge ($4.00 per page) will not be made and no reprints will be furnished free.

The Relation between Covalent and Packing Radii of Atoms

A. L. G. REES
Division of Industrial Chemistry, Council for Scientific and Industrial Research, Melbourne, Australia
August 23, 1948

ALTHOUGH a knowledge of the packing radii of covalently bound atoms is frequently necessary in problems of structural chemistry, adequate data are available for a few atoms only, and an empirical rule suggested by Pauling[1] is usually employed to evaluate the packing radius (r) from the single-bond covalent radius (r'). This rule is formulated as

$$r = r' + 0.8\text{A}.$$

In cases for which x-ray crystallographic data are available, the differences ($r - r'$) are found to vary from 0.4 to 0.9A, indicating that Pauling's rule is a very approximate statement only. However, in the light of recent calculations of electron density distributions in covalently bound atoms, there is some basis on which a more precise rule may be formulated.

Since the assignment of a single constant value for the covalent radius of an atom is well established as a good approximation, and since there is now some evidence that the packing radius of a particular atom is independent of the nature of the atom to which it is bound, it is reasonable to expect as a first approximation that the electron density distribution about such an atom would also be independent of the nature of the atom to which it is bound. Moreover, Moffitt and Coulson[2] have shown for carbon atoms in different states of sp hybridization that the transverse thicknesses of the electron clouds are surprisingly constant. This supports any assumption which requires a constant packing radius independent of the state of binding. Evidence on the experimental side can also be derived from J. M. Robertson's x-ray crystal analysis data;[3] carbon atoms involved in single, conjugated, double and triple bonds are seen to have the same radius (as measured on a contour map to the 1 electron per A^2 contour in a direction perpendicular to the bond).

On the assumption that covalent and packing radii are constant for an atom in a particular state of binding, then there should be continuity of the electron density distribution (or the electronic wave function) and its first derivative across the covalent bond. This may be more readily appreciated from Fig. 1(a) in which a bond $A-B$ is represented on an electron density contour map of a section through the nuclei. The plane XY, which is perpendicular to the internuclear line $A-B$, divides $A-B$ into the appropriate covalent radii, r_A' and r_B', of the atoms A and B, respectively. The continuity condition can only be satisfied if the charge density distribution in the plane XY is independent of the nature of the atoms A and B, but it will, of course, vary with the bond order.

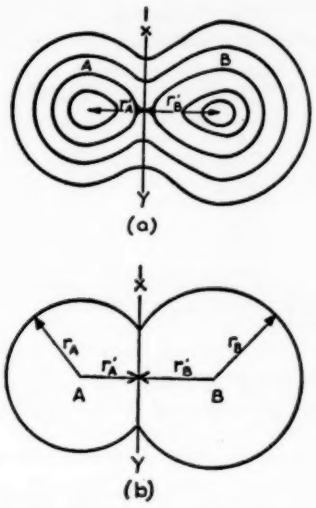

FIG. 1. Electron density contours.

If the equivalent, but less satisfactory, classical model of a covalently bound atom, *viz.*, a sphere of radius r with a spherical segment of height ($r - r'$) removed, is considered, fulfillment of the continuity condition evidently implies that the circular area of contact of the two spherical atoms in the plane XY (see Fig. 1(b)) is the same for all

TABLE I.

Atom	Single-bond covalent radius (r') A	Packing radius (r) (observed) A	k (A)	Packing radius (calculated according to rule of this paper)	Packing radius (calculated according to Pauling's rule)
H	0.37[a]	1.25[b]	1.20	1.27	1.17
O	0.730	1.39[c]	1.19	1.42	1.53
Br	1.142	1.65[d]	1.19	1.67	1.94
I	1.334	1.77[d]	1.17	1.81	2.13
Se	1.16	1.73[e]	1.29	1.69	1.96
C	0.772	—	—	1.44	1.57
Te	1.37	1.87[e]	1.26	1.84	2.17
			Mean 1.22		

[a] Covalent radii taken from Skinner, Trans. Faraday Soc. **41**, 645 (1945).
[b] Collision radius.
[c] Strukturbericht (S.B.). Vol. **II**, p. 269—smallest intermolecular O—O in N_2O_4.
[d] S.B. Vol. **IV**, p. 83, Vol. **II**, p. 5, smallest intermolecular interhalogen distance (data for Cl_2 quoted in S.B. Vol. **IV**, p. 3, and in original paper by Keesom and Taconis, Physica **3**, 237 (1936) appear to be in error).
[e] S.B. Vol **I**, p. 27, Vol. **I**, p. 63. Smallest interspiral interatomic distance.

TABLE II.

Atom	Single-bond covalent radius (r_S') A	Double-bond covalent radius (r_D') A	($r_S'^2-r_D'^2$)
B	0.89[a]	0.76[b]	0.21
C	0.772	0.665	0.16
N	0.735	0.60	0.18
O	0.730	0.55	0.22
Si	1.16	1.07	0.20
S	1.04	0.94	0.20
P	1.10	1.00	0.21
Cl	0.995	0.89	0.20

[a] Skinner, Trans. Faraday Soc. 41, 645 (1945).
[b] See reference 1, p. 164.

atoms participating in bonds of the same order. This condition is simply expressed by the relation—

$$r^2=r'^2+k^2,$$

where k is the radius of the circular contact area in the plane XY.

In Table I, single-bond covalent radii and packing radii obtained from the available x-ray crystallographic and collision data have been used to calculate the k values for various atoms. The mean of these k values has been used to calculate the packing radii included in column 5 of this table from the relation—

$$r^2=r'^2+1.22^2.$$

These are compared with packing radii calculated according to Pauling's rule and tabulated in column 6. It is evident that the rule derived here, which is still by nature very approximate, does give better agreement with the experimental data.

Electron diffraction data on molecular dimensions cannot be used in general for the derivation of packing radii , since it is only in spacial cases that the intramolecular interatomic distances represent conditions of close-packing. In the tetrahalides of tin, for example, there is ample room for the four halogen atoms around the comparatively large tin atom. In the carbon tetrahalides, however, it is evident that the halogen atoms just touch in their tetrahedral packing about the carbon atom. In CI_4 the I−I distance is 3.50A, giving the packing radius $r_I=1.75$A, which compares favorably with the value 1.77A deduced from the packing of I_2 molecules and 1.81A calculated from the rule derived here. The Br−B, distance in CBr_4 is 3.14A, giving $r_{Br}=1.58$A, compared with 1.65A from the crystal structure of Br_2 and 1.67A from this rule. Pauling's values for these radii are 2.13A and 1.94A, respectively—values which would result in repulsive forces large enough to give C−Br and C−I bond lengths larger than normal, a consequence which is not confirmed by experiment. Similarly, the carbon packing radius as deduced by this rule gives a more reasonable model for these molecules than that deduced by Pauling.

Viscosity, compressibility, and parachor data give molecular volumes which represent the total space per molecule in a close-packed liquid and are considerably larger than the true molecular volumes; these could not then be used in the evaluation of true packing radii.

It is interesting to note that the relation,

$$r_S'^2-r_D'^2=k_D^2-k_S^2=\text{constant},$$

is a consequence of the assumption that the packing radii r_S and r_D are identical, where the subscripts S and D denote the type of bond to which the quantities refer. It can be seen from Table II that this relationship between single- and double-bond radii is substantially true.

Provided its limitations are appreciated, this rule could be used with profit in the construction of molecular models and in the problems associated with structural chemistry for atoms whose packing radii are unknown.

[1] L. Pauling, *The Nature of the Chemical Bond* (Cornell University Press, Ithaca, 1945), p. 192.
[2] W. E. Moffitt and C. A. Coulson, Phil. Mag. 38, 634 (1947).
[3] J. M. Robertson, J. Chem. Soc. 249 (1945).

Ultraviolet Absorption Spectra of Substances Dissolved in Compressed Gases

B. VODAR AND S. ROBIN
Laboratoire de Physique-Enseignement, Sorbonne, Paris, France
August 26, 1948

WHEN studying the absorption of the ultraviolet spectrum in compressed liquids up to a pressure of 1.200 kg/cm², we have noticed that the commercial nitrogen, used as a compressive fluid, becomes absorbing for pressures higher than 600 kg/cm².

As we could not explain this phenomenon by the presence of any of the gaseous impurities which could be contained in the nitrogen used, we first suggested that it would be possible, perhaps, to impute this absorption to the gas itself.[1] Nevertheless, the liquid nitrogen being transparent in this region according to Ciechomski,[2] we tried to find another explanation for our results.

In order to be sure not to introduce any impurity in the gas, we have built an apparatus to liquefy the gas at a pressure of 100 kg/cm² in a tank immerged in liquid air. By heating, the gas is compressed to a pressure of 1.200 kg/cm² in a stainless steel cylinder provided with two quartz windows. Previously, all the parts of this apparatus have been carefully cleaned and backed at 350°C during several hours. All the joints used are made of silver and lead, the valves being of a special type with a packing of lead. Under these conditions we have ascertained that nitrogen has practically no absorption over 2.000A.

In fact, the absorption is due to a real dissolution phenomenon, the gas behaving like a non-polar solvent. Some very small quantities of low vapor pressure oils (high vacuum diffusion pump oil), or of organic solids (anthracene, phenanthrene), introduced in the cylinder are sufficient to make the gas absorbent. We tried to determine the order of magnitude of the quantities dissolved in the saturated gas by comparing the spectra of the solutions in the compressed gas and of solutions of phenanthrene in cyclohexane. We have found that at about 1.000 kg/cm² the gas absorbs as a solution of phenanthrene in cyclohexane of the order of 1 part in 200,000 by weight. That is, when taking into account the difference of density of the solvent

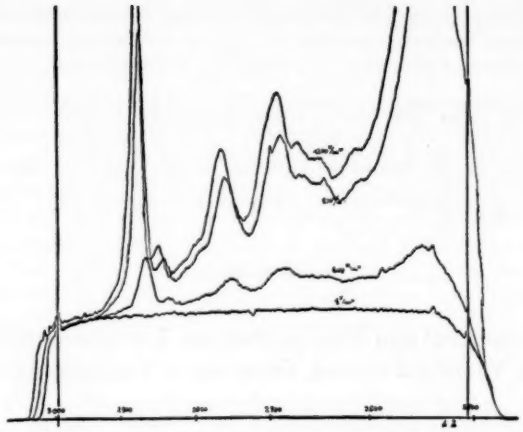

FIG. 1. Absorption spectra microphotographs of saturated solutions of phenanthrene in compressed argon (cell thickness 5 mm).

and assuming that the absorption is due only to the dissolved substance, the concentration is 1 part in 150,000 by weight in the compressed gas.

Other compressed gases also present the same character of solvent, argon under the same conditions being a better solvent than nitrogen. Compressed hydrogen also is a solvent for solids, but it dissolves much smaller quantities at equal pressure (the characteristic bands of phenanthrene do not appear until a pressure of 1.000 kg/cm² is reached, with a thickness of 4 cm).

These measures are a confirmation of older published data, such as those of Villard,[3,4] and should be compared with those obtained recently by Diepen.[5] A quantitative study of the dissolution in argon is presently in progress and is expected to give a good check of the theories of solubility.

It is known that the lack of a solvent transparent in the Schumann region makes the spectral analysis practically impossible in this region, except perhaps for the longer wave-lengths.[6] We suggest, taking advantage of the transparency of such gases as Ar, N_2, or H_2, the use of them as solvents for the investigation of the optical absorption, between 1.300 and 2.000A, of such substances which it is impossible to study in the pure solid state. This is the case, for instance, of many organic substances which cannot be deposited in vacuum as thin films, because they cannot be evaporated without decomposition.

Moreover, from the spectroscopic standpoint, the phenomenon of solubility in compressed gases makes it possible for the first time to follow quite easily and at constant temperature the displacement of the absorption bands as functions of the density of solvent (see Fig. 1). The use of this phenomenon will probably permit the drawing of some direct conclusions on the variation of intermolecular forces with intermolecular distances.

[1] S. Robin, B. Vodar, and G. Philbert, Comptes Rendus Acad. Sci. 225, 495 (1947).
[2] Ciechomski, dissertation, Fribourg (Switzerland), 1910.
[3] M. P. Villard, Comptes Rendus Acad. Sci. 9, 182 (1880).
[4] M. P. Villard, J. de Phys. 5, 453 (1896).
[5] G. A. M. Diepen, Thesis, Delft, Netherlands (1947).
[6] J. R. Platt, I. Rusoff, and H. B. Klevens, J. Chem. Phys. 11, 535 (1943).

Morphological Changes of Tactoid-Forming Particles

JOHN H. L. WATSON
The Edsel B. Ford Institute for Medical Research, Henry Ford Hospital, Detroit, Michigan,
AND
WILFRIED HELLER AND WESLEY WOJTOWICZ
Chemistry Department, Wayne University, Detroit, Michigan
July 30, 1948

THE colloidally thin platelets of FeOOH and of tungstic acid, which form schiller layers,[1] maintain long-range equilibrium distances between each other which are of the order of magnitude of optical wave-lengths.[2] In order to determine these distances and their variations very accurately, it became necessary to compile detailed distribution curves on the size and, particularly, on the thickness of these platelets. In the course of the latter studies, carried out with the electron microscope, in conjunction with the polarizing light microscope, surprising morphological changes were observed on the platelets of tungstic acid[3] which seem to have a general interest in regard to the behavior of crystals within the colloidal range.

The first particles of well defined shape to form from an aqueous solution of tungstic acid are exceedingly thin, electron-optically highly transparent platelets of surprisingly uniform elliptical shape which always seem to have a remarkably uniform initial size (major axis) of 0.2–0.3 micron. Immediately after their formation, these "nuclei" grow rapidly in length and width, with continuous perfection of their elliptical shape. These particles to be called "type *A*" (Fig. 1A) exhibit a weak positive double refraction and they possess very regular neutral lines indicating a uniform structural anisotropy, i.e., excluding a mosaic-like structure.

Whether these particles are single crystals of unusual shape or tactoid-like aggregates of nematic symmetry composed of amicronic non-spherical material cannot be decided as yet. The latter concept is supported but not proved by the interesting fact that the contours of the

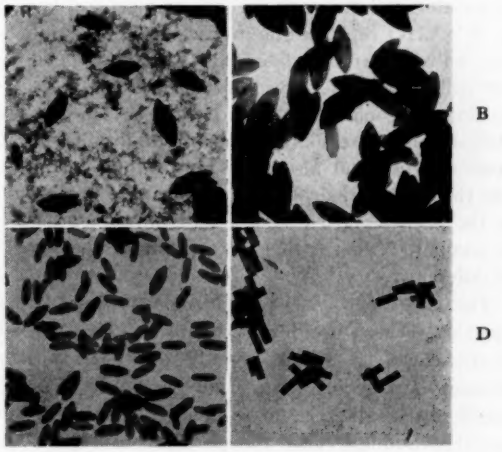

FIG. 1. Electron micrographs of tungstic acid, ×1167, to show the four main particle shapes.

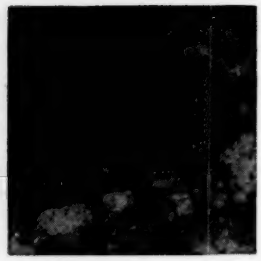

FIG. 2. Electron micrograph of the edge of a tip of a tungstic acid particle, ×12,000, showing toothed edge.

particles are frequently not smooth, but toothed (Fig. 2). In the example given, each of the remarkably uniform "steps" has a length of slightly less than 400A in the direction of the major axis. On the assumption of a tactoid-like structure, the elliptical shape could be explained as the result of an anisotropy of interfacial energy or as the result of a competition between the interfacial energy and the exceedingly weak (long-range distances!) "lattice" energy of a tactoid. If the particles represent crystals of anomalous shape, then they are related to the "somatoids" described by Kohlschuetter.[4] Generally, however, the elliptical species of somatoids does not have a shape as regular and uniform as observed in the above systems.

After a sufficient aging of the respective suspensions, particles of "type *D*" are found exclusively (Fig. 1D), i.e., exceedingly thin perfectly regular-shaped rectangular crystals. The morphological differences between the two types of particles is apparent not only in the dried-out samples studied electron-optically, but also in the original samples investigated with the polarizing light microscope. A comparison of the sharp electron diffraction diagrams obtained from particles of type *D* with the less distinct ones exhibited by particles of type *A* indicates definite differences in intrinsic structure, in addition to the morphological differences.

At intermediate ages of the suspensions, platelets of intermediate shape are observed. For purposes of statistical evaluation, we divide them into two general types: type *B* (Fig. 1B) representing particles with straight plane-parallel edges at the midsection, whereas the end sections are still elliptically curved, and type *C* (Fig. 1C) representing octagonal particles with straight edges throughout. Occasionally, irregularly shaped variants of these four general types and also twins and triplets are observed, but they are statistically unimportant. (The absolute sizes of the particles in the four photographs of Fig. 1 cannot be compared because they were obtained from suspensions of different history (see a subsequent communication).)

The existence of the intermediary types *B* and *C*, the fact that the size distribution curves compiled as a function of the age of the suspensions do not show characteristic changes or discontinuities, and the absence of definite double distributions seem to make it certain, in addition to other findings, that the particles of type *D* do not develop from dissolving particles of type *A*, but rather by their slow transformation.

The work reported in this and in the following communications was made possible by a grant for tactoid research to Wayne University by the Research Corporation.

[1] H. Zocher and K. Jacobsohn, Koll. Beih. **28**, 167 (1929); H. Zocher and W. Heller, Zeits. f. anorg. allgem. Chemie **186**, 75 (1930).
[2] W. Heller, Comptes Rendus **201**, 831 (1935); P. Bergmann, P. Loew-Beer, and H. Zocher, Zeits. f. physik **A181**, 301 (1938).
[3] See also W. Feitknecht, Vierteljahrsschrift Natur. Ges. Zuerich **161**, XC (1945).
[4] E.g., V. Kohlschuetter, C. Egg, and M. Bobtelsky, Helv. Chim. Acta **8**, 457 (1925).

Isothermal and Non-Isothermal Transformations of Tactoid-Forming Particles of Tungstic Acid

WILFRIED HELLER AND WESLEY WOJTOWICZ
Chemistry Department, Wayne University, Detroit, Michigan,
AND
JOHN H. L. WATSON
The Edsel B. Ford Institute for Medical Research, Henry Ford Hospital, Detroit, Michigan
July 30, 1948

FIGURE 1 shows on two representative samples that the isothermal habitus change (25°C) $A \rightarrow B \rightarrow C \rightarrow D$ of the particles which develop from a solution of tungstic acid[1] is accompanied by a continuous increase in the major axis (length) of the particles. The rate of change of both habitus and size are found to be highest shortly after the organization of elliptical particles (nuclei), 0.2–0.3-micron long, from electron-optically unresolved amicronic material. No nuclei have been observed in solutions less than two hours old. The results support the concept[1] that the particles of type *D* develop directly from particles of type *A* by a morphological change of the latter.

The hydrogen ion concentration decreases very strongly with increasing age of the suspensions, i.e., with the progressing development of the particles. One example is given in Table I. This is due primarily to the fact that the particles develop from tungstic acid in solution, but part of the effect apparently must be attributed also to the transformation of the particles themselves. Particularly interesting is the fact that the rate of change in habitus is faster (Table II) and the final size is smaller (Fig. 1) the lower the initial hydrogen ion concentration. (The latter is varied by varying the concentration of HCl which is present beside tungstic acid.)

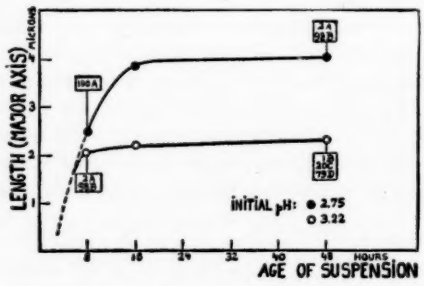

FIG. 1. Change in length (major axis) of the platelets of tungstic acid with the age of the suspensions. (Inscription in squares: percentage frequency of the four types.)

TABLE I. Change of pH with the age of suspensions of tungstic acid

Age (days):	0	3	8	16	35	240
pH:	3.22	3.77	4.49	4.71	4.96	5.03

A qualitative change in the electron diffraction pattern accompanies the isothermal morphological transformation of the particles. This suggests that the change in habitus is accompanied by and most likely is a result of an internal transformation. Such isothermal internal transformations of colloidal particles had been known before, the most extensive one being probably the transformation FeOCl→β-FeOOH→α-FeOOH, proved by x-ray diffraction and by magneto-optical measurements.[2]

This hypothesis is supported by the fact that the particles of type D evaporate uniformly under concentrated electron bombardment like typical anhydrous crystals. This suggests that they consist of single crystals of WO_3. Particles of type A, which definitely consist of tungstic acid, change, under electron bombardment, into a fibrillar structure of nematic symmetry which shows surprising sudden changes in the direction of the symmetry axis with respect to the major axis. This is illustrated in Fig. 2A and Fig. 2B on two different samples. The average distance between the centers of the "rods" is similar to the width of the steps observed in the contours of unbombarded particles.[1] This appearance of a fibrillar structure may favor the assumption of a tactoid-like structure for the unbombarded particles.[1] However, the possible sudden changes in the symmetry axis, under maintenance of a simple elliptical shape, in conjunction with the fact that the unbombarded particles show uniform neutral lines in the polarizing microscope,[1] suggest that at least the mosaic pattern, if not the fibrillar structure as such, is a quality of the particles produced by the electron bombardment.

Thermal heating and light microscopic observations of the changes produced leads to related results supporting the contention[3] that the effect of electron bombardment observed is a heating effect. Rapid heating to 650°C leads to a disintegration of the particles of type A into rectangular flat rods whose length is often of the same order of magnitude as the major axis of the original particles. Slow heating produces much shorter rods, apparently because of the lateral breakup of primary long rods. In either instance, the positive double refraction of the individual rods is uniform and much stronger than in the original particles. (Melting of the elliptical particles prior to or instead of their breakup also leads to a strong increase in double refraction with irregularly changing neutral lines.) Although a fibrillar structure of the elliptical particles could not be observed prior to their break up, according to Fig. 2, it actually is below the resolving power of a light microscope; it is safe to assume that the two phenomena, revelation or production of a fibrillar structure by electron bombardment and a break up under heating in the polarizing microscope, are conjugate. They apparently accompany the non-isothermal transformation of tungstic acid to tungstic oxide, under loss of water.

TABLE II. Shape distribution, in percent, as a function of the age of suspensions of tungstic acid (number of particles considered: 2357).

Initial pH \ Hours	8	16	48
2.75	100*A*	2*A* 96*B* 2*C*	80*B* 10*C* 10*D*
3.00	23*A* 77*B*	1*B* 99*C*	8*B* 76*C* 16*D*
3.22	2*A* 98*B*	4*B* 82*C* 14*D*	1*B* 20*C* 79*D*

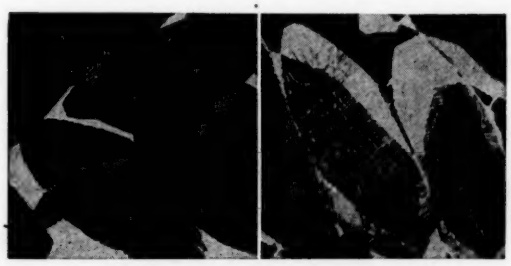

A B

FIG. 2. Electron micrographs to show effect of electron bombardment upon tungstic acid, ×10,000, (A) after bombardment, bright field, and (B) after bombardment, dark field.

[1] J. H. L. Watson, W. Heller, and W. Wojtowicz, J. Chem. Phys. preceding letter.
[2] W. Heller, O. Kratky, and H. Nowotny, Comptes Rendus **202**, 1171 (1936).
[3] J. H. L. Watson, J. App. Phys. **19**, 713 (1948).

Direct Electron Microscopic Thickness Determinations of Ultramicroscopically Thin Crystals

JOHN H. L. WATSON
The Edsel B. Ford Institute for Medical Research, Henry Ford Hospital, Detroit, Michigan
AND
WILFRIED HELLER AND WESLEY WOJTOWICZ
Chemistry Department, Wayne University, Detroit, Michigan
July 30, 1948

THE shadowcasting technique makes it possible to obtain the thickness of microscopic or ultramicroscopic particles indirectly. This technique was applied to the ultramicroscopically thin platelets which form from a solution of tungstic acid.[1] Examples for particles of type A and type D[1] are given in Figs. 1A and 1B, respectively. Chromium shadowcasting was carried out under an acute angle of less than 15°. Carbon particles, visible in the photographs, had been mixed with the preparation for calibrating purposes. The dimensions of the major axis,

(A) (B)

FIG. 1. Electron micrographs of chromium shadowcast tungstic acid ×2667.

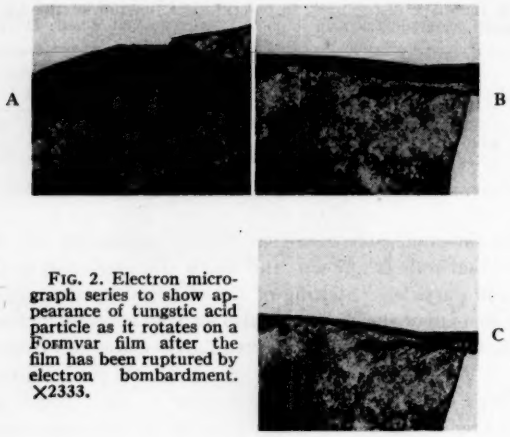

FIG. 2. Electron micrograph series to show appearance of tungstic acid particle as it rotates on a Formvar film after the film has been ruptured by electron bombardment. ×2333.

minor axis, and thickness of the elliptical platelets (only one is shown) are 11.7, 4.05, and 0.15 microns, respectively, (ratio: 100:35:1.3). The mean dimensions of the length, width, and thickness of 21 rectangular crystals (taken from a differently treated suspension) of which a few are shown in Fig. 1B are 2.27, 0.75, and 0.044 microns, respectively, (ratio: 100:33:1.95). The results show that both types of particles are very thin. This follows for the particles of type *D* also directly from the fact that a small carbon particle adjacent to one of these crystals casts part of its shadow onto the crystal (arrow).

A decrease in the azimuth between the plane of the preparation and the direction of the beam of metal atoms improves the differentiation between particles of slightly different thicknesses, but it reduces the accuracy of absolute thickness determinations. Because of the very acute angle necessary in the above experiments, an attempt was made to work out a method for direct thickness determinations. The procedure adopted is as follows: The supporting film is subjected to a concentrated electron bombardment near the particle selected for thickness determinations. If the conditions are suitable, the film ruptures in a direction parallel to the longest axis of the particle and begins to curl up because of internal strain. When the particle adheres firmly to the film, the net result is a rotation of the particle about its longest axis, i.e., about an axis perpendicular to the electron beam. Figures 2A, B, and C show a particle of type *B*, just prior to rotation, after a rotation by 80° and after a rotation by 90°, respectively. The particle which is 14.6μ long and 5.0μ wide, has, according to Fig. 2 and considering the end sections, a maximum thickness of 0.350μ. This leads to a dimensional ratio of 100:34:2.4. As regards the apparent thickening of the particle towards the center, in Fig. 2C, it is not possible at the present time to state whether this is real, i.e., whether it indicates a slightly elliptical shape perpendicular to the plane of the particles or is rather due to a deviation (by ±2°) from 90°. A slight shortening of the shadow in Fig. 1A towards the end section is an argument in favor of the former possibility.

FIG. 3. Electron micrograph of a tungstic acid (oxide?) crystal curling up with Formvar film. ×2667.

An application of this method to particles of type *D* failed, because, surprisingly, the thin crystals curled up together with the film (Fig. 3). The new method is therefore, in suitable cases, useful also for a rough comparison of the rigidity of colloidally thin crystals.

Considering the fact that the particles of type *A* and *D*, illustrated in Figs. 1 and 2, were taken from suspensions of different original *p*H at different stages of aging with a resulting appreciable difference in their absolute dimensions,[2] it is interesting to note that the ratios length/thickness differ at the most by a factor of 2 and the ratios length/width differ by a factor of less than 0.1. Particularly noteworthy is the fact that the absolute mean thicknesses of the particles of type *A* considered above are of the same order of magnitude as the dimensions of the steps in the contours of such particles.[1]

[1] J. H. L. Watson, W. Heller, and W. Wojtowicz, J. Chem. Phys. **16**, 997 (1948).
[2] W. Heller, W. Wojtowicz, and J. H. L. Watson, J. Chem. Phys. **16**, 998 (1948).

A New Type of Micelle: Solubility by Film Penetration*

WILLIAM D. HARKINS AND HANS OPPENHEIMER
George Herbert Jones Chemical Laboratory, University of Chicago, Chicago, Illinois
August 3, 1948

THE existence of a new type of soap micelle is demonstrated by earlier x-ray work[1] which proved that a *n*-long paraffin chain alcohol, amine, or another polar-nonpolar molecule can penetrate the film of a soap micelle without increasing its thickness. In later work it has been found that with certain lengths of the paraffin chain of the detergent and the polar-non-polar compound the micelle even becomes a few angstroms thinner than that of the pure detergent.

This new phenomenon is entirely different from solubilization in which the micelle is thickened by as much as 12A or even more, since the solubilized hydrocarbon is located between the ends of the hydrocarbon chains, whereas the polar-non-polar molceules line up with the soap molecules with their polar groups toward the water.

It is obvious that if all of this is true the solubility relations exhibited in film penetration should be entirely different from and much more complicated than those in solubilization. That this is true has been shown by extensive work. It would be extremely unfortunate if such entirely different phenomena were to be designated by a single term. If the term film penetration is too lengthy, then *penetration* may be used.

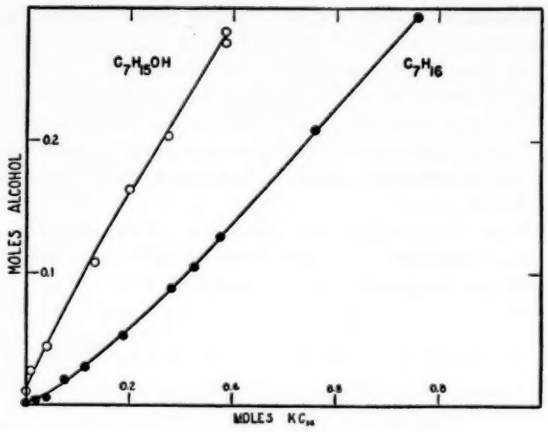

FIG. 1.

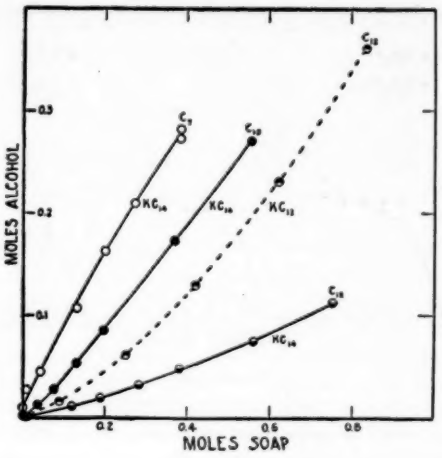

FIG. 2.

Thus we have solubility in micelles caused by *solubilization* and by *penetration*. That the latter may exhibit a greater effect is shown by Fig. 1 which in the lower curve gives the molal concentration of *heptane* (*y* axis) as a function of the concentration of potassium tetradeconoate. The solubility by penetration is from two to five times greater for the 7-carbon alcohol than by solubilization of the 7-carbon atom hydrocarbon. Also the curve for penetration is concave toward the soap concentration (*x*) axis, whereas that for solubilization is convex.

The great differences in solubility relations are illustrated in a striking way by Figs. 2 and 3. For example, in Fig. 2 the solubility by penetration of the 12-carbon atom alcohol (C_{12}) in the 12-carbon atom soap is shown to be from 2 to 3 times larger than in the 14-carbon atom (KC_{14}) soap, whereas the *solubilization* of the 12-C atom hydrocarbon is much larger in the 14 than in the 12-C atom soap.

However, the *penetration* of the 7, 10, and 12-C atom alcohols into the micelles of the 12-C atom soap follows the same rule as for solubilizations: i.e., the solubility decreases rapidly with the length of the hydrocarbon chain of the oil.

The complicated solubility relations which emerge in penetration are exhibited in Fig. 3. The solubility of the alcohols of 7, 8, and 9-C atoms increases rapidly, but not regularly, for any one alcohol as the length of the hydrocarbon chain of the soap increases from 8 to 14-C atoms. However, except for heptanol, the solubility of all of the alcohols up to 12-C atoms increases the most rapidly as the number of C atoms in the soap increases from 8 (the lowest investigated) up to 9. In general, the solubility is favored by an oddness in the number of C atoms in the soap. The increment of solubility per C atom decreases as the number of C atoms in the soap molecule increases up to 14.

This decrease in increment becomes most marked in the 12-C atom alcohol or amine which above the 13-C atom soap becomes a decrement so large that the 12-C atom amine or alcohol is much less soluble in the 14-C atom than in even the 9-C atom soap.

It should be noted that the solubility relations are much the same for the 10- and 12-C atom amines as for the corresponding alcohols.

The solubility by penetration of any one of the alcohols of from 7- to 12-C atoms is found to be from 10 to 30 percent higher in sodium dodecyl sulfate than in potassium dodecanoate. The amount of solubilization of a hydrocarbon in the sulfate is also higher.

In a 10 percent solution of potassium myristate, 28 grams of decyl alcohol became dissolved in 1000 grams of soap solution. The introduction of a second OH− group, at the other end of the hydrocarbon chain, gives decanediol (1, 10), a solid. Its solubility in the same soap solution is very low, less than 4.6 grams per 1000 grams of soap solution. The high insolubility of this alcohol is related to the occurrence of a polar −OH group at both ends of the molecule, so it is attracted more by the water, and the decrease in free energy on entering the hydrocarbon part of the micelles is less than when the group is present at only one end of the molecule.

The solubility relations which have been found in this laboratory exhibit the following relations (Table I).

1. In solubilization the relations are simple. The solubility *increases* with the length of the hydrocarbon chain of the colloidal electrolyte and decreases with the length of that of the hydrocarbon. This decrease is related to the decrease of activity of the hydrocarbon with chain length.

2. In film penetration the solubility decreases rapidly with the length of the hydrocarbon chain of the alcohol,

TABLE I. Effect of the nature of the polar group on the solubility of derivatives of dodecane by aqueous solutions of 0.3 mole of sodium lauryl sulfate per 1000 grams of detergent solution.

"Oil"	Grams "oil" (per 1000 grams of detergent solution)	Moles "oil" (per 1000 grams of detergent solution)
Dodecane (solubilization)	<1.72	<0.01
Dodecylchloride	<1.82	<0.01
Dodecylmercaptan	6.55	0.03
Dodecylamine (penetration)	20.6	0.11
Dodecylalcohol (penetration)	22.8	0.12
Dodecylic acid (penetration)	26.3	0.13

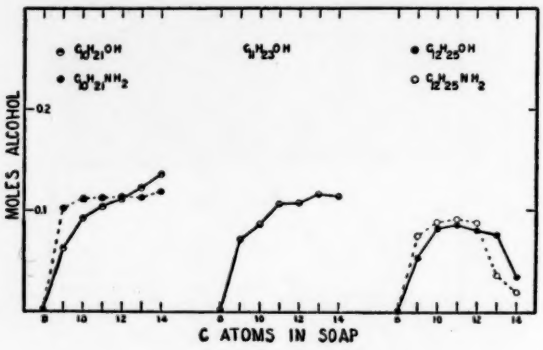

FIG. 3.

amine, etc., since in this case also the activity of the compound decreases rapidly with chain length. However, most of the relations are complex, and there is evidence that what may be described as molecular fitting enters, especially if the lengths of the soap chain and that of the polar-non-polar-non-ionic chain are not too different. For example, the solubility of the 11-C atom alcohol is in general higher than that which corresponds to the solubility of the 10- and 12-C atom alcohols.

Substances which enter the micelle by film penetration lower the critical micelle concentration. The rate of lowering with film concentration increases with extreme rapidity with the length of the molecule.[2] Substances which enter by solubilization have little effect upon the critical micelle concentration.

* This investigation was carried out under the sponsorship of the Reconstruction Finance Corporation, Office of Rubber Reserve, in connection with the Government's synthetic rubber program.

[1] W. D. Harkins, R. W. Mattoon, and R. Mittelmann, J. Chem. Phys. **15**, 763 (1947).

[2] M. L. Corrin and W. D. Harkins, J. Chem. Phys. **10**, 640 (1946), and later work with higher alcohols.

The Moment of Inertia of CF_3CH_3

WALTER F. EDGELL, *Department of Chemistry,*
AND
ARTHUR ROBERTS, *Department of Physics,*
The State University of Iowa, Iowa City, Iowa

August 25, 1948

THE C−C bond distance in polyfluorinated compounds is a subject of much interest. On the basis of electron diffraction measurements Brockway, Secrist, and Lucht[1] reported a distance of 1.45A in C_2F_6. On the other hand, nearly normal hydrocarbon bond distances for both the single and double bond in hexafluoropropene—namely, 1.52 and 1.31A, were found by Buck and Livingston[2] in their electron diffraction study. As an initial step in determining the bond distances and angles in CF_3CH_3 we have made a preliminary study of its microwave spectrum near 1.5-cm wave-length. The absorption cell was a five-foot section of standard 1.25-cm wave guide, used as a Hughes-Wilson[3] Stark effect spectrometer.

Two lines were found. The first had a frequency of 20,741±2 megacycles and had an absorption coefficient of the order of 2×10^{-6} cm^{-1}. It is due to the $J=1$ to $J=2$ transitions (for $K=0$ and $K=1$) in the ground state. Both linear and quadratic Stark effects were observed. The second line at 20,710±2 megacycles appeared with an intensity of about half that of the first line, and is probably caused by the same rotational transition in a low lying, excited vibrational state. A second-order Stark effect was observed.

These data permit the calculation of the moment of inertia perpendicular to the threefold axis. Using Birge's[4] values for the fundamental constants,

$$I_B=161.80\pm0.07\times10^{-40}\text{ g cm}^2$$

in the ground state; for the unidentified excited state,

$$I_B=162.04\pm0.07\times10^{-40}\text{ g cm}^2.$$

It is not possible to determine bond distances from these data alone, yet it is interesting to note several combinations which are in harmony with the observations. The electron diffraction measurements of Shand and Spurr[5] yield C−C=1.52±0.02A, C−F=1.37±0.02A, <C−C−F =112° 10′±2°, <F−C−F=107° 32′±2° when a tetrahedral methyl group with C−H=1.09A was assumed. The moment of inertia[5] calculated from these values, $I_B=166.7\pm5.8\times10^{-40}$, while in agreement within the stated limits with the microwave value, does not represent the best choice of the distances and angles.

Before beginning the search for the microwave spectrum, a calculation of the microwave line positions was made with the following parameters: C−C=1.54A, C−F =1.33A, C−H=1.093A, F−F=2.16A, <H−C−H =109° 28′, H=1.008, C=12.01, F=19.00, and N=6.0228 $\times10^{23}$. These lead to $I_B=161.9\times10^{-40}$, the close agreement with experiment probably being fortuitous. A shorter C−C distance of 1.45A with all other distances and angles as listed immediately above gives $I_B=154.7\times10^{-40}$. Such a distance requires compensation elsewhere; for example, $I_B=161.7\times10^{-40}$ when C−C=1.45A and C−F=1.38A, the other distances and all angles remaining as before.

If recent work[2,6] may be interpreted as favoring the shorter C−F bond distance and angles which are nearly tetrahedral, the present results would favor a C−C distance in CF_3CH_3 more nearly like that in ethane than like that reported for C_2F_6.[1]

Work is planned on the preparation of isotopic molecules from which these distances may be determined unambiguously, within the limits imposed by zero-point vibration corrections.

The CF_3CH_3 used in this work was part of a sample furnished Professor Glockler by Dr. A. F. Benning, Jackson Laboratory, E. I. du Pont de Nemours Company. Thanks are due them for the loan of the material and to Mr. Donald A. Gilbert for assistance in the microwave measurements.

[1] L. O. Brockway, J. H. Secrist, and C. M. Lucht, Abstracts, American Chemical Society Meeting, Buffalo, New York, 1942.

[2] F. A. M. Buck and R. Livingston, J. Am. Chem. Soc., in press. Thanks are due these authors for permission to use their data in advance of publication.

[3] R. H. Hughes and E. B. Wilson, Jr., Phys. Rev. **71**, 562 (1947).

[4] R. T. Birge, Rev. Mod. Phys. **13**, 233 (1941).

[5] W. Shand and R. A. Spurr, quoted by H. Russell, Jr., D. R. V. Golding, and D. M. Yost, J. Am. Chem. Soc. **66**, 16 (1944).

[6] H. J. Bernstein and G. Herzberg, J. Chem. Phys. **16**, 30 (1948).

Crystal Structures of a Series of Rare Earth Phosphates

ROSE C. L. MOONEY
Newcomb College, Tulane University, New Orleans, Louisiana
August 25, 1948

THE crystal structures of the phosphates of trivalent lanthanum, cerium, praseodymium, and neodymium were determined by x-ray diffraction techniques in 1944 for the Manhattan Project. It was found that the crystals are dimorphic. One phase is monoclinic, isomorphous with the mineral, monazite; the other is a hexagonal structure of a new type, which easily converts to the monoclinic form at moderately high temperatures.

Hexagonal modification. There are three molecules of XPO_4, where X may be La, Ce, or Nd, in the unit hexagonal cell. The cell constants and calculated densities for the isomorphous series are as shown in Table I.

The space group is $D_3^4-C\,3_1\,2\,1$ (D_3^6). The atomic positions, in fractions of the unit cell, are given for $CePO_4$ as a representative of the series as follows:

(a) Three Ce atoms in $x\ 0\ \frac{5}{6}$, $0\ x\ \frac{1}{6}$, $\bar{x}\ \bar{x}\ \frac{1}{2}$ where $x=\frac{1}{3}$.
(b) Three P atoms in $x\ \frac{1}{3}$, $0\ x\ \frac{2}{3}$, $\bar{x}\ \bar{x}\ 0$, where $x=\frac{1}{2}$.
(c) Two sixfold sets of oxygens in

$$x\,y\,z;\ \bar{y}\ x-y,\ \tfrac{1}{3}-z;\ y-x,\ \bar{x},\ \tfrac{2}{3}+z;$$
$$y\,x\,\bar{z};\ \bar{x},\ y-x,\ \tfrac{1}{3}-z;\ x-y,\ \bar{y},\ \tfrac{2}{3}-z,$$

where the parameter values are:

	x	y	z
O_1	0.446	0.147	0.473
O_2	0.554	0.853	0.473

In this structure, cerium is coordinated to either oxygens—four at 2.30A and four at 2.66A—in such a manner as to form open oxygen-lined channels along the hexagonal axis. The presence of zeolithic water in these channels [$XPO_4(0-0.5H_2O)$] is probably necessary to stabilize the structure.

Monoclinic modification. Four molecules of XPO_4 occupy the unit cell. Cell constants and densities for the isomorphous series are as shown in Table II. The space group is $C_{2h}^5-P\,2_1/n$. The atoms are all in fourfold general positions, namely, $\pm(xyz;\ \frac{1}{2}-x,\ \frac{1}{2}+y,\ \frac{1}{2}-z)$. The structural parameters, in fractions of the unit cell, are given in Table III for $CePO_4$ as a representative of the series. The cerium atom is coordinated to eight oxygens—four at an average distance of 2.37A—and four more at 2.66A. Though the coordination distances are closely analogous to those in the hexagonal structure, the arrangement is such as to form a tightly packed structure. In consequence, there is an unusual difference in the densities of the two modifications of XPO_4, the monoclinic being about 25 percent heavier than the hexagonal form.

A detailed account of these investigations will be published later.

TABLE I.

XPO_4	a_1 (A)	a_2 (A)	$a3/a_1$	ρ g/cm$_3$
$LaPO_4$	7.081 ±0.005	6.468 ±0.008	0.9134	4.122
$CePO_4$	7.055 ±0.003	6.439 ±0.005	0.9127	4.193
$NdPO_4$	6.98 ±0.01	6.34 ±0.02	0.9083	4.328

TABLE II.

XPO_4	a_1 (A)	a_2 (A)	a_3 (A)	β	ρ g/cm^3
$LaPO_4$	6.89 ±0.02	7.05 ±0.02	6.48 ±0.02	103° 34′ ±15′	5.087
$CePO_4$	6.76	7.00	6.44	103° 38′	5.234
$PrPO_4$	6.75	6.94	6.40	103° 21′	5.344
$NdPO_4$	6.71	6.92	6.36	103° 28′	5.500

TABLE III.

	x	y	z
Ce	0.292	0.156	0.083
P	0.292	0.156	0.581
O_1	0.211	0.990	0.423
O_2	0.374	0.323	0.464
O_3	0.467	0.786	0.765
O_4	0.116	0.235	0.680

Evidence for the Planar Structure of the Urea Molecule

W. E. KELLER
Mallinckrodt Chemical Laboratory, Harvard University, Cambridge, Massachusetts
August 11, 1948

FROM x-ray data on crystals of urea[1] it is known that the heavy atoms, C, N, O, of each molecule lie in a plane and have symmetry C_{2v}, whereas the positions of the H atoms, too light to scatter x-rays, must be inferred. Though considerations of resonance[2] in the urea molecule, giving each of the two C−N linkages approximately 20 percent double-bond character, leads to favoring an entirely planar structure, the only published vibrational analysis[3] has employed a model in which the H atoms lie in planes perpendicular to the plane of the remaining atoms. We believe that evidence from infra-red spectra obtained by directing plane-polarized radiation through oriented urea crystals provide support for the planar structure.

If the urea molecule possesses either of the configurations described above, the point-group for the molecule is C_{2v}. Furthermore, urea crystallizes in the tetragonal system with space-group $V_d^3(P\bar{4}2_1m)$ and two molecules per unit cell;[1] the molecules are at sites having symmetry C_{2v}. Halford's method[4] is considered to yield valid selection rules for molecular crystals and, when applied to the data for urea, indicates that the molecule in the crystal should give rise to the same active frequencies as the free molecule. There should be 6 modes belonging to the totally symmetric representation (A_1) if the molecule is non-planar and 7 if planar. Since the crystal is uniaxial, there will be but two principal directions in which there will be a change of electric moment during a molecular vibration; modes belonging to A_1 will be polarized along the tetragonal axis, while the remaining active representations will have modes polarized in the plane perpendicular to this axis. We

should thus expect 6 or 7 fundamental modes polarized A_1, depending on the configuration, but only if 7 are accounted for can the results be interpreted with any certainty.

Samples of oriented urea crystals were prepared by evaporation of urea from a methanol solution onto a AgCl plate. The evaporation was controlled by placing at one edge of the plate a heated transite rod; the crystals grew with the tetragonal axis parallel to the changing thermal gradient thus produced.

Assuming for the moment that urea is planar, representation A_1 will contain three groups of modes: two symmetrical H stretches; modes principally C−O stretch, symmetrical N−C−N bent and stretch; and two symmetrical H bends. The H stretch modes occur in a region (about 3200 cm^{-1}) where the resolving power of our instrument is inadequate, so that polarization data is poor. In the non-planar model only one of these modes should be active. We found two bands polarized A_1 at 1680 and 546 cm^{-1}, assignable to the C−O stretch and N−C−N bend, respectively. The N−C−N stretch has been found at 1010 cm^{-1} but is too weak to give good polarization data. Raman work,[5] however, provides ample evidence for this assignment. These three modes would be polarized similarly in the non-planar structure. The most crucial data concerns the H bends, only one of which would be expected to be active in the non-planar model. We found two bands at 1160 and 1590 cm^{-1} polarized along the tetragonal axis and attributable to these modes. It is true that all first overtones, as well as certain combinations, will be polarized A_1, but none of the frequencies observed by us or by other investigators would be expected to contribute to the spectrum at the frequencies listed above.

Our ability to account satisfactorily for 7 fundamental frequencies polarized A_1 leads us to choose the entirely planar structure for the urea molecule in the crystal.

The author wishes to acknowledge gratefully the suggestions given him during the course of the work by Professor E. B. Wilson, Jr. and Mr. W. L. Hyde.

[1] R. W. G. Wyckoff, Zeits. f. Krist. **81**, 102 (1932); R. W. G. Wyckoff and R. B. Corey, *ibid.* **89**, 462 (1934).
[2] L. Pauling, *The Nature of the Chemical Bond* (Cornell University Press, Ithaca, 1939), p. 212*ff*.
[3] L. Kellner, Proc. Roy. Soc. **177A**, 546 (1941).
[4] R. S. Halford, J. Chem. Phys. **14**, 8 (1946).
[5] For example, J. W. Otvos and J. T. Edsall, J. Chem. Phys. **7**, 632 (1939).

Polarization of Raman Lines of *s*-Dichloroethane

JOHN T. NEU, ABRAHAM OTTENBERG, AND WM. D. GWINN
Department of Chemistry, University of California, Berkeley, California
July 30, 1948

IN a recent paper Gwinn and Pitzer[1] use the *s*-dichloroethane frequency assignments of Wu[2] with the exception that a C_2 (staggered configuration) rather than a C_{2v} (eclipsed configuration) model is taken as one of the two forms. Ananthakrishnan's[3] evaluations of the 123-cm^{-1} and 1206-cm^{-1} lines as depolarized are not consistent with this C_2 assignment, however. Other investigators[3] have reported polarization on dichloroethane but only Ananthakrishnan has evaluated the 123-cm^{-1} line and his work was qualitative. The C_2 configuration, in which the 123-cm^{-1} line is polarized, is similar to the C_{2v} configuration, in which the 123-cm^{-1} line would be depolarized, differing only in an internal rotation of 60°. It would not be expected, therefore, that the 123-cm^{-1} line, corresponding to the torsional vibration, would be strongly polarized. Since the 123-cm^{-1} line is somewhat obscured by the background from the exciting line, it is not surprising that the other investigators did not obtain polarization data, nor is it unlikely that a qualitative estimate of polarization, where the background intensity is high, might be in error if the polarization is not pronounced. The 1206 line is reported as depolarized by Ananthakrishnan and as polarized ($\rho=0.36$) by Cheng.[3] In order to assign the polarization of these lines definitely, the writers have made a quantitative determination of the polarization.

The sample of dichloroethane obtained from Eastman Kodak Company was purified by washing with sulfuric acid, steam distilling, drying over $MgSO_4$, and finally distilling into the Raman tube through a thirty-theoretical-plate fractionating column. A Steinheil GH type spectrograph with *f*:10 collimator and *f*:3 camera was used with a slit of 0.017 mm. The method used to obtain polarization was a combination of schemes either cited or described by Glockler and Baker.[4] Illumination was furnished by two G.E. AH11 mercury arcs lying in a plane inclined 45 deg. to the vertical. Wratten 2*A* gelatin filters and baffles to eliminate light not perpendicular to the Raman tube were interposed between the arcs and the Raman tube. A quartz Wollaston prism with its axis inclined 45 deg. was placed between the collimator lens and the first prism of the spectrograph. Thus a single exposure produced two representations of the spectrum, one above the other and shifted slightly, in which the polarized lines appeared less intense in one representation than in the other. Differential reflection at the prism surfaces was eliminated by the device of inclining the plane of illumination and the Wollaston prism at an angle of 45 deg. Spectra were recorded on Eastman 103 *H* spectroscopic plates with exposure time varying from 6 to 24 hours. Intensity calibrations were placed on each plate by means of a rotating stepped sector disk, and intensity traces of plates were made with a microphotometer of our own design. Wave number assignments were taken from the work of Ananthakrishnan.[3] A graph was obtained by plotting the photometer reading of the intensity calibration at the frequency of the particular line against the intensity of the light that produced the calibration. Line intensities were

TABLE I.

cm^{-1}	ρ	cm^{-1}	ρ	cm^{-1}	ρ
123	0.63	880	0.88	1302	0.45
263	0.31	940	0.26	1429	0.82
302	0.40	989	*P**	1440	*D**
411	0.81	1052	0.47	2844	*P**
654	0.18	1144	*D**	2872	*P**
675	*D**	1206	0.65	2956	0.23
754	0.23	1262	*D**	3002	*D**

* This line was too weak for quantitative evaluation of ρ. *P* (polarized) or *D* (depolarized) represents a qualitative estimate.

evaluated in the usual manner by subtracting the background intensity from the line intensity as evaluated from the graph. In the special case of the 123-cm^{-1} line, the apparent background was sketched in and the intensities of the Raman line at small increments of frequency were plotted against a uniform scale. This served to show that the background had been sketched in so that the line had the correct shape and was symmetric.

Indeed, a visual estimate of the polarization seemed to indicate that the 123-cm^{-1} line was depolarized, but careful determination of the value of ρ indicated that the line was polarized. The average value from five plates was 0.63, the average deviation from this value being 0.06. The 1206-cm^{-1} line was also found to be weakly polarized. Table I below lists the values of ρ for all the lines.

These data indicate that the high energy form of *s*-dichloroethane is C_2 and not C_{2v}.

[1] W. D. Gwinn and K. S. Pitzer, J. Chem. Phys. **16**, 303 (1948).
[2] Ta-You Wu, *Vibration Spectra and Structure of Polyatomic Molecules* (Edwards Brothers, Inc., Ann Arbor, Michigan, 1946), second edition, pp. 306–312.
[3] R. Ananthakrishnan, Proc. Ind. Acad. Sci. **5A**, 285 (1937).
[4] G. Glockler and H. T. Baker, J. Chem. Phys. **11**, 446 (1943).

Note on the Theory of Ethylene

RODOLFO H. BUSCH
Facultád de Ciencias Exactas, Físicas y Naturales, Perú 222, Buenos Aires, Argentina
August 6, 1948

IN a recent paper, Mulliken and Roothaan[1] use the semi-empirical linear combination of atomic orbitals, the molecular orbital method for some computations on the ethylene molecule. The purpose of this note is to direct the attention to another starting point in the double-bond problem, which is suggested by the following.

In its ground state, the carbon atom is divalent. To account for the fact that it is normally quadrivalent it must be postulated that in carbon compounds the atom is in an excited state with one *s* and three *p* electrons, all with unpaired spins.

There is no doubt of the correctness of this assumption in a great number of cases, but in the treatment of the double-bond problem there seems to exist another possibility, consisting in emphasizing the fact that the carbon atom does have the alternative of being two- or quadrivalent, and seek for the explanation of its chemical particularities by the systematic application of this argument.

The starting point may be the consideration of the problem of methylene, which is known to exist in two forms (Pearson, Purcell, and Saigh;[2] Burton, Davis, Gordon, and Taylor[3]), as the "molecule" CH_2 and as the short lived "radical" $>CH_2$. The energy required to raise the CH_2 molecule to the radical structure is about 15 kcal. (Long and Norrish[4]).

In the photolysis of ketene, investigated by Norrish, Crone, and Saltmarsh,[5] the products obtained were quantitatively carbon monoxide and ethylene. Ross and Kistiakowsky[6] suggested the following mechanism:

$$CH_2CO+h\nu=CH_2+CO,$$
$$CH_2+CH_2=C_2H_4.$$

This reaction may be the key for the theory of ethylene. We assume that the formation of ethylene is due to the interaction of the two forms of methylene:

$$CH_2+>CH_2=C_2H_4.$$

If we label the two carbon atoms as C(*a*) and C(*b*), it follows that the system consisting of a "molecule" CH_2 and a "radical" $>CH_2$ at great distances is doubly degenerate:

$$C(a)H_2 \qquad >C(b)H_2, \qquad (1)$$
$$>C(a)H_2 \qquad C(b)H_2. \qquad (2)$$

The symmetry of this problem is in some respects similar to that of the hydrogen molecule ion; at shorter distances the interaction between the two forms may give rise to two solutions, one of which may correspond to the ethylene molecule.

The double bond might be thus interpreted as a kind of "excitation resonance." Using the data of the paper of Long and Norrish,[4] the interaction energy results in the order of 130 kcal.

In view of the preceding discussion, we think it would be interesting to compute the interaction energy by the methods of quantum mechanics.

[1] R. S. Mulliken and C. C. J. Roothaan, Chem. Rev. **41**, 201 (1947).
[2] Pearson, Purcell, and Saigh, J. Chem. Soc. **1**, 459 (1938).
[3] Burton, Davis, Gordon, and Taylor, J. Am. Chem. Soc. **63**, 1956 (1941).
[4] Long and Norrish, Proc. Roy. Soc. **A187**, 337 (1946).
[5] Norrish, Crone, and Saltmarsh, J. Chem. Soc. 1533 (1933).
[6] Ross and G. B. Kistiakowsky, J. Am. Chem. Soc. **56**, 1112 (1934).

Addendum: Continuous Spectra and OH Absorption in Carbon Monoxide-Oxygen Explosions

G. A. HORNBECK
Applied Physics Laboratory, The Johns Hopkins University, Silver Spring, Maryland
August 3, 1948

THE structural part of the CO-oxygen spectrum referred to as flame bands in a recent note[1] have been identified as belonging to the $^3\Sigma\rightarrow{}^3\Sigma$ transition of the neutral oxygen molecule. The agreement of our measurements with those of Lochte-Holtgreven and Dieke[2] of the oxygen bands observed in a high tension arc by Runge are generally better than 0.2 cm^{-1}. Current measurements confirmed the existence of several bands of the $^3\Sigma\rightarrow{}^3\Sigma$ transition in the spectra obtained from the CO-oxygen explosion. The bands found thus far are the (0–12), (0–13), (0–14), (0–15), and the (2–15). A detailed discussion of this spectrum as observed in CO-oxygen combustion will be reported in the near future.

[1] G. A. Hornbeck, J. Chem. Phys. **16**, 845 (1948).
[2] W. Lochte-Holtgreven and G. H. Dieke, Ann. d. Physik **3**, 937 (1929).

Raman Spectrum of Trimethyl Silicon Chloride

JULES DUCHESNE
Institut d'Astrophysique, Université de Liège, Liège, Belgium
August 18, 1948

THE analysis of the Raman spectra of substances like trimethyl-silicon chloride, which belongs to the symmetry C_{3v},[1] seems highly desirable in connection with the study of the structural properties of silanes and with recent theoretical considerations put forward for the similar carbon compounds.[2]

Our results for the Raman spectrum of this substance in the liquid state are given in the following table, in which we indicate the Raman frequencies (cm^{-1}), the rough relative intensities, and the exciting mercury lines which are referred to by letters as follows: $e=4358$A, $k=4047$A. The spectrograph was a "Huet" glass prism instrument giving a dispersion of about 20A/mm in the region involved. Diffuse and sharp lines are designated *d* and *s*, respectively. The mean error of our measurements is about 3 cm^{-1} for most lines.

±187 (3,*dd*) (*e*,*k*)	846 (*o*,*dd*) (*e*,*k*)
±242 (3,*dd*) (*e*,*k*)	1260 (*o*,*sd*) (*e*,*k*)
330 (*oo*,*d*) (*e*)	1315 (*oo*,*dd*) (*e*)
±467 (5,*d*) (*e*,*k*)	1375 (*oo*,*d*) (*e*)
±637 (6,*s*) (*e*,*k*)	1415 (1,*d*) (*e*,*k*)
700 (1,*dd*) (*e*,*k*)	1446 (*oo*,*d*) (*e*)
760 (2,*sd*) (*e*,*k*)	2902 (5,*d*) (*e*,*k*)
	2970 (4,*dd*) (*e*,*k*)

The intense lines observed at 2902 and 2970 cm^{-1} correspond, respectively, to symmetric and antisymmetric valency C−H vibrations. These values are in agreement with the frequencies found with hydrocarbons. The C−H deformation frequencies appear at 1375 (1315) and 1415 (1446) cm^{-1} and are abnormally weak. If we can correlate the former with the symmetric vibration and the latter with the antisymmetric one, these too are in good agreement with the frequencies found with the corresponding vibrations in hydrocarbon compounds. Finally, the line observed at 1260 cm^{-1} may involve hydrogen motions as well, and in that case would be assigned to a methyl rocking frequency in agreement with the interpretation given to an infra-red band situated at 1257 cm^{-1} in methyl-polysiloxanes.[3] It should be remarked, however, that in our experiments this line could be considered alternatively as the first overtone of the 637-cm^{-1} frequency.

Assuming now that the methyl groups behave like single atoms R of atomic weight 15, six vibrations are to be expected to characterize the $ClSiR_3$ radical.

In order to correlate the observed frequencies with the normal modes, we have used a simple valency force field and have adopted for the force constants the values

$$f_1(\mathrm{Si-R})=3.3\times10^5 \text{ dynes/cm};$$
$$f_\theta(\mathrm{R-Si-R})=0.13\times10^5 \text{ dynes/cm};$$
$$f_\beta(\mathrm{Cl-Si-R})=0.2\times10^5 \text{ dynes/cm};$$
$$f(\mathrm{Si-Cl})=5\times10^5 \text{ dynes/cm}.$$

The excellent agreement obtained between calculated (in brackets) and observed frequencies justifies the following assignment, where ν_1, ν_3, ν_5 are the parallel and ν_2, ν_4, ν_6 the perpendicular frequencies according to the usual notation:

$\nu_1=760$ cm^{-1} (810),	$\nu_2=846$ cm^{-1} (850),
$\nu_3=187$ cm^{-1} (191),	$\nu_4=242$ cm^{-1} (224),
$\nu_5=637$ cm^{-1} (595),	$\nu_6=330$ cm^{-1} (330).

The constants f_1 and f_θ are nearly the same as those found by Wall and Eddy[4] for tetramethylsilicon, whereas f_β has been chosen by analogy with the ratio f_θ/f_β present in CH_3Cl. f_{Si-Cl} has been adjusted to calculate a satisfactory value for ν_5 (symmetric Si−Cl vibration) which we had already assigned to 637 cm^{-1} because of its sharpness and intensity. It should be noticed that the infra-red spectrum of compounds such as the linear methylpolysiloxanes, which contain the group $Si(CH_3)_2$, show bands at 753 and 841 cm^{-1} which have been assigned to Si−C vibrations.[3] This provides further evidence of the correctness of our assignments.

The 467- and 700-cm^{-1} frequencies must remain unassigned until a more detailed analysis of the vibrational modes has been made.

It will be observed that the value of f_{Si-Cl} is greater than the corresponding value for the C−Cl bond in CH_3Cl(3.30). This result is in qualitative accordance with recent measurements[1] showing that the Si−Cl bond distance in $ClSi(CH_3)_3$ is markedly contracted (2.09A) with respect to the sum of the covalent radii (2.16A), whereas this is not the case with the C−Cl bond length. On the other hand, there is an increase in the Si−Cl bond as well as in the C−Cl bond in going from $SiCl_4$ to $Si(CH_3)_3Cl$ (or SiH_3Cl), or from CCl_4 to CH_3Cl.

These facts can be explained in terms of two distinct effects: (1) resonance effect, and (2) changes of hybridization at the central atom.

The resonance effect must be due to the part played by structure like $(CH_3)_2(\overline{CH})_3Si=Cl^+$ which strengthen the Si−Cl bond. The changes of hybridization at the silicon atom with respect to an sp^3 state are illustrated by the opening of the C−Si−C angle to about 113°, which means more *s*-character in the hybridized Si orbital from which the Si−C bonds are formed, and more *p*-character in the corresponding orbital for the Si−Cl bond. This results in the Si−Cl bond increasing and in the Si−C bond decreasing. This agrees qualitatively with the facts, as the SiCl bond is only 2.02A in $SiCl_4$ and as Si−C is a little smaller (1.88A) than the sum of the covalent radii (1.94A). Hence this second factor which seems to exert only a small influence in carbon compounds such as CH_3Cl (2) is much enhanced in the silicon compounds.

Thus we believe that we have here an important indication in favor of the existence of the small effects predicted for the carbon compounds which are probably so small that it would be difficult to measure them directly. It should also be noticed that the frequencies of the methyl group are not noticeably affected when it is bound to a silicon atom.

A full account of this work will be published later. We are very indebted to Dr. W. F. Gilliam and to Dr. E. L.

Warrick who have kindly supplied us with samples of the trimethyl silicon chloride.

Our best thanks are due Professor C. A. Coulson and to Dr. D. M. Simpson who have read the manuscript and kindly revised the English.

[1] R. L. Livingston and L. O. Brockway, J. Am. Chem. Soc. **68**, 719 (1946).
[2] C. A. Coulson, *V. Henri Memorial Volume* (Deseer, Liége, 1947); C. A. Coulson, J. Duchesne, and C. Manneback, *ibid.*; A. D. Walsh, Trans. Faraday Soc., meeting on free radicals (in the press); J. Duchesne, Nature **159**, 62 (1947).
[3] N. Wright and M. J. Hunter, J. Am. Chem. Soc. **69**, 803 (1947).
[4] F. T. Wall and C. R. Eddy, J. Chem. Phys. **6**, 107 (1938).

Errata: A Relation between Bond Order and Covalent Bond Distance

[J. Chem. Phys. **15**, 284 (1947)]
H. J. BERNSTEIN
National Research Council, Ottawa, Canada

IN the table for CN, CO, and NO bonds, the bond orders are 0, 1, and 2 for single, double, and triple bonds instead of 1, 2, and 3 as in the table; the C≡O distance is 1.11 instead of 1.15.

Errata: "Volume Effect" and Random Flights

[J. Chem. Phys. **16**, 839 (1948)]
R. C. BRIANT
Mellon Institute, Pittsburgh, Pennsylvania

IN a previous Letter to the Editor the proposed solution is wrong, in part, because the definition of "loop" is ambiguous. Also, multiple loop configurations are overweighted. The writer regrets the error.

A Note on the Structure of Insulin*

DOROTHY WRINCH
Department of Physics, Smith College, Northampton, Massachusetts
August 16, 1948

A COMPREHENSIVE x-ray study of a "wet" insulin crystal has been carried out by Dr. Crowfoot and her collaborators. Much of the work is at present unpublished because of the war. A preliminary publication gave the space group $R3$, cell dimensions $a=83.0A$, $c=34.0A$, and the Patterson projection on the basal plane.[1] A report to the Rockefeller Foundation in 1942 by Dr. Crowfoot included her calculation of the basal section of the Patterson-Harker map and calculations by Dr. K. Schiff of lines parallel to the trigonal axis, including those extending over a $5A$ region about it and an estimate of molecular weight 36,000. A general account based on this report appeared in Russian in 1946.[2] Dr. Crowfoot has generously given me a list of the intensities recorded. We are very greatly indebted to Dr. W. J. Eckert and the International Business Machine Corporation for making available the facilities of the Watson Scientific Computing Laboratory, to Dr. L. H. Thomas for planning, and to Miss E. A. Stewart for carrying out the calculation of the complete three-dimensional Patterson-Harker map derived from these intensities, for z in thirtieths, and for x and y in sixtieths.

Figure 1 shows sections from this map parallel to the basal plane, in the neighborhood of the trigonal axis. The following features may be remarked: a *positive* region A enclosing the origin with circumscribing sphere of radius 8.2A; a *negative* region B completely inclosing A; and a *positive* region C extending slightly further than from $z=\frac{1}{2}\pm\frac{1}{6}$. Since the full extent of the insulin structure or of any molecule in it cannot be represented by so small a region as A, the region B suggests the presence of a lower electron density distribution within each molecule, i.e., a cage structure for each molecule comprising a closely integrated space-enclosing atomic fabric. Structures of this morphological type[3] were suggested for protein molecules in 1936. These include the C_1 cage which, it is now seen,[4] can comprise 72 to 48 residues per skeleton, the C_2, $\cdots C_n$, $\cdots$ cages with maximum skeletal residue numbers 288, $\cdots 72n$,[2] $\cdots$.

A possible picture of the insulin structure is thus as follows: each particle comprises m trigonal molecules ($m=0, 1, \cdots$) and n triads of molecules not necessarily trigonal ($n=0, 1, \cdots$), each being a cage structure. Oncley's recent finding[5] that the insulin structure ($MW\sim 36{,}000$) may be dissociated into 3 subunits suggests that $m=0$, leaving n, the number of molecules per subunit, to be determined.

These new data, so far as suggestions of the "cage" type are concerned, thus appear to favor the suggestion of an insulin structure made up of C_1 cages[6]—say 6—or of 3

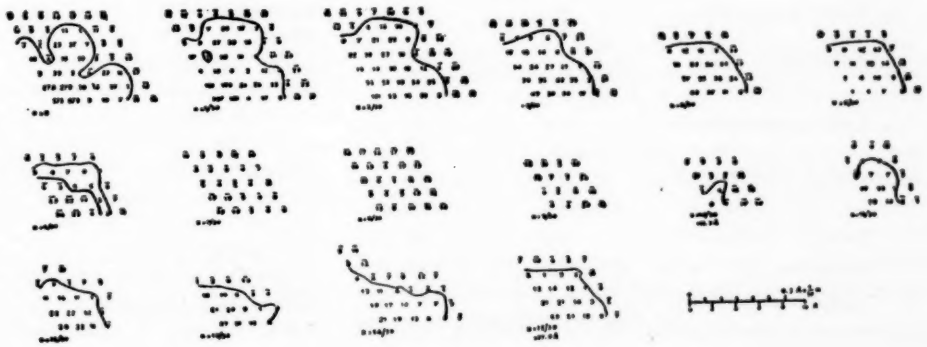

FIG. 1. Sections of the Patterson-Harker map of the "wet" insulin crystal in the neighborhood of the trigonal axis, parallel to the basal plane, calculated from Crowfoot's intensities.

pairs of C_1 cages forming *intramolecular* parallel intergrowths on cube faces, rather than a single C_2 cage.[7] Either of the first two suggestions places cyclic hexapeptides carrying closely packed *R*-substituents on antipodal faces normal to the trigonal axis, which interact in Patterson space to yield a local maximum at rather more than 12A from the origin which may be compared with the maximum in the region *C* which falls at $z\sim\frac{2}{5}$, i.e., at 13.6A from the origin.

* This work is supported by the Office of Naval Research under Contract N8onr—579.

[1] Crowfoot and Riley, Nature **144**, 1011 (1939).
[2] Crowfoot, Chem. J. G15, 215 (1946).
[3] D. Wrinch, Proc. Roy. Soc. London A161, 505 (1937).
[4] D. Wrinch, Science **107**, 445 (1948).
[5] Oncley, Science **106**, 509 (1947).
[6] D. Wrinch, Phil. Mag. **26**, 325 (1938).
[7] D. Wrinch, J. Am. Chem. Soc. **60**, 2005 (1938).

Vibrational Bands Measured with a Thallium Bromide-Iodide Prism

EARLE K. PLYLER
National Bureau of Standards, Washington, D. C.
August 11, 1948

IN recent papers[1] the writer has shown the method of calibration and use of the thallium bromide-iodide prisms for measurements to 40 microns. It was also found that polyethylene and polystyrene, in thin layers, are highly transparent in the 24- to 40-micron region and are well suited for window materials.

TABLE I. List of observed bands.

Substance	Wave-length (μ)	Wave number (cm^{-1})
Trichloroethylene	22.3	448
	25.9	386
	36.0	278
Tetrachloroethylene	23.4	427
	24.8	403
	28.8	347
	34.8	287
Benzene	24.8	403
Isobutylbenzene	22.5	444
	23.7	422
	24.9	402
	28.9	346
Methylene chloride	34.9	286
Carbon tetrachloride	30.5	328
	32.3	310
Bromoform	23.1	433
	25.8	388
	26.4	379
1,3,5-trimethylbenzene	30.0	333
	36.4	275
S-tetrabromoethane	22.4	446
	25.1	398
	35.5	282
Toluene	28.7	348
Chloroform	27.1	369
Carbon disulfide	25.2	397

A study has been made of the absorption spectra of about 30 substances in the long wave-length region, and bands have been found for molecules containing C=S, C−Cl, C−Br, and C−I and other atomic groups. In nearly all cases, cells of 0.4 mm or more in thickness are necessary for the observation of the bands. In Table I are given the wave-lengths and the frequencies of the observed bands for a selected group of substances.

Some of these frequencies have been predicted in studies of the molecular structure of these molecules.[2] In the gaseous state the bands are broad, and the regions of maximum absorption are not so clearly defined. The CS_2 band, as measured in the vapor state at 25.2μ, is strong and is suitable for checking the calibration of the instrument. The absorption band of CCl_4 at 32.3μ has been observed in the vapor. Propane has a band in the region of 26μ and some general absorption beyond 30μ. A detailed discussion of these absorption bands, as well as those of other substances comprising a total of thirty, will be given in a publication now in preparation.

[1] E. K. Plyler, J. Chem. Phys. **15**, 885 (1947), J. Opt. Soc. Am. **38**, 664 (1948).
[2] W. J. Taylor and R. S. Pitzer, J. Research Nat. Bur. Stand. **38**, 1 (1947); G. Herzberg, *Infrared and Raman Spectra of Polyatomic Molecules* (D. Van Nostrand Company, Inc., New York, 1945).

Mass Spectrometric and Infra-Red Study of Rates of Deuterium Exchange, Isomerization, and Hydrogenation of the *n*-Butenes

VERNON H. DIBELER* AND T. IVAN TAYLOR
Department of Chemistry, Columbia University, New York, New York
August 18, 1948

MUCH work has been reported on the nickel-catalyzed deuterium exchange, isomerization, and hydrogenation of the *n*-butenes. The use of mass spectrometric and infra-red analyses to determine the rate constants for the initial stages of these processes seemed to us to offer certain advantages over methods used in previous studies. In particular, mass spectral data should give information on the rates of exchange and addition as well as the position of the exchanged deuterium atom in the molecule. The "hydrogen-switch" mechanism recently proposed by Turkevich and Smith[1] for isomerization and tritium exchange is supported by our results. In certain respects we differ from the results of earlier studies by Twigg[2] and others.[3]

The reactions were carried out with equimolar quantities of hydrogen and olefin in a 400-cc Pyrex vessel containing an 80-cm length of 0.25-mm diameter nickel wire activated by heating alternately in oxygen and hydrogen. Rates of formation of deuterobutenes and of butane were observed by mass spectrometric analysis. Infra-red absorption at 925 cm^{-1} was used to follow the rate of isomerization of 1-butene to 2-butene.

During the initial stages of the reaction between deuterium and 1-butene, in the temperature range 93 to 130°C, the rate of isomerization was only slightly (1.0 to

1.2 times) greater than the rate of exchange. The latter was measured by the increase in abundance of the ion $m/e=57$, due to ionization of $CH_2D-CH=CH-CH_3$ in the mass spectrometer. Activation energies for isomerization and exchange were found to be 7.8 ± 0.7 kcal. and 7.1 ± 0.7 kcal., respectively. The essential equality of these two rates supports the idea that each isomerization is accompanied by an exchange; e.g.,

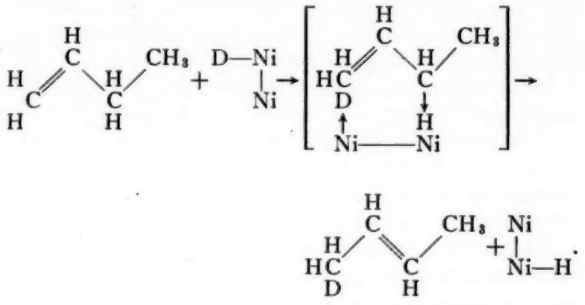

As the reaction progresses, the deuterium is diluted with protium, and the apparent exchange rate decreases. At the same time the isomerization rate increases, as evidenced by the observation that in the presence of pure protium at 100°C, the isomerization rate constant is ten times that in the presence of deuterium. This may account for the difference between our results and those of Twigg, who reported an isomerization rate six times the deuterium exchange rate.[2]

Initially, the rate constant for the second deuterium atom exchanged into the butene molecule is approximately one-fifteenth that of the first deuterium atom. This was measured by observing the rate of increase in abundance of the $m/e=58$ ion. On the basis of the "hydrogen-switch" theory, the second deuterium atom should be introduced primarily by 2-butene reverting to 1-butene to form (I) $CHD=CH-CHD-CH_3$ or (II) $CH_2D-CHD-CH=CH_2$. The observed difference in the above rate constants corresponds roughly to the value that one would predict from the observed equilibrium concentration of 2-butene, i.e., 95.0 ± 2.0 percent and 93.0 ± 2.0 percent at 93 and 130°C, respectively. The mass spectral data indicated provisionally that approximately two-thirds of the butene-d_2 molecules had the (I) structure. The significance of this observation is being investigated further.

Initially, the rate constant for deuterium-induced isomerization was about 20 times that of deuterium addition; while the rate of protium-induced isomerization (activation energy 5.0 ± 0.5 kcal.) was approximately twice that of protium addition (activation energy 2.0 ± 0.3 kcal.). This suggests that the addition and the isomerization-exchange mechanisms are different.

More nearly complete details of this study will be published at a later date.

* National Institute of Health Research Fellow, 1947–48.
[1] J. Turkevich and R. K. Smith, J. Chem. Phys. **16**, 466 (1948).
[2] G. H. Twigg, Proc. Roy. Soc. **A178**, 106 (1941).
[3] For a comprehensive presentation of early work on this subject see the Faraday Society's general discussion on hydrocarbon chemistry, Trans. Faraday Soc. **35**, 806 (1939).

Raman Spectrum of Tetraethyl Orthosilicate

JULES DUCHESNE
Institut d'Astrophysique, Université de Liège, Liège, Belgium
August 18, 1948

THE analysis of the Raman spectra of substances like tetraethyl orthosilicate $Si(OC_2H_5)_4$ seems of some general interest, mainly on account of the SiO_4 group which they possess in common with other molecules such as the siloxanes. The purpose of the present note is to report briefly our investigations on the vibration spectrum of this compound and to discuss the skeletal frequencies of SiO_4 and C_2H_5.

Our results for tetraethyl orthosilicate in the liquid state, together with the rough relative intensities, are listed in the following table. Diffuse and sharp lines are designated, respectively, by *d* and *s*, and the exciting mercury lines are referred to by the letters $e=4358$A and $k=4047$A. The spectrograph was a "Huet" glass prism instrument giving a dispersion of about 20A/mm in the region investigated. The mean error of our measurements is about ±2 cm^{-1} for most lines. Microphotometer records were made, and the weakest diffuse lines were measured on these with errors of about ±10 cm^{-1} for the three lower frequencies.

2975 (5,*s*) (*e*,*k*)	1392 (2,*sd*) (*e*,*k*)	280 (*o*,*dd*) (*e*)
2929 (7,*s*) (*e*,*k*)	1293 (5,*sd*) (*e*,*k*)	236 (*o*,*dd*) (*e*).
2888 (6,*s*) (*e*,*k*)	1087 (6,*d*) (*e*,*k*)	
2867 (4,*sd*) (*e*,*k*)	970 (2,*d*) (*e*,*k*)	
2766 (1,*d*) (*k*)	932 (2,*s*) (*e*,*k*)	
2718 (1,*sd*) (*e*,*k*)	810 (2,*dd*) (*e*,*k*)	
1483 (6,*s*) (*e*,*k*)	790 (2,*dd*) (*e*,*k*)	
1456 (6,*sd*) (*e*,*k*)	652 (5,*s*) (*e*,*k*)	
1443 (5,*sd*) (*e*,*k*)	318 (*o*,*dd*) (*e*)	

The intense lines observed at 2975, 2929, 2888, and 2867 cm^{-1} must correspond to C–H valency vibrations. We may correlate them, respectively, with $\nu_\perp(CH_3)$, $\nu_\parallel(CH_3)$, $\nu_\perp(CH_2)$, and $\nu_\parallel(CH_2)$, in good quantitative agreement with the assignments made for ethers.[1] The C–H deformation frequencies are probably to be identified with the lines at 1392, 1443, 1456, and 1483 cm^{-1}, which are also intense. We suggest that the lines 1443 and 1483 cm^{-1} may be due to a splitting of the doubly degenerate $\delta_\perp(CH_3)$ vibration, as has been assumed in the interpretation of the spectrum of methyl alcohol,[2] whereas 1392 and 1456 cm^{-1} may both be assigned as either $\delta_\parallel(CH_3)$ or $\delta(CH_2)$. The intense line at 1293 cm^{-1} can be associated with an ethyl rocking frequency, and the weak one at 790 cm^{-1} may perhaps arise from a methylene rocking vibration, as suggested by recent observations made with paraffins.[3] 2718 and 2766 cm^{-1} are probably the first overtones of the fundamentals 1390 and 1443 cm^{-1}. Three lines with frequencies 810, 932, 970 cm^{-1} are thus left for consideration; the others will be interpreted as vibrations of the SiO_4 group. These are probably fundamentals corresponding to valency vibrations of C–C–O. Any further attempt at making an exact assignment of these lines would be speculative, until the normal modes have been analyzed in detail.

Assuming that the SiO_4 group is tetrahedral and behaves independently from the rest of the molecule, four vibrations should appear. Thus by analogy with the behavior of the fundamental frequencies of tetrahedral pentatomic molecules, we should expect $\nu_3 > \nu_1 > \nu_4 > \nu_2$, where ν_1 is the non-degenerate symmetrical vibration, ν_2 is the doubly degenerate one, and ν_3 and ν_4 are the triply degenerate ones. The 652-cm^{-1} intense line which appears also in methyl silicate, where it is strongly polarized,[4] remains, according to preliminary results obtained by Thosar and Bapat,[5] practically constant in a series of homologous molecules. It must presumably correspond to ν_1. If so, ν_3 is to be identified with 1087 cm^{-1} and ν_4 and ν_2 are to be chosen among 236, 280, 318 cm^{-1}. The value obtained for ν_3 is in close agreement with that found for methylpolysiloxanes,[6] which give rise to an antisymmetrical stretching vibration of the Si−O bonds at 1050 cm^{-1}. Deformation vibrations involving the Si−O bond occur in the vicinity of 400 cm^{-1} in the Raman spectrum of crystalline quartz.[7] This too supports our assignment of ν_2 and ν_4 and accounts for a certain similarity of the Si−O bonds in these different kinds of molecules.

If we suppose that a valence force field is able to represent the vibrations of SiO_4, two relations between the frequencies and the masses of atoms result. The following assignment,

$\nu_1 = 652$ cm^{-1}, $\nu_2 = 236$ cm^{-1}, $\nu_3 = 1087$ cm^{-1}, $\nu_4 = 280$ cm^{-1},

verifies the relations satisfactorily. The values of the stretching and deformation force constants deduced are 5 and 0.2×10^5 dynes/cm, respectively; they enable one to recalculate the observed frequencies with a maximum error of ten percent. This result would not be appreciably modified by an alternative assignment for ν_2 and ν_4.

On the whole, the consistency for the valence force system is rather satisfactory, and the reasonable values obtained for the force constants give some evidence of the symmetrical tetrahedral character of SiO_4. Further, the Si−O bond distance seems to be the same in the silicate as in the polysiloxanes, as is shown by the equality of the force constants.[6] It would seem that the C_2H_5 and SiO_4 groups are relatively independent and behave quite normally so far as the intensity and magnitude of their frequencies are concerned.

A full account of this work will be published later.

We are very indebted to Dr. D. M. Simpson who has read the manuscript and kindly revised the English.

[1] Cleveland, Murray, Haney, and Schackelford, J. Chem. Phys. **48**, 153 (1940).
[2] H. D. Noether, J. Chem. Phys. **10**, 693 (1942).
[3] N. Sheppard and G. B. B. M. Sutherland, Nature **159**, 739 (1947).
[4] J. Weiler and R. Signer, Helv. Chim. Acta **16**, 115 (1933).
[5] Thosar and Bapat, Zeits. f. Physik **109**, 472 (1938).
[6] N. Wright and M. J. Hunter, J. Am. Chem. Soc. **69**, 803 (1947).
[7] B. D. Saksena, Proc. Ind. Acad. Sci. **16A**, 270 (1942) (mentioned by Wright and Hunter).